QC
1
.U56
vol. 64-A
no. 2

THE UNIVERSITY
OF MICHIGAN
APR 8 1960
LIBRARY

Volume 64A
Number 2
Mar.–Apr. 1960

Journal of Research

of the

NATIONAL BUREAU OF STANDARDS

A. PHYSICS AND CHEMISTRY

Journal of Research
of the
National Bureau of Standards

A. Physics and Chemistry

MAR.–APR. • 1960

VOLUME • 64A

NUMBER • 2

Editor: U. Fano

Associate Editors: L. M. Kushner
J. M. Richardson

Publication dates:
Feb. 1, Apr. 1, June 1, Aug. 1, Oct. 1, Dec. 1, 1960.

JOURNAL OF RESEARCH

The National Bureau of Standards Journal of Research reports research and development in the fields of activity shown at right. Also included from time to time are survey articles and compilations of information on topics closely related to the Bureau's scientific and technical program.

The Journal is published in four separate sections as follows:

A. Physics and Chemistry

Contains papers of interest primarily to scientists working in these fields. Issued six times a year. Annual subscription: domestic, $4.00; foreign, $4.75.

B. Mathematics and Mathematical Physics

Presents studies and compilations designed mainly for the mathematician and the theoretical physicist. Issued quarterly. Annual subscription: domestic, $2.25; foreign, $2.75.

C. Engineering and Instrumentation

Reports research and development results of interest chiefly to the engineer and the applied scientist. Issued quarterly. Annual subscription: domestic, $2.25; foreign, $2.75.

D. Radio Propagation

Reports work in radio propagation, upper atmospheric physics, and communications. Issued six times a year. Annual subscription: domestic, $4.00; foreign, $4.75.

Functions and Activities

The functions of the National Bureau of Standards are set forth in the Act of Congress, March 3, 1901, as amended. These include the development and maintenance of the national standards of measurement and the provision of means and methods for making measurements consistent with these standards; the determination of physical constants and properties of materials; the development of methods and instruments for testing materials, devices, and structures; advisory services to government agencies on scientific and technical problems; invention and development of devices to serve special needs of the Government; and the development of standard practices, codes, and specifications. The work includes basic and applied research, development, engineering, instrumentation, testing, evaluation, calibration services, and various consultation and information services. The Bureau also serves as the Federal technical research center in a number of specialized fields. The scope of activities of the National Bureau of Standards is suggested in the following listing of the divisions and sections engaged in technical work.

Washington, D.C.

Electricity and Electronics. Resistance and Reactance. Electron Devices. Electrical Instruments. Magnetic Measurements. Dielectrics. Engineering Electronics. Electronic Instrumentation. Electrochemistry.

Optics and Metrology. Photometry and Colorimetry. Optical Instruments. Photographic Technology. Length. Engineering Metrology.

Heat. Temperature Physics. Thermodynamics. Cryogenic Physics. Rheology. Molecular Kinetics. Free Radicals Research.

Atomic and Radiation Physics. Spectroscopy. Radiometry. Mass Spectrometry. Solid State Physics. Electron Physics. Atomic Physics. Neutron Physics. Radiation Theory. Radioactivity. X-ray. High Energy Radiation. Nucleonic Instrumentation. Radiological Equipment.

Chemistry. Organic Coatings. Surface Chemistry. Organic Chemistry. Analytical Chemistry. Inorganic Chemistry. Electrodeposition. Molecular Structure and Properties of Gases. Physical Chemistry. Thermochemistry. Spectrochemistry. Pure Substances.

Mechanics. Sound. Mechanical Instruments. Fluid Mechanics. Engineering Mechanics. Mass and Scale. Capacity, Density, and Fluid Meters. Combustion Controls.

Organic and Fibrous Materials. Rubber. Textiles. Paper. Leather. Testing and Specifications. Polymer Structure. Plastics. Dental Research.

Metallurgy. Thermal Metallurgy. Chemical Metallurgy. Mechanical Metallurgy. Corrosion. Metal Physics.

Mineral Products. Engineering Ceramics. Glass. Refractories. Enameled Metals. Constitution and Microstructure.

Building Technology. Structural Engineering. Fire Protection. Air Conditioning, Heating, and Refrigeration. Floor, Roof, and Wall Coverings. Codes and Safety Standards. Heat Transfer. Concreting Materials.

Applied Mathematics. Numerical Analysis. Computation. Statistical Engineering. Mathematical Physics.

Data Processing Systems. SEAC Engineering Group. Components and Techniques. Digital Circuitry. Digital Systems. Analog Systems. Applications Engineering.

• Office of Basic Instrumentation. • Office of Weights and Measures.

Boulder, Colorado

Cryogenic Engineering. Cryogenic Equipment. Cryogenic Processes. Properties of Materials. Gas Liquefaction.

Radio Propagation Physics. Upper Atmosphere Research. Ionosphere Research. Regular Prediction Services. Sun-Earth Relationships. VHF Research. Radio Warning Services. Airglow and Aurora. Radio Astronomy and Arctic Propagation.

Radio Propagation Engineering. Data Reduction Instrumentation. Radio Noise. Tropospheric Measurements. Tropospheric Analysis. Propagation-Terrain Effects. Radio-Meteorology. Lower Atmosphere Physics.

Radio Standards. High-Frequency Electrical Standards. Radio Broadcast Service. Radio and Microwave Materials. Electronic Calibration Center. Microwave Circuit Standards.

Radio Communication and Systems. Low Frequency and Very Low Frequency Research. High Frequency and Very High Frequency Research. Modulation Systems. Antenna Research. Navigation Systems. Systems Analysis. Field Operations.

U.S. DEPARTMENT OF COMMERCE
Frederick H. Mueller, Secretary

NATIONAL BUREAU OF STANDARDS
A. V. Astin, Director

Order all publications from the Superintendent of Documents,
U.S. Government Printing Office, Washington 25, D.C.

Use of funds for printing this publication approved by the Director of the Bureau of the Budget (June 24, 1958).

DEPOSITED BY THE
UNITED STATES OF AMERICA

JOURNAL OF RESEARCH of the National Bureau of Standards—A. Physics and Chemistry
Vol. 64A, No. 2, March–April 1960

A Carbon-14 Beta-Ray Standard, Benzoic Acid-7-C^{14} in Toluene, for Liquid Scintillation Counters

W. F. Marlow and R. W. Medlock

(October 16, 1959)

A carbon-14 beta-ray standard for use in liquid scintillation counting has been prepared and standardized. The sample consists of benzoic acid-7-C^{14} dissolved in toluene. Samples of the solution were oxidized quantitatively in a Paar oxygen bomb, and the radioactivity of the carbon dioxide was compared with the radioactivity of carbon dioxide prepared quantitatively from the Bureau's sodium carbonate-C^{14} standard.

1. Introduction

With the greatly increased use of liquid-scintillation counting as a means of measuring carbon-14 activity, particularly in biochemical and medical studies, the need has also arisen for a suitable carbon-14 standard sample. Since the solvent in most liquid-scintillation systems is generally toluene or xylene, the standard sample should be readily soluble in, and compatible with toluene or xylene. Benzoic acid-7-C^{14} dissolved in toluene was decided upon as a suitable sample.

It was decided to standardize the sample by quantitative oxidation of the benzoic acid and toluene, with quantitative collection of the carbon dioxide produced, followed by measurement of the level of radioactivity of this carbon dioxide in an ionization chamber.

It has been reported by W. D. Armstrong and coworkers [1] [1] that $C^{14}O_2$ and $C^{12}O_2$ are evolved at different rates during oxidation of organic compounds. They report that on wet combustion of xanthydrourea (using the Van Slyke-Folch oxidizing mixture), the $C^{14}O_2$ came off to a very small extent in the first portions of reactant gasses and to a very large extent in the latter portions. Severe treatment was necessary to effect complete combustion; a small amount of nonoxidized material could, therefore, result in a disproportionately large loss of $C^{14}O_2$. When the same compound was oxidized in a stream of oxygen (Pregl's method), it was found that more $C^{14}O_2$ came off in the first half of the reaction than in the last half.

In order to avoid the possibility of error due to this possible isotope effect in either method, it was decided to use a method certain to effect complete combustion of the sample and complete mixing of the $C^{12}O_2$ and $C^{14}O_2$ produced. After consultation with personnel of the Bureau's Thermochemistry Section, it was decided to burn the sample in a modified Paar oxygen bomb and separate the carbon dioxide produced from the oxygen and water.

[1] Figures in brackets indicate the literature references at the end of this paper.

2. Preparation of the Standard Sample

The benzoic acid-7-C^{14} used was prepared by the Bio-Organic Group, Radiation Laboratory, University of California at Berkeley, Calif. The procedure consisted of the carbonation of phenyl magnesium bromide, ether extraction from the reaction mixture, extraction from the ether layer with sodium carbonate solution, and concentration, neutralization, and crystallization.

Seventy milligrams of the dry benzoic acid-7-C^{14}, containing approximately 0.77 mc of C^{14} were placed in a dry 3-neck 3,000-ml round bottom flask protected from the atmosphere by a magnesium perchlorate—Ascarite trap. Reagent-grade toluene that had been dried over sodium was then distilled from freshly added sodium, and 1,500-ml of the fraction boiling between 109.8° and 110.6° C were distilled directly into the 3,000-ml round bottom flask. The mixture was thoroughly agitated to effect a homogeneous solution. The flask was then set up as shown in figure 1. A 5-ml syringe with hypodermic needle, set to deliver 3 ml, was used to transfer the toluene solution of benzoic acid-7-C^{14} to 500 round bottom glass ampoules. The ampoules were cooled in a dry ice—alcohol—water bath (−30° C) and flame-sealed. Figure 2 shows apparatus and techniques used.

3. Combustion of the Sample and Collection of the Carbon Dioxide

Samples of the contents of several of the individual ampoules were taken for analysis after the ampoules had been sealed at least 6 months. This elapsed time presumably allowed any adsorption of benzoic acid on the walls of the ampoules to reach equilibrium. This was verified by the agreement obtained on analyses of contents of ampoules performed 6, 10, and 12 months after preparation.

F. N. Hayes [2, 3] reported that no apparent adsorption effects occurred in liquid-scintillating counting with benzoic acid-7-C^{14} if the total concentration of benzoic acid was above 2 mg/liter; below this

535595—60——1

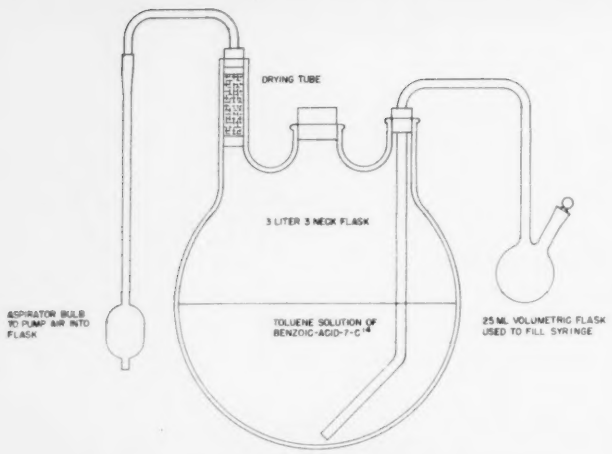
DRYING TUBE
3 LITER 3 NECK FLASK
ASPIRATOR BULB TO PUMP AIR INTO FLASK
TOLUENE SOLUTION OF BENZOIC-ACID-7-C14
25 ML VOLUMETRIC FLASK USED TO FILL SYRINGE

FIGURE 1. *Reservoir for toluene solution of benzoic acid-7-*C^{14}.

value, adsorption apparently became serious. Hayes also reported that concentrations of benzoic acid above approximately 1,300 mg/liter apparently had a quenching effect in liquid-scintillation counting. With the amount of carrier benzoic acid used in the present samples (total concentration of benzoic acid was approximately 47 mg/liter), neither adsorption nor quenching effects will be present according to Hayes' data.

The standard solution was diluted quantitatively with 1 or 2 parts, by weight, of pure toluene before sampling; this was done to obtain a solution of low enough specific activity so that a large enough sample could be taken to give sufficient carbon dioxide for analysis without yielding too much radioactivity to be measured in the ionization chamber. The ampoule used to weigh and introduce the samples into the Paar bomb is shown in figure 3. The sample was drawn in through capillary *A* by applying very mild suction to capillary *B*; capillary *A* and then *B*

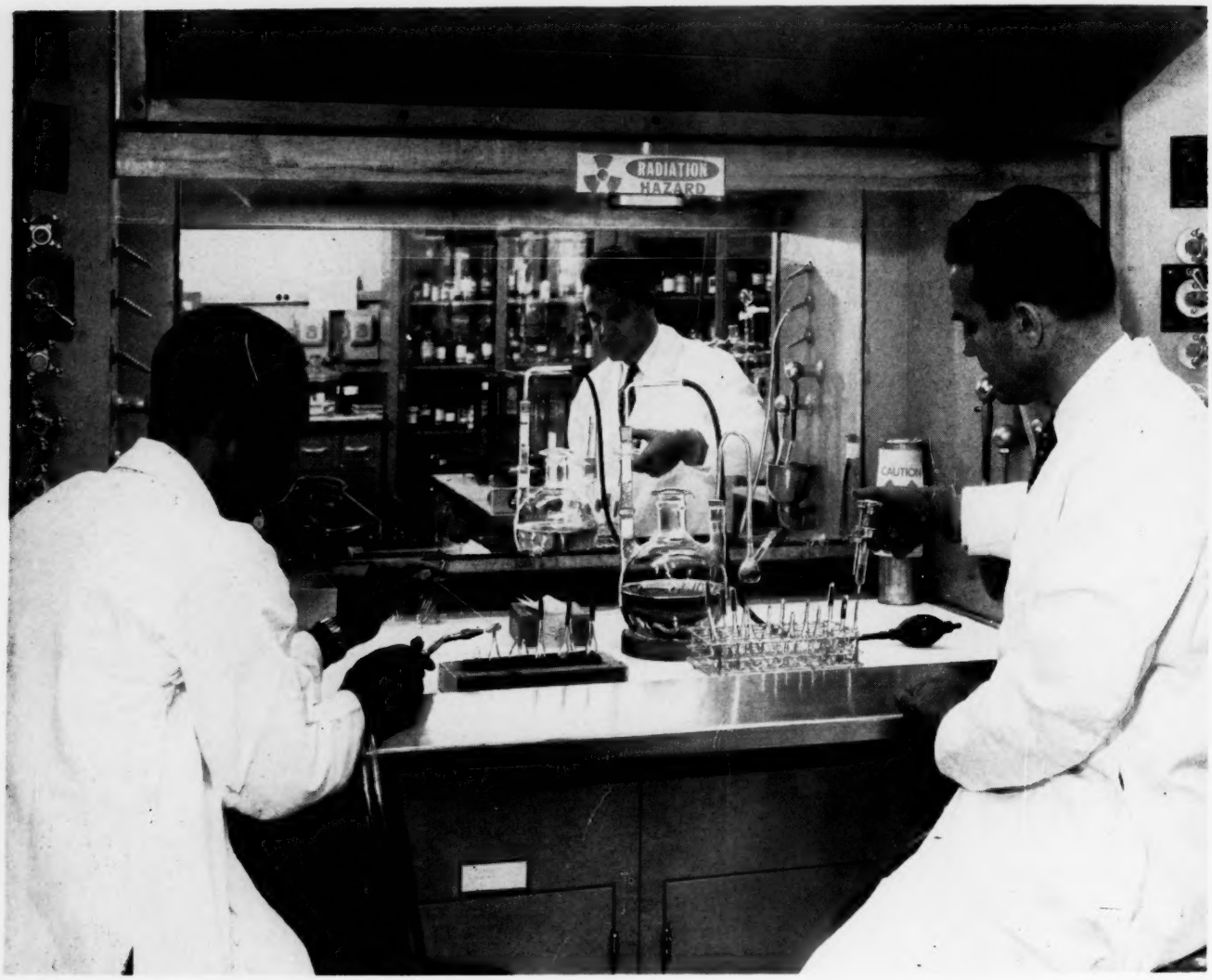

FIGURE 2. *Setup and procedure for filling and sealing ampoules with benzoic acid-7-*C^{14}.

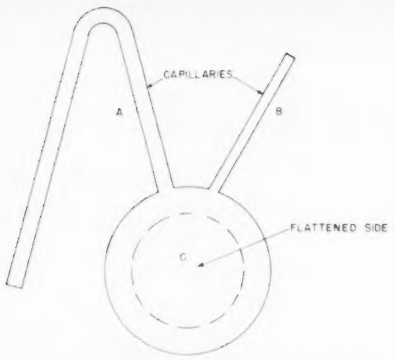

FIGURE 3. *Glass ampoule for sampling toluene solution of benzoic acid-7-C^{14} and introducing it into Paar bomb.*

were sealed, using a pinpoint oxygen-gas flame. The ampoule had to be completely filled, since any air bubble in the sealed ampoule could cause the ampoule to break in the Paar bomb as the oxygen pressure was introduced. The ampoules used held from 0.12 to 0.21 g of the sample.

After the combustion, the gases were bled very slowly through a magnesium perchlorate trap, dry ice—alcohol trap, flowmeter, two liquid nitrogen traps, where the carbon dioxide was frozen out, and finally out through a vacuum pump (see fig. 4). The exit pressure was kept between 70 and 80 mm Hg for best results. When all the gases had been removed from the bomb and passed through the traps, as evidenced by zero flow rate on the flow meter and minimum pressure on the barometer, all of the carbon dioxide was frozen into one of the liquid nitrogen traps and the trap pumped down for 15 to 20 min to less than 1 mm Hg pressure. The carbon dioxide was then transferred to the calibrated gas-collecting and measuring system, figure 5, where its volume and pressure were measured to determine the yield. Nonradioactive carbon dioxide was added to bring the gas to the desired pressure (1 atm) and the gases thoroughly mixed by repeated freezing and expanding of the carbon dioxide. A known fraction was collected in a 250-ml ionization chamber.

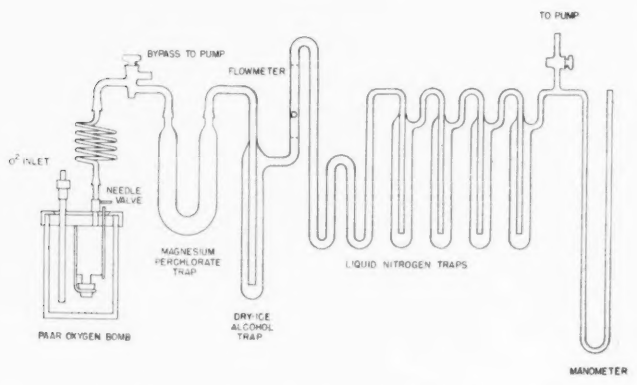

FIGURE 4. *System for collection of CO_2 from combustion products in Paar bomb.*

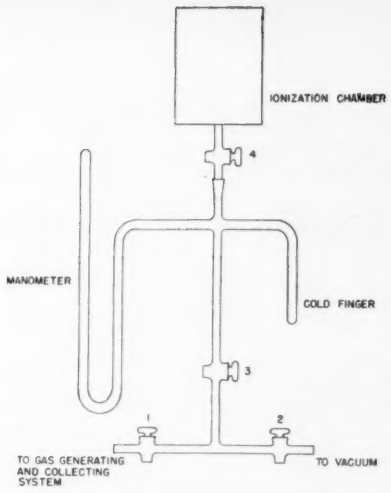

FIGURE 5. *Gas measuring system.*

4. Measurement of Radioactivity of the CO_2

The ionization chamber containing the known portion of the collected carbon dioxide was placed on the electrometer head of a vibrating reed electrometer and the drift rate measured. After correcting for background, the net drift rate was compared with the net drift rate of carbon dioxide, at the same pressure, quantitatively generated from a National Bureau of Standards sodium carbonate-C^{14} beta-ray standard, and the activity was calculated.

5. Calculations and Results

The data and calculations are given in table 1 and in the graph, figure 6.

The graph, with the drift rate in millivolts per second per sample plotted versus the weight of the sample shows the reproducibility of the method over the range of sample weights used.

TABLE 1

Run	Wt of sample	X Wt of standard in sample	Y mv/sec/ sample	Y/X mv/sec/g standard	$\overline{(Y/X)}-(Y/X)$ Deviations(d)
	g	*g*			
1	0.1546	0.0519	9.213	177.44	+3.72
2	.2047	.0687	12.076	175.68	+1.96
3	.1996	.0670	11.864	177.00	+3.28
4	.2044	.1011	18.345	181.45	+7.73
5	.1520	.0752	13.199	175.62	+1.90
6	.2012	.1012	17.025	168.25	−5.49
7	.1682	.0846	14.829	175.20	+1.48
8	.1508	.0759	12.693	167.28	−6.44
9	.1513	.0761	12.788	167.98	−5.74
10	.1611	.0811	13.803	170.28	−3.44
11	.1287	.0433	7.557	174.74	+1.02

$\overline{(Y/X)}=173.72$

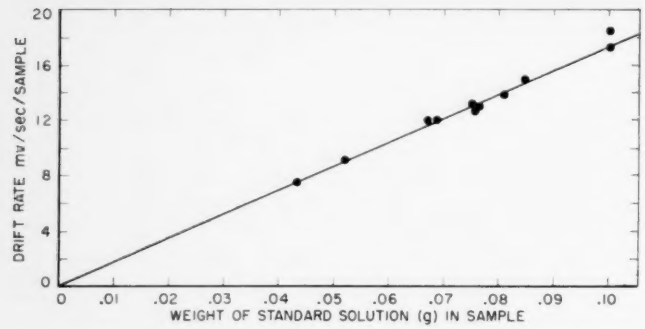

FIGURE 6. *Graph showing drift rate on vibrating reed electrometer for CO_2 from toluene solution of benzoic acid-7-C^{14} versus weight of sample of toluene solution of benzoic acid-7-C^{14}.*

Standard deviation:

$$\sigma=\sqrt{\frac{\sum d^2}{n(n-1)}}=\sqrt{\frac{211.43}{110}}=\sqrt{1.92}=\pm 1.386$$

$$1.386/173.72=\pm 0.80 \text{ percent.}$$

Therefore, the drift rate for the carbon dioxide obtained from the combustion of the benzoic acid-7-C^{14} in toluene, under the conditions used here, was expressed as 173.7 ± 0.8 percent mv/sec/g standard.

The drift rate for the carbon dioxide obtained from the quantitative conversion of the sodium carbonate-C^{14} standard had been determined to be 13.18 mv/sec/g standard when measured under the same conditions as for the carbon dioxide from the benzoic acid. The activity of the sodium carbonate-C^{14} standard has been determined to be 1250 ± 1.5 percent dps/g by absolute counting of the carbon dioxide obtained from the quantitative conversion of the sodium carbonate.

Therefore, the activity of the benzoic acid-7-C^{14} in toluene is calculated:

$$\frac{\text{mv/sec/g benzoic acid standard}}{\text{dps/g benzoic acid standard}}=\frac{\text{mv/sec/g } Na_2CO_3 \text{ standard}}{\text{dps/g } Na_2CO_3 \text{ standard}}$$

$$\text{dps/g benzoic acid standard}=\frac{173.7\times 1250}{13.18}=16.47\times 10^4.$$

The value assigned was 16.5×10^4 dps/g of solution, with a precision of ± 1 percent on comparison with sodium carbonate-C^{14} standard, whose value is known with an accuracy of ± 1.5 percent.

The authors gratefully acknowledge the assistance and cooperation of the following personnel: H. H. Seliger of the Radioactivity Section who suggested the Paar bomb method; I. Jaffee, W. H. Johnson, J. I. Minor, and Mrs. M. V. Kilday, of the Thermochemistry Section, who helped develop the combustion technique; and W. J. Youden, of the Applied Mathematics Division, who greatly assisted in the statistical treatment of the data.

6. References

[1] W. D. Armstrong, L. Singer, S. H. Zbarsky, and B. Dunshee, Errors of combustion of compounds for C^{14} analysis, Science **112**, 531 (1950).

[2] D. L. Williams, F. N. Hayes, R. J. Kandel, and W. H. Rogers, Preparation of C^{14} standards for liquid scintillation counting, Nucleonics **14**, 62 (1956).

[3] F. N. Hayes, Liquid solution scintillators LA–1639, 70 (1954).

WASHINGTON, D.C. (Paper 64A2–36)

JOURNAL OF RESEARCH of the National Bureau of Standards—A. Physics and Chemistry
Vol. 64A, No. 2, March–April 1960

A Comparison of Experimental and Theoretical Relations Between Young's Modulus and the Flexural and Longitudinal Resonance Frequencies of Uniform Bars

S. Spinner, T. W. Reichard, and W. E. Tefft

(December 17, 1959)

The relations from which Young's modulus may be computed from mechanical flexural and longitudinal resonance frequencies have been established by an empirical method using two sets of steel bars. Both sets contained rectangular and cylindrical specimens. For longitudinal vibration of cylindrical specimens, the agreement between the empirical curves and Bancroft's corresponding theoretical relation was within experimental error if Poisson's ratio for both sets is taken to be 0.292. For flexural vibrations, the agreement between the empirical curve and the corresponding theoretical relation developed by Pickett is also within experimental error for about the same value of Poisson's ratio for the rectangular specimens of both sets; but for cylindrical specimens, the empirical values are somewhat lower than those predicted by the theory.

1. Introduction

In a previous paper, [1] [1] an empirical relation was established from which the shear modulus could be calculated from the torsional resonance frequency using uniform steel bars of different rectangular cross sections. The empirical relation was compared with corresponding theoretical approximations. The purpose of the present paper is to establish similar relations from which Young's modulus may be determined from the flexural and longitudinal mechanical resonance frequencies for bars of round and rectangular cross section. These empirical relations are also compared with corresponding theoretical equations when feasible.

As in the previous work, advantage is taken of the fact that these resonance frequencies can be determined to an accuracy which, when combined with comparable accuracy of dimensions, is sufficient to yield empirical results good to four significant figures.

In fact, it is this increased accuracy to which modern experimental techniques have advanced dynamic elastic measurements that has made it possible to check in a more precise manner the theoretical results of such analysts as Rayleigh, Kelvin, Poisson, and Stokes [2].

As usually happens in such cases, this increased experimental accuracy has, in turn, led to a refinement and extension of the theory. Some equations had lain dormant for many years because, though presumably "complete" and "correct," they were nevertheless expressed in so general a form that numerical solutions for most real cases were too cumbersome to be of practical value. Such equations have recently been solved for given boundary conditions. These solutions have often taken advantage of modern computing devices. A particular case in point is the set of Pochhammer-Chree equations, relating the most general case of elastic waves in rods to their elastic moduli. These equations, almost forgotten for more than 50 years, were solved by Bancroft [3] for the case of longitudinal waves and by Hudson [4] for flexural waves. A recent article by Davies [5] presents a comprehensive review and bibliography of the advances in this field up to the present time.

For Young's modulus, the problem of establishing an empirical relation is complicated by the fact that the cross sectional correction for both flexural and longitudinal vibrations depends upon Poisson's ratio as well as the dimensions. This is in contrast with shear for which the cross sectional correction is independent of Poisson's ratio. Consequently, the results to be presented here are more limited than those previously given for shear since these results apply mainly to those materials having Poisson's ratios approximately equal to those used here. Furthermore, when comparing the empirical with theoretical relations, any error in the value of Poisson's ratio assigned to the specimens would result in a corresponding error in the comparison of the correction factors. This error would increase as the ratio of cross section to length increased.

2. Experimental Procedures

2.1. General

The basic experimental approach consists in determining the flexural and longitudinal resonance frequencies of specimens of known mass and dimensions, and assuming their uniformity of Young's modulus and density, to derive the empirical relation needed for the determination of Young's modulus from the mechanical resonance frequency. Data to

[1] Figures in brackets indicate the literature references at the end of this paper.

be presented later will show that the assumption of uniform density and Young's modulus is quite justified.

2.2. Specimens

Two separate sets of steel specimens were used in this investigation. Each set of specimens was cut from its own parent piece to insure the greatest possible uniformity of intrinsic Young's modulus and density from specimen to specimen within each of the two sets.

One source was a cylindrical bar of cold drawn steel about 1 in. in diameter, designated as SAE No. 1020. Originally 18 specimens, I–5 through I–22, ranging in length from about 3 to 12 in. were cut from the parent stock. Subsequently some of these rods were further shortened or machined to square cross section to extend the range of the experimental data. All of the specimens from this source are henceforth classified as set I. Exact dimensions and other related data for set I are given in table 1.

TABLE 1. *Data for specimens of set I*[a]

Specimen	Length l	Density ρ	f(long)[b]	f(flex)[b]	k/l[c]	v/v_0 empirical	T empirical
	cm	*g/cm³*	*cps*	*cps*			
I–1	5.050	7.849	50,253	31,310	0.12565	0.9851	2.1234
I–2	5.118	7.850	49,606	30,650	.12396	.9857	2.0997
I–3	5.354	7.849	.....	28,624	.11850	.....	1.9998
I–4	5.639	7.850	.....	26,401	.11251	.....	1.9206
I–5	7.511	7.851	34,051	16,605	.08447	.9929	1.5424
I–6	7.584	7.851	33,752	16,341	.08366	.9938	1.5320
I–7	7.760	7.851	32,975	15,733	.08176	.9934	1.5077
I–8	10.117	7.847	25,370	9,939	.06272	.9965	1.3085
I–9	10.224	7.846	25,107	9,755	.06206	.9966	1.3024
I–10	14.790	7.851	17,389	4,955	.04289	.9985	1.1475
I–11	14.958	7.853	17,190	4,859	.04241	.9982	1.1447
I–12	14.968	7.854	17,185	4,854	.04238	.9986	1.1438
I–13	15.118	7.853	17,014	4,765	.04196	.9985	1.1410
I–14	15.235	7.851	16,883	4,695	.04164	.9986	1.1395
I–15	19.736	7.851	13,037	2,866	.03214	.9989	1.0832
I–16	19.985	7.852	12,875	2,799	.03174	.9989	1.0829
I–17	22.951	7.849	11,213	2,139	.02766	.9991	1.0564
I–18	25.641	7.850	10,039	1,725	.02475	.9993	1.0525
I–19	29.987	7.852	8,587	1,271	.02116	.9997	1.0360
I–20	30.201	7.853	8,525	1,253	.02101	.9995	1.0359
I–21	30.500	7.852	8,442	1,229	.02080	.9996	1.0353
I–22	30.554	7.850	8,427	1,225	.02076	.9995	1.0350
I–12b	5.177	7.849	.....	26,704	.10020	.....	1.7649
I–12c	6.942	7.849	.....	16,415	.07473	.....	1.4445
I–12a	14.968	7.850	17,188	4,043	.03464	.9988	1.1016
I–15a	19.736	7.848	13,039	2,370	.02627	.9991	1.0610
I–18a	25.641	7.847	10,038	1,421	.02023	.9992	1.0360

[a] All specimens except those followed by a letter are 2.5378 cm in diameter. Those followed by a letter are 1.796-cm square.

[b] Fundamental longitudinal and flexural resonance frequencies.

[c] k=radius of gyration of the cross sectional area about an axis perpendicular to the plane of vibration

for round specimens $k=\frac{1}{4}$ diam=0.63445 cm.

for square specimens k=edge/$\sqrt{12}$=0.51846 cm.

for cylindrical specimens, $D/\lambda=2k/l$

where D=diameter of specimen and λ=wavelength of longitudinal wave.

The other source of specimens was a bar of 2-in. square stock of hot rolled and annealed tool steel designated by the trade name "Stentor." The original specimens from this source were the same 12 pieces (II–1 through II–12) of equal lengths but different rectangular cross sections that were used in the investigation for shear modulus [1]. As for set I, some of these specimens were further reduced in dimensions or machined to circular cross section. All specimens from the second source are classified as set II and data for these specimens are given in table 2.

The dimensions of both sets of specimens are accurate to ±.001 cm. The density was calculated from the mass and the dimensions of the specimens. The average density for the specimens of set I was 7.851 g/cm³, and that of set II was, as previously given [1], 7.814 g/cm³. The standard deviation of this measurement was 0.002 g/cm³ for both sets. This small variation in density is good evidence for the intrinsic uniformity of the specimens of each set. Although the density variations are within the error of the measurement, the mass and dimensions of each particular specimen were used in most calculations rather than the average value of density. The density of some randomly selected specimens of both sets was also checked by weighing in air and while immersed in liquid and was found to agree with the above values within the error of their determination.

Actually, for the specimens of set II, the density, ρ, by the immersion technique was found to be 7.816 g/cm³. Subsequent determination of ρ, calculated from the mass and volume of two specimens machined to a higher degree of accuracy than the others (specimens II–4r_1 and II–4r_2), agreed with the value obtained by immersion and is believed to be the most reliable value for the specimens of set II.

2.3. Method

The mechanical longitudinal and flexural resonance frequencies of both sets of specimens were determined by the dynamic method previously described [1]. Briefly, one of the mechanical resonance frequencies of the specimen is excited by an electromagnetic driver. The increased amplitude of vibration of the specimen at resonance is detected by a crystal pickup whose output, together with a signal of the same frequency, produces a Lissajou pattern on a cathode-ray oscilloscope. The different types of vibrations are obtained by appropriate placement of the driver and pickup with respect to the specimen.

As with torsional vibrations the longitudinal and flexural resonance frequencies were excited and detected by more than one method.

In the first method the specimens were supported on foam rubber in the vicinity of the nodal points and driven through air by a tweeter type driver. A crystal pickup placed lightly against the proper part of the specimen detected the vibrations. Both longitudinal and flexural vibrations could be obtained by this method.

The second method could be used only to obtain flexural vibrations and was most appropriate for the lighter specimens. This method consisted in suspending the specimens from two cotton fibers, one fiber being attached to a phonograph record cutting head as the driver and the other fiber being attached to a crystal pickup. Unlike the case for torsion, it

TABLE 2. *Data for specimens of set II*

Specimen [a]	Length l	Width w	Depth d	Density ρ	Flatwise			Edgewise			f (long)
					k/l [b]	f(flex)	T	k/l [b]	f(flex)	T	
	cm	*cm*	*cm*	*g/cm³*		*cps*			*cps*		*cps*
Rectangular specimens											
II–1	15.202	3.1496	3.1496	7.817	0.05981	6411	1.2915	0.05981	6411	1.2915	17,046
II–2	15.202	3.1433	2.5405	7.819	.04825	5379	1.1936	.05969	6399	1.2910	17,053
II–3	15.202	3.1433	1.9055	7.814	.03619	4183	1.1112	.05969	6398	1.2923	17,062
II–4	15.202	3.1433	1.5875	7.817	.03015	3538	1.0775	.05969	6400	1.2909	17,065
II–5	15.202	3.1433	1.4300	7.814	.02716	3208	1.0635	.05969	6397	1.2926	17,066
II–6	15.202	3.1433	1.2708	7.816	.02413	2867	1.0514	.05969	6399	1.2915	17,066
II–7	15.202	3.1433	1.1120	7.812	.02112	2523	1.0403	.05969	6399	1.2921	17,071
II–8	15.202	3.1433	0.9530	7.812	.01810	2172	1.0309	.05969	6394	1.2941	17,067
II–9	15.202	3.1433	.7943	7.813	.01508	1820.6	1.0189	.05969	6400	1.2916	17,075
II–10	15.202	3.1433	.6363	7.815	.01208	1463.4	1.0118	.05969	6400	1.2912	17,070
II–11	15.202	3.1433	.4773	7.811	.00906	1101.1	1.0061	.05969	6400	1.2919	17,070
II–12	15.202	3.1433	.3172	7.814	.00602	733.0	1.0028	.05969	6396	1.2927	17,064
II–2a	7.882	3.1433	2.5405	7.814	.09306	16,941	1.6660	.11513	19,203	1.9849	----------
II–2b	7.010	3.1433	2.5405	7.817	.10463	20,432	1.8297	.12945	22,934	2.2232	----------
II–3a	7.546	3.1433	1.9055	7.818	.07290	14,983	1.4255	.12026	20,495	2.0732	----------
II–3b	7.249	3.1433	1.9055	7.817	.07589	16,052	1.4584	.12519	21,789	2.1535	----------
II–10a	15.202	2.0574	0.6363	7.816	.01208	1460.7	1.0147	.03907	4475	1.1314	----------
II–10b	15.202	0.6426	.6363	7.814	.01220	----------	----------	----------	----------	----------	17,100

	Length l	Diameter D	Density ρ	k/l [c]	f(flex)	T	f(long)	v/v_0
Cylindrical specimens								
II–1r	14.364	3.1252	7.816	0.05439	6303	1.2384	18,057	0.9978
II–2ar	7.315	2.4460	7.812	.08359	17,102	1.5329	35,329	.9944
II–3br	6.447	1.8124	7.812	.07029	17,141	1.3882	40,145	.9957
II–4r$_1$	14.669	1.2845	7.816	.02189	2708.9	1.0404	17,714	.9996
II–4r$_2$	14.668	1.2843	7.816	.02189	2708.3	1.0407	17,715	.9996

[a] Letter following specimen number indicates that the specimen has been redimensioned. Number denotes original specimen. A second letter indicates a second change in dimension.

[b] k=radius of gyration of the cross sectional area about an axis perpendicular to the plane of vibration. For rectangular specimens in flatwise vibrations, $k=d/\sqrt{12}$; for edgewise vibration $k=w\sqrt{12}$.

[c] For cylindrical specimens, $k=D/4$. Since, for the fundamental longitudinal resonance frequency, $\lambda=2l$, $k/l=d/2\lambda$.

was not necessary for the points of suspension to be at opposite faces of the specimen.

A third method, combining certain features of the first two, consisted in suspending the specimens from two cotton fibers as in the second method but driving them through air with a tweeter and detecting the vibrations with a crystal pickup as in the first method. This third method could be used to obtain both flexural and longitudinal vibrations and was satisfactory for heavy as well as light specimens. The highest resonance frequencies could be obtained most readily by this method.

The accuracy of the resonance frequencies obtained by the last two methods was usually somewhat better than that obtained by the first method. However, by any of these methods, the accuracy of the resonance frequencies was usually better than 1 part in 4,000 [1].

The fundamental longitudinal and flexural resonance frequencies for the specimens of sets I and II are given respectively in tables 1 and 2. Inasmuch as the specimens of set II are rectangular in cross section, two separate flexural resonance frequencies occur about both longitudinal planes of symmetry (flatwise and edgewise). The fact that the edgewise flexural frequency is the same for specimens II–2 through II–12 is of considerable significance as will be explained. Table 3 gives frequencies of overtones of longitudinal resonance vibrations of four specimens of set I and one specimen of set II.

It may be observed that longitudinal resonance frequencies of over 50,000 cps are recorded for both fundamentals and overtones. These remarkably

TABLE 3. *Overtones of logitudinal resonance vibrations of several cylindrical specimens*

		Frequency	$D/\lambda=r/l$	v/v_0 [a]
Set I Specimen I–20	Fundamental ($n=1$)	8525	0.04202	0.9995
	1st overtone ($n=2$)	17027	.08405	.9982
	2d overtone ($n=3$)	25491	.12607	.9963
	3d overtone ($n=4$)	33898	.16809	.9936
	4th overtone ($n=5$)	42218	.21012	.9900
Set I Specimen I–21	Fundamental ($n=1$)	8442	.04160	.9996
	1st overtone ($n=2$)	16858	.08321	.9981
	2d overtone ($n=3$)	25238	.12481	.9961
	3d overtone ($n=4$)	33560	.16642	.9935
	4th overtone ($n=5$)	41800	.20802	.8999
Set I Specimen I–19	Fundamental ($n=1$)	8587	.04232	.9997
	1st overtone ($n=2$)	17154	.08464	.9985
	2d overtone ($n=3$)	25683	.12696	.9966
	3d overtone ($n=4$)	34146	.16928	.9938
Set I Specimen I–16	Fundamental ($n=1$)	12875	.06348	.9989
	1st overtone ($n=2$)	25692	.12696	.9967
Set II Specimen II–1r	Fundamental ($n=1$)	18057	.10878	.9978
	1st overtone ($n=2$)	35823	.21756	.9898
	2d overtone ($n=3$)	52884	.32634	.9741

[a] For set I specimens, $v_0=5152$ m/sec; for set II specimens, $v_0=5199$ m/sec.

high values of resonance frequency which can be excited and detected by a method sometimes described as "sonic," are explained by the nature of the specimens and also by the fact that the response of both driver and pickup, though reduced, persists at frequencies considerably above their rated upper frequency limit. This reduced response is amplified and detected as a recognizable pattern on the scope.

Since the upper frequency response obtained is more than 2½ times higher than the nominal upper limit of the sonic range and will probably go higher as experimental techniques improve, it is felt that the term, "mechanical resonance methods," would be more appropriate than "sonic methods" to describe the experimental procedure used.

3. Calculations, Results, and Discussion

3.1. Longitudinal Resonance Frequencies for Cylindrical Specimens of Sets I and II

The following relations for this type of vibration are recalled. First, a rod vibrating in this manner satisfies the condition that

$$l=n\lambda/2 \tag{1}$$

where l=length of specimen, n=order of resonance frequency. For the fundamental, $n=1$, for the first overtone $n=2$, etc., λ=wavelength of the vibration in the specimen. This leads to the well-known relation between the velocity of the longitudinal wave, v, and the longitudinal resonance frequency, f_n,

$$v=\frac{2lf_n}{n}. \tag{2}$$

The subscript after the f indicates the order of the resonance frequency.

For an infinitely thin specimen of length l, v becomes the "rod velocity," v_0. Rayleigh's familiar approximation, given below, shows the amount by which v, in a specimen of finite circular cross section is reduced from v_0.

$$v=v_0\left[1+\left(\frac{\pi n\mu r}{2l}\right)^2\right]^{-1} \tag{3}$$

where μ=Poisson's ratio and r=radius of the rod.

The relation showing the effect of cross section is often expressed in terms of v/v_0 as a function of D/λ, D being the diameter of cross section. This convention will be followed here. From eq (1) it is seen that $D/\lambda=nr/l$.

Empirical values of v/v_0 can be conveniently calculated after the value of v_0 has been determined. We consider first the specimens of set I. Substitution of the appropriate values for the longest specimen, I–22, (having the lowest r/l) in eq (3) shows that $v=0.9996v_0$. Specimens I–19, I–20, and I–21 are sufficiently long to give an average for the ratio, v/v_0, from eq (3) equal to that for specimen I–22. At the low values of r/l associated with these specimens, the choice of a proper value of μ is no problem, since any reasonable variation about the selected value of 0.3 (say from 0.26 to 0.32) will have only a negligible effect on the result. Also, at such low values of r/l any difference between Rayleigh's and corresponding equations, such as Bancroft's, will also be negligible. Therefore, the average value of $v_0=5152$ m/sec, obtained by substituting the values for these four longest specimens in eq (2) and dividing by 0.9996, is taken to be the rod velocity for the specimens of set I. The empirical values of v/v_0 for the remainder of the specimens of set I are then found from the following equation

$$v/v_0=\frac{2lf_n}{5152n}. \tag{4}$$

These v/v_0 values are given numerically in table 1 and graphically, as a function of D/λ in figure 1.

The empirical values of v/v_0 for the specimens of set II are found in the same manner. The reference specimens in this case, having the lowest value of r/l, were II–4r_1 and II–4r_2. These are recalled to be the specimens that were more accurately machined. The purpose of this was to obtain a more reliable base value. For these specimens, $v/v_0=0.9996$, $v_0=5199$ m/sec, and empirical values for the other specimens are found from the equation

$$v/v_0=\frac{2lf_n}{5199n}. \tag{4a}$$

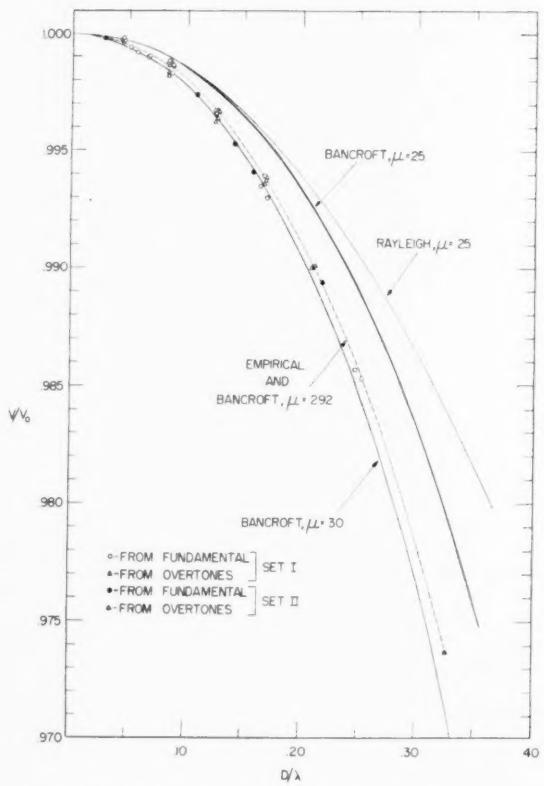

FIGURE 1. *Effect of the ratio of diameter* (D) *to wavelength* (λ) *on the ratio of the velocity of the longitudinal wave* (v) *to the rod velocity* (v_0) *for two sets of cylindrical steel specimens.*

Theoretical curves are included for comparison.

Numerical values of v/v_0 for these specimens are given in table 2 and are plotted along with those of set I in figure 1.

For both sets of specimens, v/v_0 for higher values of D/λ was obtained both by vibrating the shortest specimens at their fundamental resonance frequency and also (since $D/\lambda=n\ r/l$) by vibrating some specimens at higher overtones. The data for these overtones are found in table 3.

It is observed from figure 1 that not only do the empirical points fall on the same curve, within experimental error, whether determined from the fundamental or overtones of either set of specimens, but also the points for both sets of specimens also fall on this same curve.

Since v_0 and the density, ρ, are known, Young's modulus, E, can be determined for each set of specimens from the equation,

$$E=v_0^2\ \rho \tag{5}$$

for set I, $E=2084\times10^9$ dynes/cm^2=2084 kilobars, and for set II, $E=2113$ kilobars.

Bancroft's [3] numerical solution of the Pochhammer-Chree equation for longitudinal waves has already been mentioned. His values for $\mu=0.25$ and $\mu=0.30$ are plotted, along with values based on Rayleigh's equation for $\mu=0.25$, in figure 1. Bancroft's solution is seen to reduce v/v_0 by a greater amount than Rayleigh's for a given value of μ. Since Bancroft's solution is considered more exact than Rayleigh's, comparison of the empirical points will be made with Bancroft. Graphical interpolation between Bancroft's values for $\mu=0.25$ and $\mu=0.30$ at $D/\lambda=0.25$ shows the empirical curve to agree with Bancroft for the case where $\mu=0.292$. That is, if the μ of the specimens of sets I and II is 0.292, then agreement of the empirical with Bancroft's solution would be within the error of the measurement.

It would be desirable then to obtain an independent value of μ as a further check. The method that appeared most feasible for this was to determine the shear modulus, G, from the torsional resonance frequency and then, since E is already known, to compute μ from the well-known relation between E and G for isotropic materials,

$$\mu=\frac{E}{2G}-1. \tag{6}$$

For the specimens of set II, G is already known from the previous investigation [1] to be 822.1 kilobars. For the specimens of set I, however, it was not possible (at first) to detect the torsional resonance frequency of the round bars by any of the variations of the method previously described.[2] To circumvent this difficulty, three of the specimens were machined to square cross section. This was in fact the original reason for squaring some of the round specimens of set I. (These squared bars incidentally provided additional specimens for which longitudinal and flexural resonance frequencies could be determined. It can be seen from table 1 that for specimens of this size, the effect of cross section in reducing the rod velocity is of the same order of magnitude as for circular cross section.) For square specimens the torsional resonance frequency, and hence G, can be obtained in the manner described in the previous paper [1].

Two of the longer and one relatively short specimen were selected. A square rather than rectangular cross section was chosen because the shape factor for square cross section is believed to be more accurate [1] and would therefore lead to a more accurate value of G.

The value of G obtained for specimens I–12a, I–15a, and I–18a, of set I, were 820.5, 821.6, 820.5 respectively, with an average of 820.9 kilobars.

Substituting the known values of E and G for both sets of specimens in eq (6) yields the following values for μ: For set I, $\mu=0.269$ and for set II, $\mu=0.285$.

The physical constants obtained for sets I and II are now summarized in table 4.

It appears far more likely that the value of $\mu=0.292$ is closer to the true value for both sets of specimens than the values obtained from eq (6). This belief is supported by the following evidence.

TABLE 4. *Physical constants of two different sets of steel specimens*

	Set I	Set II
v_0, "rod velocity" ..... m/sec	5152	5199
ρ, density ..... g/cm^3	7.851	7.816
E, Young's modulus ..... kilobars	2084	2113
G, shear modulus ..... kilobars	820.9	822.1
μ, Poisson's ratio	0.269[a]	0.285[a]

[a] Derived from E and G values and eq (6). From Bancroft, $\mu=0.292$ for both sets.

The value of μ for steel usually found in the literature is around 0.29. Markham [6], for instance, measured E and G for 10 different types of steel by an ultrasonic method and, from these elastic moduli, calculated μ. His values for μ varied between 0.286 and 0.292 with an average of 0.289. Analysis of Markham's data shows that the variation in values of μ given for the different types of steel can be accounted for completely by precision in measurements of E and G, given by Markham, rather than by any differences in the values of E and G themselves. Therefore, the average value of $\mu=0.289$ for all the steels may be taken as characteristic of each of them. Thus it appears that though E and G may be different for different types of steel, these elastic moduli vary concomitantly so that μ remains constant.

If $\mu\approx0.292$ is correct for the specimens of sets I and II, then a possible explanation for the lower

[2] Subsequently, by the use of an improved driver and suspension of the specimens from strings as already described, the torsional resonance frequencies were obtained for cylindrical bars of sets I and II. The average values of G, calculated from these resonances, were in agreement with those given in the text.

values of μ obtained from eq (6) lies in the fact that a preferred crystal orientation develops in the steel during the process of manufacture. Consequently, the assumption of macroscopic isotropy resulting from a completely random crystal orientation is not entirely fulfilled, and eq (6) which is based on this assumption, is not entirely valid for these specimens. Frankland and Whittemore [7] have demonstrated that the average E for specimens of "black" sheet steel cut perpendicular to the direction of rolling is significantly different from the average E of specimens cut parallel to the direction of rolling. In this connection, it is noteworthy that for the specimens of set I, in which the process of repeated cold working of the parent stock results in a more pronounced crystal orientation, the value of μ departs by a greater amount from the "correct" value, than for the specimens of set II, where the process of annealing of the parent stock largely restores the random crystal orientation. Indeed, the value of μ in the specimens of set II from eq (6) is in good agreement with the values found in the literature and with that based on Bancroft in this investigation.

Also, it appears from the fact that the empirical points of v/v_0 for sets I and II lie on the same line, that the value of μ for both sets of specimens is the same. This does not prove that the value of μ based on Bancroft is "correct" but it does make it improbable that sets I and II should have different values as the results based on eq (6) would indicate, for it would be a most unlikely coincidence that any error resulting from interpolation from Bancroft should lead to the same value of μ, if the μ of both sets of specimens were actually different. Furthermore, the agreement in μ for both sets of specimens is in accordance with Markham's data.

The alternative possibility to explain the discrepancy in μ, is that the values based on eq (6) are correct, and that Bancroft's correction for cross section and consequently, the value of μ based on it are incorrect. Inasmuch as this alternative involves the (at least partial) rejection of Bancroft's theoretical equation as well as the value of μ for steel found in the literature, both widely accepted, its correctness appears most unlikely.

3.2. Longitudinal Resonance, Rectangular Specimens

The longitudinal resonance frequencies of the rectangular specimens of both sets are listed in tables 1 and 2 but will not be considered here. It is planned to discuss these in a subsequent paper. It will merely be noted here that specimen II–10 b, having a small nearly square cross section, had a considerably higher resonance frequency (17,100 cps) than the other specimens of the same set. Substituting the resonance frequency and length for this specimen in eq (2) yields a value of $v=5199$ m/sec in agreement with v_0 for this set. This value would be expected for a round specimen of the same k/l.

3.3. Flexural Vibrations, Sets I and II

Flexural vibrations are probably of more practical importance than longitudinal as a means of determining Young's modulus because flexural vibrations can usually be excited more easily than longitudinal. This is especially true for thin specimens. Thus, for these thin specimens where any error in E due to an error in the correction for cross section would be minimized, the longitudinal resonance frequency is relatively difficult to obtain, whereas the flexural resonance frequency becomes experimentally easier to excite. Hence a reliable relationship from which E may be determined from the flexural resonance frequency becomes important.

Hudson's [4] numerical solution of the Pochhammer-Chree equations for flexural waves has already been mentioned. Unfortunately, no comparison can be made between Hudson's results and the empirical ones, because no simple or clear-cut relation has been found to exist between the length of a traveling flexural wave in a very long bar and the length of bars vibrating in flexural resonance. Consequently, one relies on a direct relation between Young's modulus and the flexural resonance frequency.

Goens [8] has solved Timoshenko's [9] equation relating Young's modulus to the flexural resonance frequency for bars of different cross section. Pickett [10] has further simplified Goen's solution. Goen's solution can be expressed in the following form:

$$E=\left[\frac{2\pi l^2 f}{km^2}\right]^2 \rho T \tag{7}$$

where f, in this case, is the flexural resonance frequency; k is the radius of gyration of the cross sectional area about an axis perpendicular to the plane of vibration. For a rectangular cross section $k=t/\sqrt{12}$, t being the dimension in the direction of vibration. (The depth and width interchange as t depending on whether the vibration is flatwise or edgewise.) For a circular cross section, $k=r/2$; m is a constant which has higher values for higher overtones, for the fundamental $m=4.730$; T is a correction factor which varies with k/l and μ. Pickett used subscripts for m and T since both factors vary with the order of vibrations. Since only the fundamental flexural resonance frequency is considered here, the subscripts are dropped.

For cylindrical bars eq (7) becomes

$$E=1.2619\left[\frac{l^2 f}{D}\right]^2 \rho T, \tag{7a}$$

and for rectangular bars eq (7) becomes

$$E=0.9464\left[\frac{l^2 f}{t}\right]^2 \rho T. \tag{7b}$$

Pickett gives algebraic equations relating T to k/l for $\mu=0$, $\frac{1}{6}$, and $\frac{1}{3}$. In addition he gives numerical solutions of these equations for particular values of k/l and graphs based on these solutions. The graphs for $\mu=\frac{1}{6}$ and $\frac{1}{3}$, the two values which span the range of interest for steel, are reproduced in figure 2 from Pickett's numerical values. T approaches 1 as k/l approaches 0 for all values of μ.

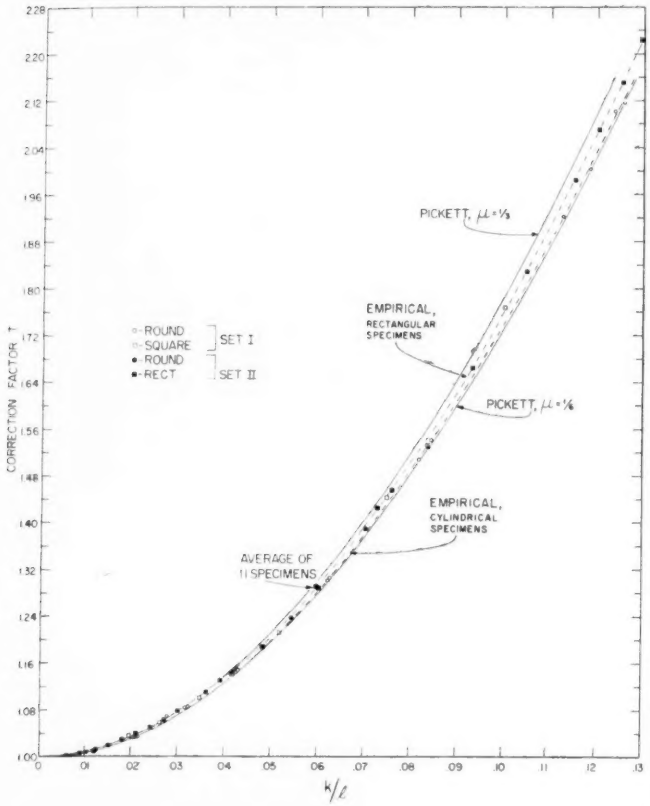

FIGURE 2. *Empirical and theoretical curves showing the effect of* k/l *on the correction factor,* T, *for flexural vibrations.*

k/l is the ratio of the radius of gyration of the cross sectional area about an axis perpendicular to the plane of vibration to the length of the specimen. Sets I and II represent two separate sets of steel bars.

According to eq 7b, for a given value of E, the flexural resonance frequencies of rectangular specimens are independent of the dimension perpendicular to the plane of vibration. Pickett shows in the appendix of his paper, which deals with the problem more rigorously, that in the extreme cases of an infinitely thin bar or an infinitely wide slab, this dimension (perpendicular to the plane of vibration) does slightly affect the flexural resonance frequency. However, for the specimens used in this investigation, this correction would be insignificant.

This means that if the specimens of set II are really uniform with respect to E as well as ρ, then the edgewise flexural resonance frequency of specimens II–2 through II–12 should all be equal, since the only variable for these specimens is the dimension perpendicular to the plane of vibration. The degree of agreement in this frequency is a critical indication of the intrinsic uniformity of the specimens. The variation in frequency is insignificantly small, as shown in table 3. Therefore, the specimens must be uniform with respect to E as well as ρ. The importance of this result can hardly be overemphasized, since the uniformity of the specimens with respect to E and ρ is the foundation of the entire empirical approach.

For the specimens of set I no such conclusive check on the uniformity of E is possible, so that the uniformity of ρ must serve as indirect evidence of the uniformity of E. However, the evidence just presented for the specimens of set II makes it more likely that the same situation holds for the specimens of set I.

The empirical values of T are obtained by substituting the base value of E for each set of specimens, given in table 4, and the other appropriate parameters for each specimen, all of which are known from tables 1 and 2, in eq 7a or 7b.

It is interesting to compare the values of E which result from a determination based on eq 7a and 7b, using T obtained directly from Pickett, with the base values of E used above. For this purpose, only those specimens of each set are used which have the lowest values of k/l because for these, as was the case for longitudinal vibrations, it can be seen from the theoretical curves in figure 2 that an error in the choice of μ would cause only a negligible error in T. Values of E for these specimens of low k/l are given below:

Set I, average of specimens I–19, I–20, I–21, and I–22—2085 kilobars;
Set II, average of specimens II–4r_1 and II–4r_2—2113 kilobars;
Set II, average of specimens II–11 and II–12—2115 kilobars.

These values are seen to be in excellent agreement with those based on longitudinal vibrations and given in table 4. The values based on longitudinal vibrations are used in establishing the empirical values of T because the equations on which they are based are established by long usage.

The empirical values of T are given numerically in tables 1 and 2 and are plotted as a function of k/l in figure 2. The average value of T obtained from the edgewise flexural resonance frequency for specimens II–2 through II–12 of set II provide a single point which is designated in the figure. Figure 3 shows the same data in an expanded form.

The values for T from Pickett, for $\mu=0.29$ given in figure 3, were obtained by a quadratic interpolation from Pickett's equations for $\mu=0$, 1/6, and 1/3.[3]

[3] The actual equation used for this interpolation was:

$$T=1+79.02\,(1+0.0752\,\mu+0.8109\,\mu^2)\,(k/l)^2 - 125\left(\frac{k}{l}\right)^4 - \frac{1201\,(1+0.2093\,\mu+2.173\,\mu^2)\,(k/l)^4}{1+76.06\,(1+0.14081\,\mu+1.536\,\mu^2)\,(k/l)^2}.$$

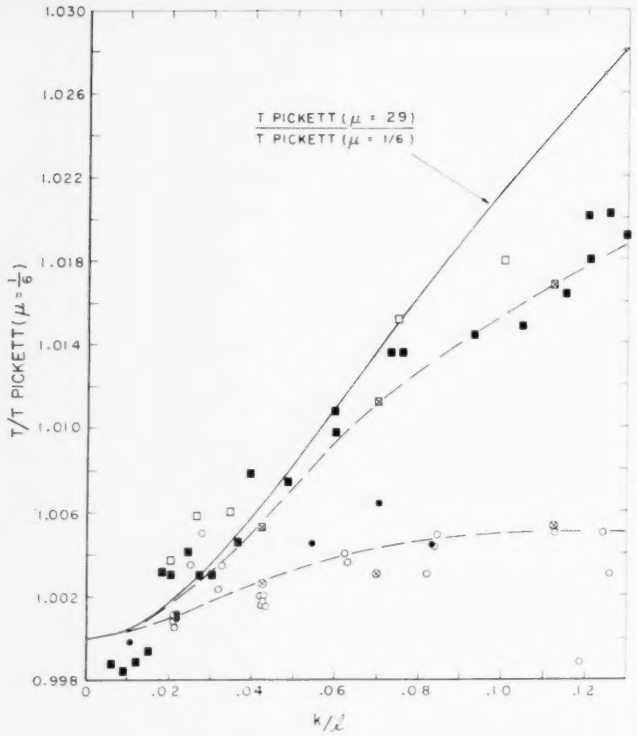

FIGURE 3. *Expanded method of showing data in figure 2 illustrating (a), separation of empirical correction factor for round and rectangular specimens, and (b), departure of all empirical points from theoretical (solid) curve for $\mu = 0.29$.*

Square symbols represent rectangular specimens; round symbols represent cylindrical specimens; hollow symbols, set I; solid symbols, set II; symbols with crosses, special group (footnote 4).

The computations involved in obtaining T for a given value of μ from this equation are obviously more cumbersome than from the corresponding one given in the ASTM Book of Standards, pt. 3, p. 1355, 1955 (C215–55T). However, the equation given in the ASTM is inadequate necessitating the use of the equation given here.

Inspection of figures 2 and 3 shows the empirical points to fall on two distinctly separate curves. The points determining these curves are not grouped on the basis of which set of specimens they are comprised but rather on the basis of whether the specimens are cylindrical or rectangular. All of the points forming the upper curve are derived from the rectangular specimens of sets I and II, while all of the points forming the lower curve are derived from the cylindrical specimens of both sets.

Inasmuch as the empirical curves are developed without any assumption for the value of μ, these data support the conclusion drawn previously from longitudinal vibrations; namely, that the specimens of both sets have the same value of μ.

However, the separation of the empirical points into two curves, one for cylindrical and one for rectangular specimens, is unexpected; for, according to Pickett, the value of T at any given k/l should depend only upon μ and not upon whether the bars are circular or rectangular in cross section.[4] Actually, Pickett recognizes that an assumption is involved in the equality of T for specimens of circular and square cross section.

Since the two empirical curves do diverge, especially at higher values of k/l, it is relevant to inquire which empirical curve is in better agreement with Pickett's theoretical relation. An estimate of the probable values of μ for the two curves may be made on the basis of their relative positions from Pickett's curves for $\mu = 1/3$ and $\mu = 1/6$. Such an estimate leads to a value of μ for the upper curve of around 0.26 to 0.30 while for the lower curve μ appears to be around 0.17 to 0.19. Inasmuch as the μ value so estimated for the upper curve is in agreement with the literature as well as earlier parts of this investigation, while the similar estimate for the lower curve leads to an absurdly low value of μ for steel, one concludes that the empirical curve for rectangular specimens is in better agreement with Pickett than the empirical curve for cylindrical specimens. It also appears that Pickett's curve for $\mu = 1/6$ would give reasonably good values of T for cylindrical specimens having an actual value of $\mu \approx 0.29$.

Inspection of figure 3 also shows that the empirical curve for rectangular specimens departs from the theoretical curve for $\mu = 1/6$ by an increasing amount as k/l increases. For the cylindrical specimens the curve appears to level off to a value slightly above Pickett's curve for $\mu = 1/6$.

4. Summary

1. Empirical relations have been developed from which Young's modulus may be determined from the longitudinal and flexural resonance frequencies. Two sets of steel bars were used as specimens. Both sets were composed of cylindrical and rectangular specimens. These empirical relations have been compared with corresponding theoretical ones. The accuracy of the empirical determinations are such that numerical comparisons with the theory to four significant figures are justified.

2. For longitudinal vibrations, the empirically determined curve for the cylindrical specimens, agrees with the corresponding theoretical one (based on Bancroft's numerical solution of the Pochhammer-Chree equations for this particular boundary condition) if a value of Poisson's ratio of 0.292 is assumed for both sets of specimens. This value is in agreement with that found in the literature for steel.

3. For flexural vibrations two separate empirical curves develop. One curve is formed by the rectangular specimens of both sets and a second curve is

[4] This unexpected result was further tested using an entirely different group of six specimens all cut from the same soft steel. Special care was taken to have the specimens homogeneous and isotropic. The six specimens were divided into three pairs, each pair having the same length and the same value of k. One specimen of each pair was circular and the other square in cross section.

If Pickett's assumption of the equality of the correction factor T for square and cylindrical bars of the same k/l is correct, then each of the above pairs should have the same flexural resonance frequency. However, the frequencies of each pair were found to differ from each other by an amount in agreement with the empirical results already obtained for sets I and II. Points representing these specimens are included in figure 3.

formed by the cylindrical specimens of both sets. The curve formed by the rectangular specimens is in fair agreement with the corresponding theoretical relation (based on Timoshenko, Goens, and Pickett) if a value of Poisson's ratio about 0.292 is again assumed. However, the empirical curve formed by the cylindrical specimens would agree with the theoretical one only if a Poisson's ratio of about ⅛ is assumed for them. Since this value is obviously too low for steel, based on the literature and the present study, it is concluded that the experimental results agree with the theory for rectangular specimens but that Pickett's equations give too high a value for the correction factor for cylindrical specimens.

The authors express their appreciation for the invaluable help of J. B. Wachtman, both for information of a general background nature and also for clarifying many particular problems which arose during the course of the investigation.

Washington, D.C. (Paper 64A2–37)

5. References

[1] S. Spinner and R. C. Valore, Jr., Comparison of theoretical and empirical relations between the shear modulus and torsional resonance frequencies for bars of rectangular cross section, J. Research NBS **60,** p. 459 (1958) RP2861.

[2] H. Kolsky, Stress waves in solids, Preface (Oxford at the Clarendon Press, Oxford, England, 1953).

[3] D. Bancroft, The velocity of longitudinal waves in cylindrical bars, Phys. Rev. **59,** p. 588 (1941).

[4] G. E. Hudson, Dispersion of elastic waves in solid circular cylinders, Phys. Rev. **63,** p. 46 (1943).

[5] R. M. Davies, Stress waves in solids, Surveys in Mechanics edited by G. K. Batchelor and R. M. Davies, pp. 64–137. (Cambridge University Press, 1956.)

[6] M. F. Markham, Measurement of elastic constants by the ultrasonic pulse method, Brit. J. Appl. Phys. Suppl. No. 6, pp. 556 to 563 (1957).

[7] J. M. Frankland and H. L. Whittemore, Tests of cellular sheet steel flooring, J. Research NBS **9,** 136 (1932) RP463.

[8] E. Goens, Uber die Bestimmung des Elastizitatsmoduls von Staben mit Hilde von Biegung Schwingungen, Ann. der Phys., B. Folge, Band 11, pp. 649 to 678 (1931).

[9] S. P. Timoshenko, On the transverse vibrations of bars of uniform cross section, Phil. Mag. Ser. 6, **43,** pp. 125 to 131 (Jan. 1922).

[10] G. Pickett, Equations for computing elastic constants from flexural and torsional resonant frequencies of vibration of prisms and cylinders, Proc. ASTM **45,** pp. 846 to 865 (1945).

JOURNAL OF RESEARCH of the National Bureau of Standards—A. Physics and Chemistry
Vol. 64A, No. 2, March–April 1960

Determination of Copolymer Composition by Combustion Analysis for Carbon and Hydrogen [1]

Lawrence A. Wood, Irving Madorsky,[2] and Rolf A. Paulson

(October 12, 1959)

A detailed description is given of the method of combustion analysis for carbon and hydrogen to determine the composition of a copolymer from its carbon-hydrogen ratio. The apparatus and procedures have been developed at the National Bureau of Standards over a period of years. The method has been applied chiefly to determine what fraction of a styrene-butadiene copolymer is derived from styrene. Minor ingredients are removed by extraction, with the exception of the bound mercaptan residue for which correction must be made. The amount of bound mercaptan residue is determined from measurements of the sulfur content of the copolymer by the Carius method. Measurements are made of the oxygen content and the ash content, although these do not enter into the calculations. The standard deviation of a measurement of carbon-hydrogen ratio is approximately 0.0010 and is independent of styrene content. This corresponds to a standard deviation of about 0.036-percent bound styrene for polymers of low styrene content and 0.018 percent for polymers of high styrene content. The accuracy of the method is demonstrated by the fact that observations of carbon-hydrogen ratio for four out of five samples of polybutadiene differed by less than one standard deviation from the theoretical value.

1. Introduction

Elemental analysis is probably the most fundamental and unambiguous method of determining the composition of many polymers. When the polymer is a copolymer of two components differing appreciably in carbon-hydrogen ratios, the analyses for carbon and hydrogen by combustion may be used to determine the relative amounts of the two components. It is perhaps the only method that is completely free from possible structural effects. The present work describes in detail the method of combustion analysis used at the National Bureau of Standards to determine the ratio of bound styrene to butadiene in different samples of styrene-butadiene synthetic rubber (SBR, formerly called GR–S). Little modification would be required to apply the method to other hydrocarbon copolymers. Further study of each system would be required to determine its applicability to copolymers containing elements that might cause interference with the determinations of carbon and hydrogen.

References to carbon-hydrogen determinations on polymers in other laboratories are relatively rare. Kemp and Peters [1][3] in 1943 at the Bell Telephone Laboratories, in conjunction with their work on unsaturation as determined by iodine chloride addition, published some results of carbon and hydrogen determinations on butadiene-styrene copolymers and used them to make calculations of the bound styrene. No details of their procedure of measurement have been published. With the exception of this publication and two others [2, 3] which give results as a very minor adjunct to other work, we are not familiar with any other carbon and hydrogen determinations on polymers. Consequently, it has seemed desirable to describe in detail the practices employed at the National Bureau of Standards in such determinations.

Carbon and hydrogen determinations have been made with high precision at NBS since about 1929. References to the earlier work are given in a paper by Wagman and Rossini [4]. The method was employed to give information regarding the composition of purified natural rubber by Smith, Saylor, and Wing [5, 6]. The present work was initiated in 1944 as a part of the government synthetic rubber program [7, 8]. Slight modifications and improvements in the method were made over the following years until about 1951. Since then the procedure has remained essentially unchanged.

The procedure is too time consuming and tedious to be applied to routine determinations on samples of only casual interest. It likewise calls for so much care in order to make the determinations with the requisite precision that it can not be recommended for general use. However, it is well adapted to use in measuring the copolymer composition of reference samples intended for standards in developing new procedures. For example, the standards may be used to determine the relationship between the composition and some other property that can be easily measured. In the present instance one of the chief

---

[1] This work was performed as part of a research project sponsored by the Federal Facilities Corp., Office of Synthetic Rubber, and its predecessors in connection with the Government Synthetic Rubber Program. This paper was presented before the Southeastern Regional Meeting of the American Chemical Society, Gainesville, Fla., December 12, 1958.

[2] Present address: U.S. Industrial Chemicals Co., Division of National Distillers & Chemical Corp., 1275 Section Road, Cincinnati 37, Ohio.

[3] Figures in brackets indicate the literature references at the end of this paper.

applications of the method was to measure the bound styrene content of samples to be used in determining the relationship of refractive index to the composition of SBR (GR–S) polymers [9 to 11]. Many of these samples were also used in studies of heats of combustion [12], specific heats, and other thermal properties [13 to 15] at NBS. The results of the analyses of these samples have already been reported in the published papers.

2. Methods of Calculation

2.1. Calculation for a Pure Copolymer

In a copolymer of two hydrocarbon monomers, one of composition C_jH_k and the other of composition C_pH_q, let the percentage of the weight arising from the first monomer be denoted by X, and the carbon-hydrogen ratio of the polymer be denoted by R. Analysis then requires the calculation of values of X from observed values of R. By expressing both of these quantities one can derive the following equation:

$$\frac{X}{100}=\left[\frac{jA_C}{jA_C+kA_H}-\frac{pA_C}{pA_C+qA_H}\right]^{-1}\left[\frac{qA_H}{pA_C+qA_H}-\frac{1}{R+1}\right] \quad (1)$$

where A_C and A_H, the atomic weights of carbon and hydrogen, are 12.011 and 1.0080, respectively [16].

If the equation is applied to a copolymer of styrene (C_8H_8) and butadiene (C_4H_6), one has $j=8$, $k=8$, $p=4$, and $q=6$. The equation then becomes

$$X=29.0831[11.1809-100/(R+1)]. \quad (2)$$

For the purpose of calculation of theoretical values, the constants in this equation are given to one more significant figure than would be justified by the probable uncertainty in the accepted atomic weights.

Table 1 shows the values given by this equation for butadiene, styrene, and several of their copolymers. Differentiation of the equation shows that each percent change in styrene content produces a change in carbon-hydrogen ratio ranging from about 0.0275 for polymers of low styrene content to about 0.057 for polymers of high styrene content. In the range of normal SBR, containing about 24-percent styrene, the value is about 0.032. The relation has been presented in graphical form by Kemp and Peters [1].

TABLE 1. *Theoretical carbon-hydrogen ratios*

Butadiene, C_4H_6		7.9438
Butadiene: %	Styrene: %	
80	20	8.5299
79	21	8.5613
78	22	8.5928
77	23	8.6245
76	24	8.6565
75	25	8.6887
Styrene, C_8H_8		11.9157

It is clear that the carbon-hydrogen ratio must be measured with considerable accuracy if an accuracy of a few hundredths of a percent in styrene content is to be obtained. However, there need be no concern for the uncertainty introduced into the calculations by uncertainty in the accepted values of the atomic weights of carbon and hydrogen, since it is of the order of magnitude of hundredths of a percent styrene.

2.2. Corrections for Minor Constituents

The discussion thus far has related to an ideal copolymer containing only material arising from the two hydrocarbon monomers. Actual copolymers, especially those made by emulsion polymerization, contain minor constituents. Some of the minor constituents are readily removable by extraction or by solution and precipitation of the polymer. Soap, fatty acid, and stabilizer should normally be removed in this manner so that corrections for their carbon-hydrogen ratios need not be made. The effort spent on such purification is well-justified in terms of increased accuracy. Table 2 shows the carbon-hydrogen ratios of some of these constituents. Special pains should be taken to free the polymer from those minor constituents with carbon-hydrogen ratios differing widely from that of the copolymer. Equal attention should be given to the removal of traces of liquids used in purification.

TABLE 2. *Theoretical carbon-hydrogen ratios*

Dodecyl mercaptan $C_{12}H_{25}SH$	5.4995
Phenyl-beta-naphthylamine $(C_6H_5)NH(C_{10}H_7)$	14.6654
Stearic acid $CH_3(CH_2)_{16}COOH$	5.9578
Sodium stearate $CH_3(CH_2)_{16}COONa$	6.1281
Benzene C_6H_6	11.9157
Methanol CH_3OH	2.9789

It should be pointed out that minor constituents containing neither carbon nor hydrogen can be tolerated, since their presence does not affect the carbon-hydrogen ratio. Of course, elements that can cause interference with the actual experimental measurements of carbon and hydrogen should be avoided. Likewise, the addition of oxygen to the polymer at room temperatures may be presumed to be without effect, since there is no evidence of evolution of carbon dioxide or water by the polymer during such oxidation. These facts are the fundamental reason why it is desirable to base calculations of this sort on the carbon-hydrogen ratio rather than the percent carbon or the percent hydrogen in the sample. As would be expected, experimental accuracy is found to be much better when this is done.

According to modern ideas of polymerization [17], the mercaptan used as modifier in the emulsion polymerization of SBR is split into a free radical and a hydrogen ion, one of which initiates and the other terminates a polymer chain. Consequently, the mercaptan is chemically bound in the polymer and cannot be removed by the methods employed to remove the other minor constituents. It has been

the practice at NBS to measure the amount of sulfur in the purified polymer and to calculate from it the amount of bound mercaptan. The presence of the sulfur is, of course, of no consequence, as shown by direct experiments mentioned later, but the carbon-hydrogen ratio of the mercaptan assumed to be bound in the polymer is even lower than that of polybutadiene, as may be noted in table 2. The carbon content and the hydrogen content of the portion of the sample consisting of bound mercaptan are subtracted from the directly-observed carbon and hydrogen contents in the calculation of the carbon-hydrogen ratio of the pure copolymer.

The modifier commonly used in butadiene-styrene emulsion polymerizations at 50° C is a mixture of mercaptans, with the major constituent *n*-dodecyl mercaptan. Next in importance in the mixture are tetradecyl and decyl mercaptans. It has been found sufficiently accurate for present purposes to make calculations as if the mixture consisted entirely of dodecyl mercaptan. For low temperature (i.e., 5° C) polymerizations the modifier most commonly used is Sulfole B–8. This is chiefly tertiary dodecyl mercaptan, which of course has the same elementary composition as the *n*-dodecyl mercaptan.

3. Apparatus and Procedure

3.1. Apparatus

The apparatus used for the combustion was developed from that used in the analysis of benzoic acid by Wagman and Rossini [4]. In the present work the polymer is burned in a stream of oxygen in a quartz combustion tube. That portion of the tube which is in the combustion furnace is packed with cupric oxide wire. The oxygen is first freed of combustible impurities, carbon dioxide, and water by passage through a combustion tube and a train of Ascarite, magnesium perchlorate, and phosphorus pentoxide before it comes into contact with the polymer.

Each sample is placed in a small Pyrex test tube capped with platinum gauze. This arrangement controls the rate of combustion much more satisfactorily than is possible with a platinum boat. This control is especially important when the styrene content of the copolymer is low.

The furnace is a common commercial type with fixed and movable electrical heating units.

The products of combustion are collected in absorption tubes of a design [18] differing from the U-type formerly employed. One of the tubes is packed with magnesium perchlorate and phosphorus pentoxide to absorb the water formed in the combustion. The other tube is packed with Ascarite to absorb carbon dioxide, and with magnesium perchlorate and phosphorus pentoxide to retain water liberated by the reaction of the carbon dioxide with the Ascarite. Weighings are made to hundredths of a milligram on a high-precision analytical balance.

3.2. Preparation of Polymer Sample

Purification of the sample of polymer is of the highest importance, as already mentioned. The purification procedure now employed was developed in the course of the present work. The later stages of the development and the application to the samples here described were carried out by Max Tryon. The polymer is first dissolved in benzene and the solution is added dropwise to well-stirred methyl alcohol to coagulate the polymer. The coagulated polymer is then redissolved in benzene. The solution and precipitation processes are carried out three times. This procedure serves to eliminate fatty acids and their salts, stabilizer, and some of the low-molecular-weight polymer. The solution of polymer in benzene is finally frozen by the use of solid carbon dioxide. The refrigerant is then removed and the benzene is sublimed from the system at a low pressure produced by a vacuum pump. This process yields a spongy mass of polymer, which is stored at a low temperature in a vacuum desiccator over magnesium perchlorate until it is cut up for individual analyses. Any possible oxidation during storage, should be at a minimum under these conditions.

3.3. Procedure

A sample is removed from the desiccator and cut into small pieces. Eight or more Pyrex test tubes (75-mm long, 12-mm in diam) are cleaned, dried, and weighed. All of the test tubes are filled at the same time with samples weighing between 0.5 and 2 g. The filled test tubes are dried in the vacuum desiccator for 2 hr to remove moisture picked up during the cutting and filling. They are then weighed. Samples are prepared at the same time for determination of sulfur and oxygen.

When a determination is begun the preheater and combustion coils are turned on and the flow of oxygen is adjusted to 250-ml per min. When the fixed unit of the furnace has reached its operating temperature of 800° C, a filled test tube is capped with a piece of platinum gauze, placed on a support of platinum gauze, and is inserted, capped end first, into the combustion tube until the capped end is 6 cm from the end of the fixed heating unit. The combustion tube is swept out with oxygen for 20 min and then the weighed absorption tubes are attached. The absorption tubes are flushed with hydrogen prior to each weighing in order to decrease the magnitude of the correction made for the increase in volume of the solid phase, with resulting decrease in the volume of the gas phase, during the run. Each tube is weighed against a counterpoise of a similar closed absorption tube filled with hydrogen. The movable heating unit is then turned on and pushed forward over the sample until it is 5 cm from the fixed unit. An asbestos pad is inserted between the units.

The temperature of the movable unit is raised rapidly to 300° C and then slowly to 400° C. If the latter temperature is approached too rapidly or if

it is exceeded, the polymer sample usually decomposes rapidly, flashes, and burns with violence. Rapid decomposition is indicated by oscillation of the mercury in the flowmeter. If the temperature of 400° C is approached too slowly, carbon forms in the test tube and can be oxidized only at a very slow rate. When conditions are satisfactory, combustion is complete in about 1½ hr. With proper control of temperature some samples are completely decomposed without ignition. Others flash lightly and afterward burn with a small flame at the mouth of the test tube. Under the best conditions no free carbon appears.

After the initial combustion the temperature is slowly increased to 600° C. This is sufficiently high for complete pyrolysis and not high enough to cause softening of the Pyrex test tube. Under normal conditions of slow combustion there is no need to cool the trap that condenses water. Five hours after the absorbers are attached the flow of oxygen is increased to 400 ml per min. Hot water is placed around the water trap and is removed. This operation is repeated several times until the condensed water has disappeared. One hour later the asbestos pad is removed and the movable heating unit is pushed against the fixed unit. The absorbers remain attached for 7 hr. They are then removed and flushed with hydrogen. After grease is dissolved from the spherical glass joints with ether, the absorber and counterpoise are placed in the balance case. They are weighed on the following morning.

The amounts of sulfur in the polymers studied were too low to affect significantly single determinations of carbon and hydrogen, as shown by check experiments utilizing mixtures of benzoic acid with a few tenths of a percent of sulfur. However, when a combusion tube had been used for a long period, it was found that traces of sulfuric acid might collect in the trap that condenses water. In this case, water was retained and the amount of hydrogen found in an analysis was lower than that in the polymer. When the presence of sulfuric acid was suspected, the combustion tube was cleaned and repacked.

3.4. Subsidiary Measurements

In the determination of sulfur, a 0.2-g sample of the purified polymer is decomposed by the Carius method [19, 20]. The sulfur is precipitated and weighed as barium sulfate by the conventional microtechnique. The Parr bomb method did not prove to be as reproducible as the Carius method. The results of the sulfur determination are used to calculate the bound mercaptan content of the copolymer, as discussed in an earlier section.

The amount of oxygen in the polymer is measured by the modified Unterzaucher method developed by Walton, McCulloch, and Smith [21]. The oxygen is converted to carbon monoxide, which is then measured by the use of the NBS colorimetric indicating gel. The ash is determined by simply weighing the sample after the combustion analysis for carbon and hydrogen. The results of the determinations of oxygen and ash are of use in estimating how well the polymer has been purified but do not enter directly into the calculations.

4. Results for Compounds of Known Composition

4.1. Benzoic Acid

In order to obtain information on the precision and accuracy of the method and to make comparisons with the work of other observers, a series of combustions of purified benzoic acid was made. The benzoic acid used was from a lot of NBS Standard Sample 39f.

Table 3 shows a comparison of values obtained by Wagman and Rossini [4] with those obtained in the first (Madorsky, 1944), and second (Cheek, 1948) stages of development of the present procedure.

It will be noted that the percentage of hydrogen found agrees with the theoretical value within the error of determination but that the percentage of carbon is significantly lower than the theoretical value in all cases. The cause of this discrepancy is not known.

TABLE 3. *Analysis of benzoic acid*

	Wagman and Rossini	Madorsky	Cheek
Carbon, %	68.8367	68.836	68.8357
Theoretical, %	68.8450	68.8450	68.8450
Difference, %	−0.0083	−0.009	−0.0093
Standard deviation, %	.0013	.0020	.00047
Hydrogen, %	4.95461	4.9542	4.9520
Theoretical, %	4.95230	4.95230	4.95230
Difference, %	+0.00231	+0.0019	−0.0003
Standard deviation, %	.0010	.0013	.00045
C/H ratio	13.8931	13.8945	13.9006
Theoretical	13.9016	13.9016	13.9016
Difference	−0.0085	−0.0071	−0.0010
Standard deviation		.0048	.0014

4.2. Polybutadiene

In order to obtain further information on the precision and accuracy of the method measurements were made on several samples of polybutadiene. These samples of known composition, of course, possessed a structure nearly the same as the copolymers in which the chief interest was centered. The samples were purified in the manner already described. The results of the analyses are given in table 4. The carbon and hydrogen results are the mean values of five determinations; the sulfur results are the mean of three. Some of these results were utilized in the thermodynamic studies already published [12, 13].

The totals in most cases are about 0.1 percent more than 100 percent. The reason for this is not apparent; it is possible that the mineral contaminants responsible for the ash contain some sulfur or oxygen

TABLE 4. *Analysis of polybutadiene*

	NE-1	GL-657	36	38	MS-1045
	%	%	%	%	%
Carbon	88.656	88.656	88.554	88.486	88.474
Hydrogen	11.1873	11.1795	11.171	11.166	11.1600
Sulfur	0.112	0.072	0.098	0.109	0.033
Oxygen	.145	.145	.16	.145	.12
Ash	.00	.097	.099	.100	.34
Total	100.1003	100.1495	100.082	100.006	100.177

(perhaps as SO_4 or CO_3) which has already been accounted for in the direct analysis for these elements. The oxygen content varies relatively little. The sulfur content depends on the amount of mercaptan used in polymerization and on other polymerization conditions. The ash content, likewise, depends on the conditions of polymerization and purification. It is notably higher for polymer MS–1045, which is the only one shown polymerized at 5° C, where the recipe would be expected to yield a much higher ash content. The sulfur and oxygen are slightly lower than in the others, so that the higher ash does not produce much increase in the total.

Table 5 shows a typical calculation of the correction of measured values of carbon and hydrogen to eliminate the effect of the bound mercaptan. The sample NE–1 polybutadiene—as noted in table 4—was found to contain 0.112 percent sulfur corresponding to 0.707 percent bound mercaptan. This in turn was responsible for 0.503 percent carbon and 0.0915 percent hydrogen. These are subtracted from the observed values, and the carbon-hydrogen ratio of the pure polymer is calculated. The mean value of this ratio R' and those for four other polybutadienes, are given in table 6. The comparison of values shows excellent agreement with the value calculated from the composition—the mean value of all differing by only one in the fifth significant figure. The individual differences from the theoretical value are shown in the last column for comparison with the standard deviations, as calculated from the separate determinations of R' for each sample. In all but one case the error is less than one standard deviation. From statistical theory this situation should occur two-thirds of the time if there are no systematic errors. We conclude that systematic errors are not significant here.

TABLE 5. *Typical calculation of corrected carbon-hydrogen ratio*

(NE-1 polybutadiene)

Determination	C	C′= (C−0.503)	H	H′= (H−0.0915)	R′= C′/H′
	%	%	%	%	
1	88.665	88.162	11.1845	11.0930	7.9475
2	88.663	88.160	11.1919	11.1004	7.9421
3	88.668	88.165	11.1913	11.0998	7.9429
4	88.701	88.198	11.1931	11.1016	7.9446
5	88.583	88.080	11.1758	11.0843	7.9464
Mean					7.9447

TABLE 6. *Precision and accuracy of corrected carbon-hydrogen ratios (polybutadienes)*

	R'	Standard deviation	Difference from theoretical
Theoretical	7.9438		
NE-1	7.9447	0.0010	+0.0009
GL-657	7.9432	.0009	−.0006
Sample 36	7.9446	.0014	+.0008
Sample 38	7.9442	.0013	+.0004
MS-1045 (5° polymer)	7.9426	.0010	−.0012
Mean	7.9439	.0011	.0008

Possible sources of systematic error, if found, would be incomplete extraction of minor constituents (other than bound mercaptan), the presence of residual solvent or precipitant following incomplete drying, and variations in the carbon and hydrogen contents of the bound mercaptan from those calculated for dodecyl mercaptan.

Both the errors and the standard deviations in four out of five cases are smaller than those previously given in table 3 for benzoic acid. This is probably the result of small improvements in technique since 1948. We conclude that the accuracy and precision of the carbon-hydrogen determination are in no way impaired by the use of a well-purified polymer instead of a compound of low molecular weight.

The generally satisfactory nature of the values shown in table 6 for polybutadiene, where the composition is known, gives us confidence in the accuracy of similar values determined for copolymers of butadience with styrene and other monomers, where there are no other satisfactory methods of determining the composition with equal precision.

5. Precision of Values for Copolymers

Table 7 shows values of the standard deviation of the carbon-hydrogen ratio R' found for a number of styrene-butadiene copolymers differing in styrene content. The elemental analyses for most of these polymers are given in papers on thermodynamic studies [12, 14, 15]. The values of standard deviation are essentially the same as those shown in table 6 for

TABLE 7. *Precision of values for butadiene-styrene copolymers*

Designation	Styrene content	Standard deviation of R'
	%	
50° copolymers		
GL-658	8.58	0.0009
MS-1726	8.69	.0006
MS-1232	10.71	.0007
MS-1728	11.4	.0016
48-B	55.73	.0006
NE-6	83.67	.0012
5° copolymers		
X-454	8.58	.0010
X-478	22.61	.0011
GL-660	36.26	.0014
GL-661	53.09	.0010
Mean value		.0010

polybutadiene. No correlation with styrene content or temperature of polymerization is apparent. From the mean value (0.0010) of the standard deviation of R' one may calculate the standard deviation of X, the bound styrene content, using the values of the derivative of eq (2) given in an earlier section. One obtains a standard deviation of 0.036 percent bound styrene for polymers of low styrene content or 0.018 percent for polymers of high styrene content. In the range of normal GR–S, containing about 24 percent styrene the value is 0.031.

6. Concluding Remarks

The procedure described attains its accuracy and precision by the refinement and improvement of conventional simple operations over a period of years. The trend in analysis recently is, of course, toward the use of rapid physical methods. In a great many instances these involve relative measurements requiring the initial establishment of reference materials with compositions determined by methods such as the one here described, which bases the numbers derived solely on readings of an analytical balance. In fact, as already mentioned, one of the principal applications of the present method has been in the establishment of the relation between refractive index and styrene content for SBR polymers so that refractive index measurements can be used in routine determinations of bound styrene content.

Contributions to the development of the method here described were made by a number of individuals whose assistance is gratefully acknowledged. Special mention should be made of the late W. H. Smith, who maintained a continuing interest in the problem for many years, and Max Tryon, who purified most of the samples. Others included F. D. Rossini, D. D. Wagman, W. W. Walton, F. W. McCulloch, and Conrad H. Cheek.

7. References

[1] A. R. Kemp and H. Peters, Unsaturation of butadiene and related polymers as determined by iodine chloride addition, Ind. Eng. Chem., Anal. Ed. **15,** 453 (1943); Rubber Chem. and Technol. **17,** 61 (1944).

[2] A. R. Kemp and W. G. Straitiff, Structural features of Buna-S. Relation to physical properties, Ind. Eng. Chem. **36,** 707 (1944); Rubber Chem. and Technol. **18,** 41 (1945).

[3] R. C. Crippen and C. F. Bonilla, Determination of styrene in hydrocarbon copolymers, Anal. Chem. **21,** 927 (1949).

[4] D. D. Wagman and F. D. Rossini, Note on the macroanalysis of carbon and hydrogen by combustion, J. Research NBS **32,** 95 (1944) RP1577.

[5] W. H. Smith, C. P. Saylor, and H. J. Wing, The preparation and crystallization of pure ether-soluble rubber hydrocarbon, BS J. Research **10,** 479 (1933) RP544.

[6] H. J. Wing, Carbon and hydrogen in rubber hydrocarbon, Science **105,** 363 (1947); Rubber Chem. and Technol. **20,** 982 (1947).

[7] I. Madorsky, D. D. Wagman, and F. R. Rossini, Private communication to Office of Rubber Reserve (unpublished rept. (CR–319), Apr. 15, 1944).

[8] I. Madorsky, Private communications to Office of Rubber Reserve (unpublished reports, Aug. 24, 1944 and Feb. 7, 1945).

[9] I. Madorsky and L. A. Wood, Private communications to Office of Rubber Reserve (unpublished reports Sept. 13, 1944 (CR–442), Nov. 30, 1944 (CR–495), and Jan. 1, 1945).

[10] A. Arnold, I. Madorsky, and L. A. Wood, Measurement of refractive index of elastomers, Anal. Chem. **23,** 1656 (1951); Rubber Chem. and Technol. **25,** 693 (1952).

[11] L. A. Wood, Physical chemistry of synthetic rubbers, ch. 10, p. 323, Synthetic Rubber, ed. by G. S. Whitby (John Wiley & Sons, Inc., New York, N.Y., 1954).

[12] R. A. Nelson, R. S. Jessup, and D. E. Roberts, Heats of copolymerization of butadiene and styrene from measurements of heats of combustion, J. Research NBS **48,** 275 (1952) RP2312.

[13] G. T. Furukawa and R. E. McCoskey, Calorimetric properties of 41° and 122° F polybutadienes, J. Research NBS **51,** 321 (1953) RP2460.

[14] G. T. Furukawa, R. E. McCoskey, and G. J. King, Thermal properties of some butadiene-styrene copolymers, J. Research NBS **50,** 357 (1953) RP2425.

[15] G. T. Furukawa, R. E. McCoskey, and M. L. Reilly, Heat capacity of some butadiene-styrene copolymers from 0° to 333° K, J. Research NBS **55,** 127 (1955) RP2610.

[16] E. Wichers, Report on atomic weights for 1956–1957, J. Am. Chem. Soc. **80,** 4141 (1958).

[17] P. J. Flory, Principles of polymer chemistry, ch. IV, p. 106 (Cornell Univ. Press, Ithaca, N.Y., 1953).

[18] E. J. Prosen and F. D. Rossini, Heats of combustion of eight normal paraffin hydrocarbons in the liquid state, J. Research NBS **33,** 255 (1944) RP1607.

[19] C. L. Gordon, Modification of the Carius combustion tube to minimize losses by explosion: Pressures attained on heating nitric acid to 300° C, J. Research NBS **30,** 107 (1943) RP1521.

[20] C. L. Gordon, W. G. Schlecht, and E. Wichers, Use of sealed tubes for the preparation of acid solutions for analysis, or small-scale refining: Pressure of acids heated above 100° C, J. Research NBS **33,** 457 (1944) RP1622.

[21] W. W. Walton, F. W. McCulloch, and W. H. Smith, Determination of small amounts of oxygen in organic compounds, J. Research NBS **40,** 443 (1948) RP1889.

Washington, D.C. (Paper 64A2–38)

JOURNAL OF RESEARCH of the National Bureau of Standards—A. Physics and Chemistry
Vol. 64A, No. 2, March–April 1960

Some Effects of Aging on the Surface Area of Portland Cement Paste

C. M. Hunt, L. A. Tomes,[1] and R. L. Blaine

(December 18, 1959)

A hardened cement paste cured at room temperature, from which part of the evaporable water has been removed by vacuum drying, has been studied. The surface area has been shown to decrease with time depending upon the amount of evaporable water left in the paste. This change is the opposite of that usually observed during hydration and probably represents some collodial growth phenomena analogous to aging observed in other collodial gels. Both water vapor and nitrogen adsorption measurements have been used to show the effects of aging in cement paste.

Wet or dry paste is shown to undergo less change than paste of intermediate evaporable water content, so that if surface area after storage is plotted as a function of evaporable water content, a curve with a minimum is obtained. With increasing storage temperature there is some indication that this minimum might shift towards lower water content.

Aging is shown to occur during the initial drying of a cement paste, so that even the initial surface area of a cement paste depends upon the manner in which the paste has been dried.

1. Introduction

Aging phenomena have been observed in many colloidal solids. Colloidal systems are unstable and with time there are usually chemical and physical changes transforming the system towards a more stable state. The gel produced by the hydration of portland cement is also subject to such processes, and this fact is undoubtedly of some importance in such properties of concrete as creep, drying shrinkage, and the development or loss of strength. However, comparatively little attention has been given to aging phenomena per se.

One of the changes usually associated with aging is a decrease in surface area [1, 2, 3, 4].[2] It is difficult to demonstrate such a decrease in cement paste, because as long as hydration continues, new gel particles are formed and surface area increases [5, 6]. However, if part of the water is removed, the hydration process is disturbed, and it is possible to observe other effects. The interruption of hydration can occur in very old specimens by self-desiccation [7, 8], or it may be brought about in younger specimens by drying. The present paper considers changes in surface area of a hardened cement paste from which enough water has been removed to stop, or at least seriously curtail hydration. Such changes are considered important, partly because they affect the reproducibility of the measurements, but they are perhaps even more important in the interpretation of vapor sorption and surface area measurements.

[1] Research Associate representing the Calcium Chloride Institute at the National Bureau of Standards.

[2] Figures in brackets indicate the literature references at the end of this paper.

2. Methods and Materials

2.1. Preparation of Cement Pastes

Pastes were prepared from cement, meeting the ASTM requirements for type I cement. Three different cements were used during the course of these experiments. Their composition is given in table 1.

To minimize contact with air during mixing, the pastes were mixed in a soil density balloon.[3] A water-cement ratio of 0.5 was used. Specimens were prepared in the form of cylinders 1/2-in. long and 1/2-in. in diam. The initial hydration of the paste, referred to here as curing, took place in the molds for the first 24 hr and thereafter in paraffin sealed quart jars. A high relative humidity was maintained by 20 to 30 ml of water in the bottom of each jar. Curing time was 1 month except where otherwise designated.

[3] Soil density balloons are supplied by the Rainhart Co., Austin, Texas. The type used in this work had a total volume of about 160 ml. The wall thickness was 0.4 to 0.5 mm, sufficiently strong to withstand the impacts of mixing.

TABLE 1. *Chemical composition of cements*

[Percentage by weight]

	Cement		
	1	3	5[a]
CaO	64.0	64.1	62.8
SiO_2	22.0	22.3	22.4
Al_2O_3	5.2	5.0	5.5
Fe_2O_3	4.6	3.0	2.8
MgO	1.6	1.9	4.2
SO_3	1.5	2.0	1.9
Ignition loss		1.0	0.4
Insoluble residue	0.1	0.3	

[a] Analysis performed on ignited paste.

2.2. Storage of Pastes

The cured pastes were crushed, divided into a number of portions, and vacuum dried in the apparatus used in the determination of nonevaporable water. The drying period of the different portions ranged from as short as 1 hr to as long as 1 week. They were dried for different periods of time in order to obtain specimens differing in evaporable water content. The partially dried pastes were stored in sealed glass tubes. Dunmore gage elements were present in some of the tubes to permit measurement of relative humidity during storage. Storage times of 1 month, 3 months, and 21 months were investigated. Specimens were stored at 21° C except in one experiment in which they were stored 1 month at 37.8° C (100° F) and 105° C.

2.3. Determination of Evaporable and Nonevaporable Water

The room temperature vacuum drying procedure used in the determination of evaporable and nonevaporable water was similar to that of Copeland and Hayes [9]. However, since the stored specimens received partial drying prior to storage, they were subsequently dried during this procedure so that each specimen ultimately received a total of 2 weeks of drying, including drying prior to storage. Poststorage drying times were as short as 1 week or as long as 2 weeks, depending on the prestorage drying treatment of the particular sample of paste. Evaporable water was the loss of weight during vacuum drying after storage. Nonevaporable water, w_n, was the subsequent loss of weight during ignition to constant weight at 1,050° C after correction for carbon dioxide in the specimen.

2.4. Measurement of Water Vapor and Nitrogen Adsorption

Water vapor adsorption measurements were made after the removal of evaporable water from the paste. The measurements were made in an apparatus which has been previously described [10] and which uses a stream of nitrogen at atmospheric pressure to transport the water vapor. Values of v_m were calculated by the BET equation [11], where p is the pressure of water vapor in equilibrium with the specimen, p_0 is the vapor pressure of pure water, C is a constant related to the

$$\frac{p}{v(p_0-p)}=\frac{1}{v_mC}+\frac{(C-1)p}{v_mC\ p_0} \qquad (1)$$

heat of adsorption, v is the amount of water adsorbed per gram of adsorbent, v_m is the amount of water required for monolayer coverage of the adsorbent.

Nitrogen adsorption measurements were made with an apparatus similar to that described by Emmett [12]. The vacuum dried specimens were further outgassed overnight at 100° C before measuring their nitrogen adsorption. BET surface areas were calculated, assuming each nitrogen molecule to cover an area of 16.2 A^2.

3. Results

3.1. Changes in Paste Stored at Room Temperature

The surface area of a hydrated cement paste was measured before and after storage, and large decreases were observed. This is illustrated in figure 1 where nitrogen areas of specimens which contained different amounts of evaporable water during storage are plotted as a function of storage time. The rate and amount of decrease in surface was profoundly affected by the evaporable water content of the paste. The specimens containing 10 to 20 percent evaporable water changed rapidly during the first month and more slowly thereafter. Specimens containing approximately 1 percent evaporable water changed very slowly throughout the 21 months of storage.

Since free water plays such an important role in the aging of hardened cement paste, it is necessary to consider its effect more fully. In figure 2a nitrogen surface areas of dried pastes are plotted as a function of the evaporable water content, as determined at the end of storage. The horizontal line, A, represents the average surface of unstored paste after 2 weeks of uninterrupted drying. It is clear from the figure that there is an "optimum" evaporable water content during storage at which the greatest decrease in surface area occurs. The "optimum" in figure 2a appears at about 10 percent evaporable water. This roughly corresponds to the amount of water required to fill the gel pores, of this particular paste as estimated by the method of Copeland and Hayes [13].

In figure 2b the same surface areas have been plotted as a function of the relative humidity in the storage tubes. The maximum decrease took place at relative humidities between 40 and 60 percent. The relative humidity increased slightly with time except in tubes containing some of the driest specimens.

Water vapor adsorption also shows the effects of storage. In figure 2c, v_m/w_n ratios have been plotted as a function of evaporable water content. A constant v_m/w_n ratio implies that the same amount of gel always requires the same amount of evaporable water for monolayer coverage. Pastes prepared from the same cement usually have the same v_m/w_n ratio regardless of curing time or water-cement ratio [5]. However the results in figure 2c show that measurable decrease in v_m/w_n ratio has taken place during storage. The decrease is related to the amount of evaporable water in the specimen during storage as in the case of nitrogen adsorption.

In figure 2d nonevaporable water content is plotted as a function of evaporable water content.

The increase in nonevaporable water during storage is seen to be negligible except for possibly one paste which was stored 21 months and contained 16 percent evaporable water at the end of storage, indicating that the changes represented in figures 2a, 2b, and 2c are due to modification in the colloidal structure of the hydration products already present.

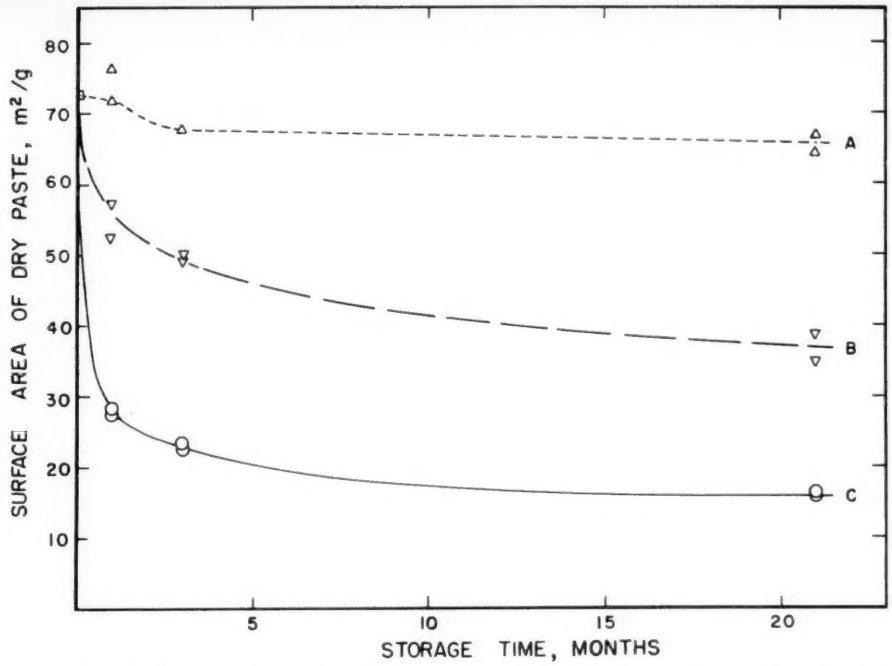

FIGURE 1. *Changes in nitrogen surface area of a hardened cement paste during storage at 21° C.*

A- - -Paste containing 1% evaporable water
B— —Paste containing 17 to 20% evaporable water
C_____Paste containing 10% evaporable water
Specimens prepared from cement No. 5.

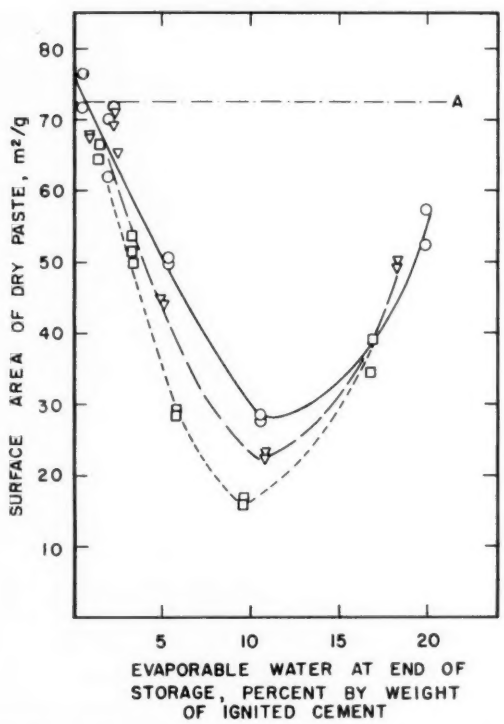

FIGURE 2a. *Changes in the nitrogen surface area of a hardened cement paste during storage as a function of evaporable water content.*

A–·–·–Original paste
○_____Paste after 1 month storage at 21° C
▽- - -Paste after 3 month storage at 21° C
□- - - -Paste after 21 month storage at 21° C
Specimens prepared from cement No. 5.

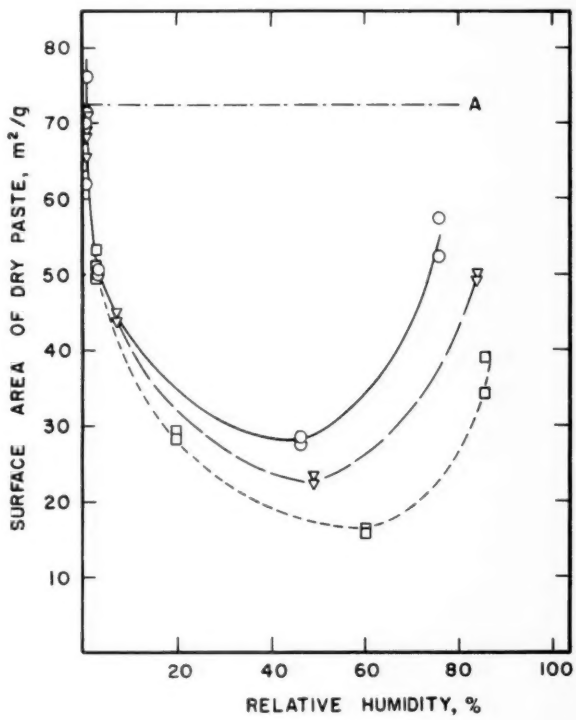

FIGURE 2b. *Changes in the nitrogen surface area of a hardened cement paste as a function of relative humidity.*

A- - -Original paste
○_____Paste after 1 month storage at 21° C
▽- - -Paste after 3 month storage at 21° C
□- - - -Paste after 21 month storage at 21° C
Specimens prepared from cement No. 5.

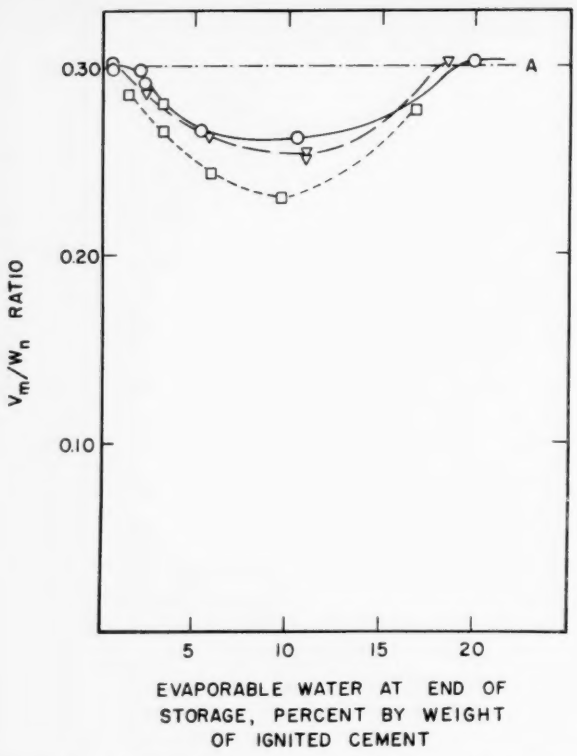

FIGURE 2c. *Changes in v_m/w_n ratio of a hardened cement paste during storage.*

A–.–.–Original paste
○——Paste after 1 month storage at 21° C
▽– – –Paste after 3 month storage at 21° C
□- - - -Paste after 21 month storage at 21° C
Specimens prepared from cement No. 5.

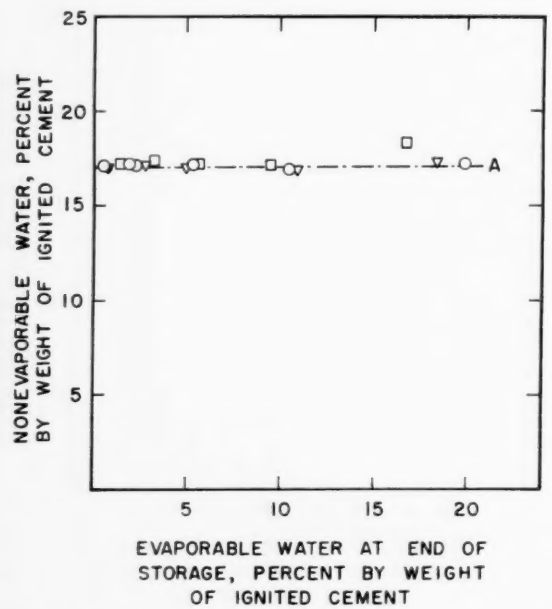

FIGURE 2d. *Changes in nonevaporable water content of a hardened cement paste during storage as a function of evaporable water content.*

A–.–.–Original paste
○ Paste after 1 month storage at 21° C
△ Paste after 3 month storage at 21° C
□ Paste after 21 month storage at 21° C
Specimens prepared from cement No. 5.

3.2. The Effect of Temperature on Storage Changes

Samples of paste containing different amounts of evaporable water were also stored 1 month at 37.8° C (100° F) and 105° C. The changes in nitrogen surface area and v_m/w_n ratio are shown in figure 3a and 3b, respectively. The corresponding curves at 21° C (from figs. 2a and 2c) are replotted in the figures for comparison. The results suggest that the minimum in the curve may be displaced to lower evaporable water contents as the temperature is raised. From figure 3a it may be seen that the decrease in nitrogen surface area during storage became less with increase in temperature for the more humid specimens, but for dryer specimens precisely the opposite behavior was observed. This statement also seems to apply to v_m/w_n ratios shown in figure 3b, when 21° and 37.8° C storage are compared, but at 105° C the decrease in v_m/w_n ratio during storage was greater for both the humid and dry specimens.

There was slightly more evidence of continued hydration during storage at the higher temperatures than at 21° C. At 105° C an increase in nonevaporable water content of 0.8 percent was observed in the most humid specimen during 1 month of storage, while nonevaporable water in the driest paste decreased 0.7 percent during this time. The corresponding changes in surface area and v_m/w_n ratio at 37.8° C were of the order of 0.2 to 0.3 percent.

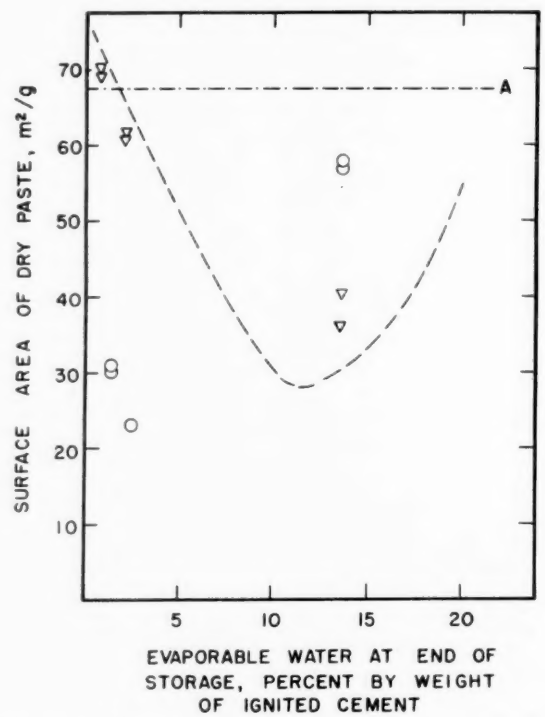

FIGURE 3a. *Changes in nitrogen surface area of a hardened cement paste stored at different temperatures.*

A– –.–Original paste
▽ Paste after 1 month storage at 37.8° C (100° F)
○ Paste after 1 month storage at 105° C
- - - - -Paste after 1 month storage at 21° C (retraced from fig. 2a)
Specimens prepared from cement No. 5.

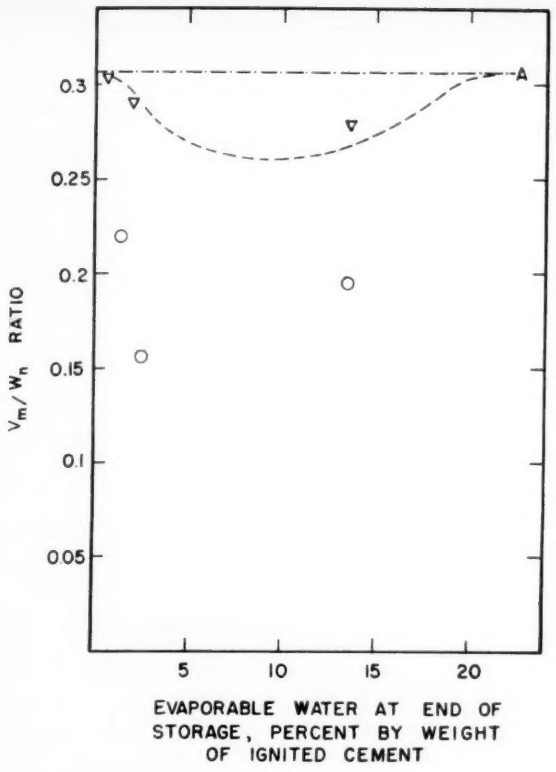

FIGURE 3b. *Changes in V_m/W_n ratio of a hardened cement paste stored at different temperatures*

A– – –Original paste
▽ Paste after 1 month storage at 37.8° C (100° F)
○ Paste after 1 month storage at 105° C
- - - - -Paste after 1 month storage at 21° C (retraced from fig. 2c)
Specimens prepared from cement No. 5.

The changes at higher temperatures were therefore accompanied by small changes in the total amount of hydration products present.

3.3. Storage Changes in Younger Pastes

Figure 4a shows the changes in nitrogen surface area which were found to occur in pastes which were cured for 1 day and 7 days respectively and stored for 3 months. Decreases, depending on evaporable water content, are shown for both groups of specimens. However considerable hydration took place during storage, especially in the 1-day specimens, as evidenced by the significant increases in nonevaporable water shown in figure 4b. It is difficult to separate the effects of continued hydration from changes in hydration products already present in younger pastes.

3.4. Effect of Drying Rate on Nitrogen Surface Area

The foregoing results showing time-dependent changes in cement pastes also have important implications with respect to the determination of surface area itself. Since, as is shown in figures 1 and 2a, most of the decrease in surface area took place

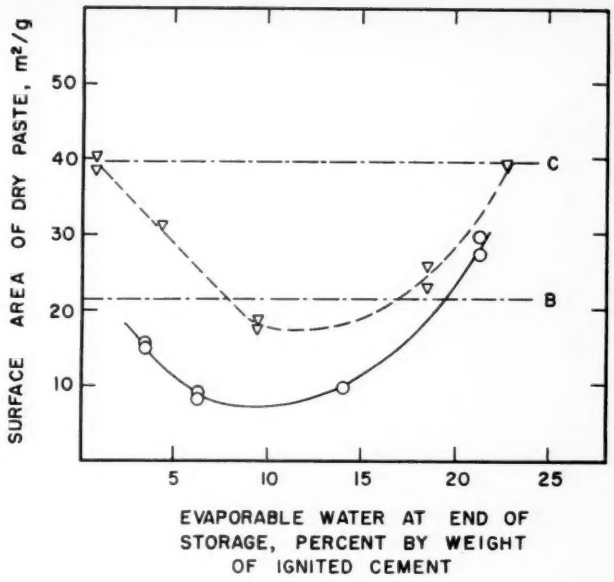

FIGURE 4a. *Changes in the nitrogen surface area of hardened cement pastes of different age as a function of evaporable water content.*

B–.–.–Original paste, cured 1 day
○——Paste cured 1 day, stored 3 months at 21° C
C–.–.–Original paste, cured 1 week
▽- - - -Paste cured 1 week, stored 3 months at 21° C
Specimens prepared from cement No. 1.

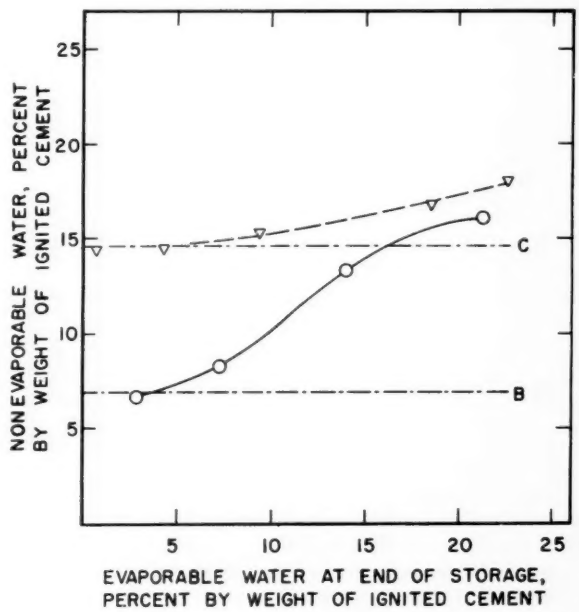

FIGURE 4b. *Changes in nonevaporable water content of hardened cement pastes of different age as a function of evaporable water content.*

B–.–.–Original paste, cured 1 day
○——Paste cured 1 day and stored 3 months at 21° C
C–.–.–Original paste, cured 1 week
▽- - - -Paste cured 1 week, stored 3 months at 21° C
Specimens prepared from cement No. 1.

during the first month of storage, it is reasonable to suppose that significant decrease must also have taken place during the first week. If this is true, aging must also take place during the initial drying, and the measured surface area of a cement paste should depend upon the rate at which the specimen is dried.

Figure 5 shows the surface areas of six specimens of 1-month cement paste which were vacuum dried at different rates for 7 days. Evaporable water content after the first 3 days drying has been selected as a measure of drying rate. A specimen containing more evaporable water after this arbitrary period of drying passed through the critical stages of drying suggested by figure 2a more slowly than a specimen containing less evaporable water. As may be seen in figure 5, it has been possible to produce a variation in surface area of nearly 30 m^2/g by merely restricting the rate of drying.

Five of the specimens represented in the figure were in the form of crushed paste while one was in the form of a ½-in. cylinder. A cylinder would dry more slowly due to restriction of diffusion by the paste itself. The largest surface area was obtained after a week of unrestricted vacuum drying of a crushed paste, a procedure similar to that of Copeland and Hayes [9]. This value is considerably greater than that obtained with the cylinder. However, when the rate of drying of crushed paste was restricted by sealing it in a closed tube with a tiny exit capillary, surface areas comparable with that of an uncrushed specimen could be obtained.

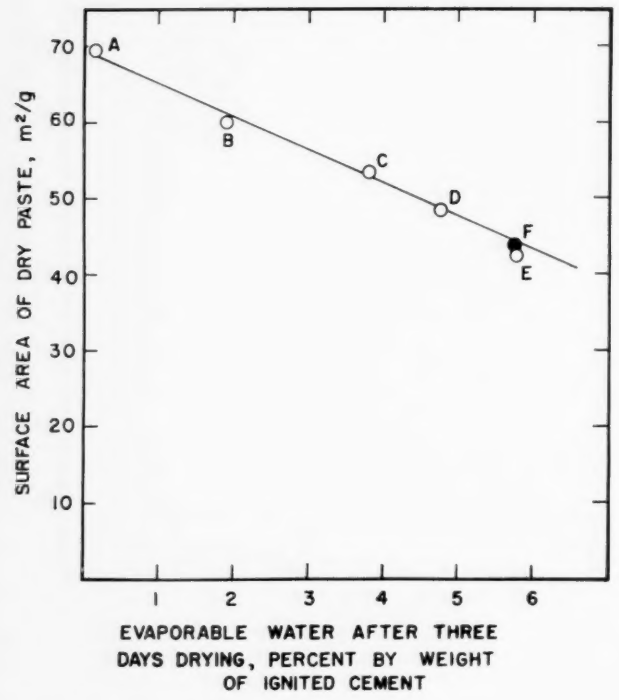

FIGURE 5. *Nitrogen surface area of a hardened cement paste after drying at different rates.*

A—Crushed paste subjected to 1 week of vacuum drying at unrestricted rate
B, C, D, E—Crushed paste subjected to 1 week vacuum drying with drying rate restricted by glass capillaries of different sizes.
F—½-in. cylinder of paste subjected to 1 week of vacuum drying at unrestricted rate.
Specimens prepared from cement No. 3.

4. Discussion

The colloidal structure of hardened cement paste cured at ordinary temperature can undergo changes leading to a decrease in surface area which in some respects resemble aging effects observed in other colloidal gels. In a mature paste (1 month or older) where the rate of hydration is small, it has been shown that decrease in surface area is not accompanied by appreciable change in nonevaporable water content and is therefore due to some time-dependent modification of the gel already present. The effects of aging are reflected in both nitrogen and water vapor adsorption measurements, but changes in nitrogen adsorption capacity are relatively greater.

Powers and Brownyard [14] sometimes observed that cement pastes which had been dried and then exposed to water vapor, first gained and then lost weight. Powers [15] has also noted decreases in water vapor surface area of pastes stored at relative humidities between dryness and complete saturation and suggested some connection between this decrease and the anomalous behavior of dried pastes in water vapor. It seems very probable that the tendency of dry pastes to gain and then lose weight in water vapor is another manifestation of aging.

The greatest amount of change occurs in pastes from which part of the evaporable water has been removed. This observation suggests the possibility of some relationship between creep in concrete and the colloidal changes detected by surface area measurements. It has been shown that partially dried concrete specimens undergo greater creep (inelastic deformation under load) than saturated [16, 17] or oven-dried [17] specimens. A further qualitative similarity between aging changes and creep is that both become slower with time. Colloidal growth phenomena may afford a partial answer to the question why creep does not continue indefinitely at the initial rate.

At high temperatures aging processes usually take place more rapidly. Digestion on a steam bath is a familiar procedure for treating precipitates before filtration. However with cement pastes stored at 105° C it is also necessary to remove most of the evaporable water to achieve minimum surface area. If aging is promoted by the increases in reaction rates, and diffusion rates which accompany rise in temperature, perhaps thermal expansion tends to offset these factors by making it more difficult for primary particles to join together and form larger particles. Removal of most of the evaporable water would be expected to reduce thermal expansion and facilitate coalescence of colloidal particles. Although this interpretation of the mechanism of aging and the effect of temperature is speculative, Meyers [18] has shown experimentally that the apparent thermal

expansion of hardened cement pastes exhibits a maximum depending upon the relative humidity at which the specimens were equilibrated before test, which in turn is a function of evaporable water content.

Not only do decreases in surface area take place during storage, but the surface area itself is dependent upon the rate of drying. This observation helps to explain the fact that larger surface areas are obtained when specimens are crushed before drying than if they are crushed after drying. Either procedure can be made reproducible, and once the specimens are dried nitrogen surface areas are quite repeatable. The effect is analogous to obtaining different surface areas when specimens of different size are dried. Such behavior is reminiscent of results obtained in drying-shrinkage experiments in which specimens of small cross-sectional area have been found to shrink more than specimens of large cross-sectional area [19, 20, 21]. However, before attempting to interpret drying shrinkage results in the light of the present experiments, it should be pointed out that the slowest drying specimens in figure 5 probably dried much faster than the fastest drying specimen in the usual drying-shrinkage experiment. Nevertheless the study of colloidal aging effects should also cast some valuable sidelights on the mechanism of drying shrinkage.

The authors are indebted to Vernon Dantzler and Alan Woolf for performing the nitrogen adsorption measurements described in this paper.

Washington, D.C. (Paper 64A2–39)

5. References

[1] H. B. Weiser, Inorganic colloid chemistry, **2,** 21 (Wiley and Sons, Inc., London, 1935).
[2] S. J. Gregg, Surface chemistry of solids, 66 (Reinhold Publishing Corp., New York, N.Y., 1951).
[3] I. M. Kolthoff, Analyst **77,** 1,000 (1952).
[4] M. R. Harris and K. S. W. Sing, J. Appl. Chem. **7,** 397 (1957).
[5] T. C. Powers and T. L. Brownyard, Proc. Am. Concrete Inst. **43,** 469 (1946); also Portland Cement Assoc. Bull. No. 22, pt. 3.
[6] R. L. Blaine and H. J. Valis, J. Research NBS **42,** 257 (1949) RP1967.
[7] T. C. Powers and T. L. Brownyard, Proc. Am. Concrete Inst. **43,** 986 (1947); also Portland Cement Assoc. Bull. No. 22, pt. 9.
[8] L. E. Copeland and R. H. Bragg, ASTM Bull. No. 204, 34 (1955); also Portland Cement Assoc. Bull. 52.
[9] L. W. Copeland and J. C. Hayes, ASTM Bull. No. 194, 70 (1953); also Portland Cement Assoc. Bull. No. 47.
[10] L. A. Tomes, C. M. Hunt, and R. L. Blaine, J. Research NBS **59,** 357 (1957) RP2806.
[11] S. Brunauer, P. H. Emmett, and E. Teller, J. Am. Chem. Soc. **60,** 309 (1938).
[12] P. H. Emmett, Symp. on new Methods for particle size determination in the subsieve range, Am. Soc. Testing Materials, 95 (March 1941).
[13] L. E. Copeland and J. C. Hayes, Proc. Am. Concrete Inst., **52,** 633 (1956); also Portland Cement Assoc. Bull. No. 68.
[14] T. C. Powers and T. L. Brownyard, Proc. Am. Concrete Inst., **43,** 274 (1946); also Portland Cement Assoc. Bull. No. 22, pt. 2.
[15] T. C. Powers (private communication).
[16] W. R. Lorman, Am. Soc. Testing Materials, Proc. **40,** 1090 (1940).
[17] R. E. Davis, H. E. Davis, and J. S. Hamilton, Am. Soc. Testing Materials, Proc. **34,** pt. 2, 354 (1934).
[18] S. L. Meyers, Proc. Thirtieth Annual Meeting of the Highway Research Board, 193 (1950).
[19] P. Schläpfers, discussion of, The physical structure of hydrated cements by S. Giertz-Hedström, Symp. Chem. Cements, Stockholm, Sweden, 534 (1938).
[20] A. D. Ross, Concrete and Constructional Engineering **39,** 193 (1944).
[21] R. E. Davis, Am. Soc. Testing Materials, Proc. **30,** 681 (1930).

JOURNAL OF RESEARCH of the National Bureau of Standards—A. Physics and Chemistry
Vol. 64A, No. 2, March–April 1960

Conformations of the Pyranoid Sugars. I. Classification of Conformers

Horace S. Isbell and R. Stuart Tipson

(August 11, 1959)

An improved system is presented for indicating the principal conformations of pyranoid sugars and derivatives, by attaching two symbols to the systematic name. The *first* symbol shows the kind of pyranoid ring; for example, B = a boat, C = the chair, and S = a skew form. (The three boat and six skew rings are distinguished by subscript numerals referring to exoplanar ring-atoms.) The *second* symbol differentiates between two conformations that have the same type of ring, by describing as A or E the axial or equatorial character of the reference group at a selected ring-atom. If the anomeric group is not quasi, the α anomeric group is used as the reference group. For sugars and derivatives having a quasi anomeric group, and for relatives lacking an anomeric group, the A or E classification is based on the reference group at the lowest numbered, nonquasi, asymmetric ring-atom.

1. Introduction

Conformation, or molecular shape, is one of the most important properties of the sugars and related compounds. Consideration of the shape of a molecule and of how the various atoms and groups in it are oriented with respect to one another leads to a better understanding and interpretation of the reactions of the compound.

The term "*conformation*" was introduced into organic chemistry by Haworth [1][1], to describe the various shapes that certain molecules may assume. Conformations have been defined by Klyne [2] as "the different arrangements in space of the atoms in a single classical organic structure (configuration), the arrangement being produced by the rotation or twisting (but not breaking) of bonds."

In contrast, the *configuration* of a compound is its unique spatial arrangement of the atoms in the compound, such that no other arrangement of these atoms is superimposable thereon to give complete correspondence, regardless of the conformation. Consequently, two compounds having *different* configurations may exist in the same general conformation; and the same compound (one configuration) may exist in different conformations.

If four atoms of the pyranoid ring are coplanar and the other two ring-atoms are *para* to each other, the latter atoms may lie on the same side (*cis*) or on opposite sides (*trans*) of the plane [3]. These two kinds of ring have been termed "boat" and "chair," respectively.

Atoms and groups are attached to ring atoms by bonds which may differ as regards their angle to the plane of the ring (or a parallel plane). Such bonds [4, 5] are designated axial (*a*) [6], equatorial (*e*), and quasi (*q*) [7]. An axial bond lies nearly perpendicular to the plane; an equatorial bond, nearly in the plane; and a quasi bond, at about 55° to the plane. Quasi bonds occur in pairs and are equally inclined to the plane of the ring; they are not present in the boat and chair forms.

The projecting bonds of the ring atoms at the ends of the boat forms are not truly axial or equatorial; they have been called [8] "flagpole" (*fp*) and "bowsprit" (*bs*), respectively. (The terms *endo* and *exo* describe them more precisely, but, for the classification presented here, they will be regarded as being axial and equatorial, respectively.)

Although the importance of pyranoid conformations has been recognized for many years, their nomenclature has been inadequate. For lack of unambiguous conventions, confusion has arisen in applying the symbols used.

Classification of conformations necessarily involves consideration of configuration.

2. Naming of Anomers

Formation of an anomeric ring-form from an open-chain sugar creates a new asymmetric center at the reducing carbon atom; the resulting isomers (anomers) are designated α and β. Anomers are named from the relationship of the configuration at the anomeric carbon atom to the configuration of a reference carbon atom of the chain of the acyclic monosaccharide. If the chain has less than five asymmetric carbon atoms, the reference atom is the highest-numbered, asymmetric carbon atom. If the acyclic chain has more than four asymmetric carbon atoms, the reference atom is the highest-numbered asymmetric carbon atom in the group of four asymmetric carbon atoms next to the functional group. The anomer having the *same* configurations at the anomeric carbon atom and the reference carbon atom is named α; the anomer having *opposite* configurations at the two atoms is named β. The α-L isomer is the mirror image of the α-D isomer, and the β-L isomer is the mirror image of the β-D isomer.

[1] Figures in brackets indicate the literature references at the end of this paper.

Enantiomorphic sugars are classified into two configurational series, respectively designated D and L, according to the configuration of the reference carbon atom. In the Fischer projection formula, the hydroxyl group on the anomeric carbon atom of the α anomers (D and L series) lies in the same direction as the hydroxyl group on their reference carbon atom, i.e., to the right in the D series and to the left in the L series.

Although the Fischer projection formulas indicate the configuration at each asymmetric carbon atom, they do *not* show the positions assumed by the atoms in space. Perspective pyranoid formulas, originated by Drew and Haworth [9], do, however, approximately depict the positions (in a planar conformation) of all the atoms in the molecule with respect to the plane of the ring. On closing the pyranoid [2] ring, carbon atom 5 of the open-chain sugar is rotated about its bond to carbon atom 4, so as to bring the ring-forming hydroxyl group into position for ring closure. With an *aldopentose*, turning carbon atom 5 in this manner merely causes a shift in the positions of the attached hydrogen atoms. With an *aldohexose*, so turning carbon atom 5 (to close the ring) causes the 5-*C*-(hydroxymethyl) group to assume a definite position with respect to the plane of the ring. When the ring is viewed in the manner shown, the 5-*C*-(hydroxymethyl) group of the D-hexopyranose lies above the plane of the ring and that of the L-hexopyranose lies below it. For the *aldohexopyranoses*, the α anomeric group is *trans* to the hydroxymethyl group, and the β anomeric group is *cis*. For the *aldopentopyranoses*, the α anomeric group is *cis* to the hydroxyl group at carbon atom 4 and the β anomeric group is *trans*.

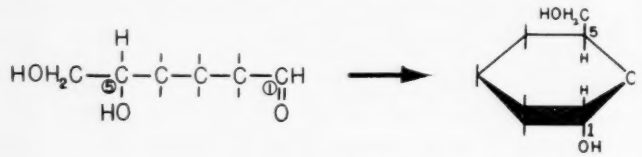

D-Aldohexose skeleton — α-D-Aldohexopyranose skeleton

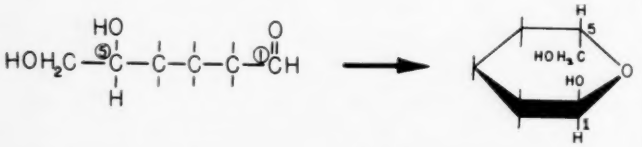

L-Aldohexose skeleton — α-L-Aldohexopyranose skeleton

3. Early Work on the Conformations of the Pyranoid Sugars

After it had been shown [10] that the stable methyl glycosides of many aldopentoses, ketohexoses, and aldohexoses have the pyranoid ring, Sponsler and Dore [3] applied the concept of the D-glucopyranose [11] unit in interpretation of the X-ray diagram of cellulose. They realized that the conformations described for cyclohexane derivatives by Sachse [12] and by Mohr [13], namely, the chair and boat forms, could be *extended to pyranoid sugars*. They found that the chair conformations of the D-glucopyranose units satisfactorily explained the spacings in the X-ray diagram of cellulose, whereas the boat conformations did not.

In 1929, Haworth [1] further developed this theme. He pointed out that each pyranoid sugar is capable of existence in several strainless ring-forms of the Sachse–Mohr types. He discussed possible conformations, mentioned the form in which all the ring atoms are coplanar, and depicted four ring skeletons for the aldohexopyranoses, as in I–IV. He noted that

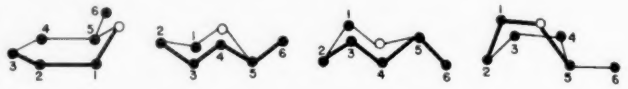

I II III IV

II and III "furnish two models for D-glucose and two for L-glucose," and that there are six boat forms for D-glucose (and six for L-glucose), "making a total of sixteen possible arrangements for D- and L-glucose."

At the time of the monumental work of Haworth and coworkers, the size, as well as the shape, of the ring in *the free sugars* was uncertain [14, 15]. In order to ascertain whether the pyranoid structures assigned (by methylation procedures) to "normal" methyl glycosides apply to the corresponding free sugars, a study of the mutarotation and oxidation reactions of aldoses was made by Isbell and coworkers [16, 17, 18]. The work had its origin in the observation of Isbell and Hudson [16] that aldoses can be oxidized by bromine to lactones *without clearage and re-forming of the ring*. It was found that the free sugars, with few exceptions, give 1,5-lactones and have the pyranose structure.

Although considerable variation in the reactivity of the individual sugars with bromine was noted, the most striking difference was observed for the reactivity of the α and β anomers of the same sugar [19]. It was reasoned that the difference in reactivity arises from an important structural difference in the two, and that, if the pyranoid sugars have strainless ring-structures, such as Haworth had suggested earlier, the α and β hydroxyl groups must be inclined at different angles to the ring and therefore react at different rates. The authors pointed out that, if the sugars are divided into two groups, α and β, according to the position of the anomeric hydroxyl group with respect to the oxygen ring-atom, there is marked similarity in the rates of oxidation of the α sugars on the one hand, and of the β on the other [20, 21, 22]. This was the first recognition of the effect of conformation on reaction rates and the first attempt to classify sugar derivatives according to what are now known as axial and equatorial groups.

On the basis of similarity in properties, Isbell and coworkers sought to classify the sugars of like configuration and conformation. The mutarotation reactions and the rates of oxidation with bromine showed satisfactory correlations for crystalline L-arabinose (now named β-L-arabinose) with α-D-galactose, for α-D-xylose with α-D-glucose, and for α- and β-D-lyxose with α- and β-D-mannose, respectively. Classification of crystalline D-ribose was found to be less clear, and this sugar was first classified with β-D-allose and later with α-L-talose. Comparisons of the optical rotations of the sugars and glycosides revealed discrepancies in Hudson's rotational difference (2A) that were ascribed to possible differences in conformation [21, 23].

[2] The terms "furanose" and "pyranose" were introduced by E. H. Goodyear and W. N. Haworth, J. Chem. Soc. **1927**, 3136.

When this study of the sugars was made, there was no known basis for predicting the stabilities of different conformations. The situation was changed by work on cyclohexane derivatives; this has been reviewed by Hassel [24], Orloff [25], and Mills [26]. The work of Hassel [4], Beckett and coworkers [5], and others led to recognition of certain factors that affect the stability of the various conformations of the cyclohexane ring. It was found that large groups attached to the *cyclohexane* ring tend to adopt ("prefer") equatorial positions, and that the chair form of the ring is generally the most stable species.

Hassel and Ottar [27] extended these ideas to the *pyranoid* ring in 1947, and Reeves developed the matter more fully in a series of papers beginning in 1949. He clarified the subject and provided a firm foundation for much subsequent work [28 to 34].

4. Nomenclature of Conformations

Reeves [28] depicted the two chair and six boat forms of the Sachse strainless-ring type (that had been discussed by Sponsler and Dore [3] and by Haworth [1]), and he assigned a symbol to each of these eight generalized, pyranoid rings as shown in figure 1. These rings consist of a chair ring, C1 (and its mirror image, 1C), and three boat rings (and their mirror images). The boat ring can be formed in three ways, according as the *cis* atoms displaced from the plane of the ring are carbon atoms **1** and 4, **2** and 5, or carbon atom **3** and the oxygen ring-atom; he designated these by the symbol B together with the numerals 1, 2, and 3, placed before or behind.

By his application of the symbols for the generalized structures (in fig. 1) to the D-glucopyranosides [28], with tabulation of bond angles, Reeves indicated that the symbols were to designate the rings of *the complete formulas containing the configurations*. In the same year, Reeves [29] showed the C1 and 1C forms of the D-hexopyranose ring with carbon atom 6 equatorial in the C1 and axial in the 1C form. He stated [29] that "the conformations involved are C1 in the D-galactopyranoside series, and, of course, the mirror image form 1C would apply to the L-galactopyranoside series." Thus, the C1 and 1C symbols were used not only for the two different chair forms of any one pyranoid sugar, but also for enantiomorphs (having the same equatorial and axial distribution of groups).

Use of *different* symbols, for the *same* molecular shapes in mirror image, is self-consistent in this system of symbols, but is difficult for many students (and even workers in this field) to comprehend. In view of this situation, Isbell suggested [35] that the symbols C1 and C2 be used for the two different chair conformations of the pyranoses, regardless of their being in the D or L series. The important feature of the revised definition was that the same symbol applied, for both the D and the L configuration of a sugar, to those conformations having *the same axial and equatorial arrangement of groups*. In

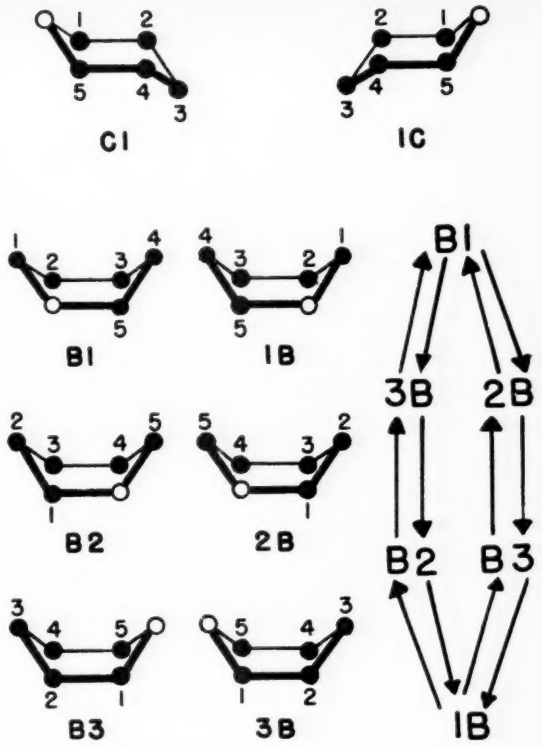

FIGURE 1. *Reeves' symbols [28] for the chair and boat forms of the pyranoid ring, and a diagram of possible pathways [34] for interconversion of boat forms.*

a later article, Isbell and coworkers [36] replaced the symbols C1 and C2 with C′1 and C′2 to avoid confusion with the C1 and 1C terms of Reeves. The authors pointed out that the axial and equatorial dispositions at each of the various ring-carbon atoms (in a strainless, pyranoid ring) have a fixed relationship to the conformation, and that the axial or equatorial disposition of the reference group attached to *any asymmetric carbon atom of the ring* could be used for description of a chair conformation. In the earlier classification, the C′1 and C′2 symbols were assigned to the chair forms according as *the reference group at carbon atom 5* was equatorial (C′1) or axial (C′2). As the aldopentopyranoses, ketohexopyranoses, and their deoxy derivatives lack a hydroxymethyl group at carbon atom 5, they could not be classified by this feature. They were, however, classified from a comparison of their physical properties with those of the structurally related aldohexopyranoses. This "classification" was empirical, and a change has seemed desirable.

Independently, Guthrie [37] and the present authors [38] have devised essentially the same solution to these problems in nomenclature. In our proposed nomenclature, the type of pyranoid ring is designated by C; B_1, B_2, B_3; and $S_{1,3}$, $S_{1,5}$, $S_{2,0}$, $S_{2,4}$, $S_{3,5}$, and $S_{4,0}$. The symbols for the chair and boat forms are analogous to those of Reeves, except that symbol C includes his C1 and 1C; symbol B_1 includes his B1 and 1B; symbol B_2 includes his B2

and 2B; and symbol B_3 includes his B3 and 3B. The symbols for the skew forms are new; the subscript numerals indicate the exoplanar ring-atoms.

The anomeric carbon atom is common to all pyranoid sugars. If the disposition of the anomeric group is not quasi, it can be used for distinguishing between the two conformations of one ring type. The symbol describing the type of ring is combined with a second symbol, A or E, to indicate whether the α anomeric group is axial or equatorial.[3] The two symbols are suffixed by a hyphen to the conventional name of the compound. For example, α-D-glucopyranose-CA indicates the chair conformation that has an axial anomeric hydroxyl group. The boat forms and those skew forms having a nonquasi anomeric group are named in like manner. The chair and boat conformations and the symbols proposed for them are given in figure 2.

All compounds classified earlier as C′1 or C′2 on the basis of the position of the reference group at carbon atom 5 are now classified as CA or CE, respectively. Compounds now designated as CA, CE, B_1A, B_1E, B_2A, B_2E, B_3A, and B_3E conformations have, in Reeves' classification, C1, 1C, 1B, B1, B2, 2B, B3, and 3B rings, respectively, when in the D series; but, when in the L series, they have 1C, C1, B1, 1B, 2B, B2, 3B, and B3 rings, respectively.

The present system defines conformations of specific structures unambiguously, but the symbols A and E do not, of themselves, represent axial or equatorial dispositions. Capital letters A and E are used in the symbols, instead of lower-case letters, because *a* and *e* show the axial and equatorial dispositions of reference groups. Occasionally, it is advantageous to cite the actual dispositions of all of the reference groups; these may be given in numerical sequence without numbers. Thus, α-D-galactose-CA (V) is α-D-galactose-C(*aeeae*) and α-L-galactose-CE is α-L-galactose-C(*eaaea*). Formulas VI, VII, and VIII depict $\beta(a)$-L-arabinopyranose-CE, α-L-galactopyranose-CA, and β-D-arabinopyranose-CE; they may also be referred to as β-L-arabinopyranose-C(*aeea*), α-L-galactopyranose-C(*aeeae*), and β-D-arabinopyranose-C(*aeea*).

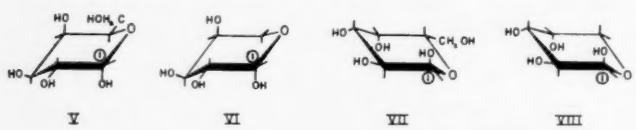

V VI VII VIII

In addition to the boat and chair rings already depicted (fig. 2), other rings, such as those shown in figure 3, are possible. In the *planar form* (IX), all of the ring-atoms are coplanar and all of the projecting bonds are quasi, although they have customarily been depicted as axial. In the *sofa forms* [39] (for example, X), all but *one* of the ring-atoms are coplanar; some of the projecting bonds of the sofa forms are quasi.

[3] For added clarity, the disposition of the anomeric group can be further designated by insertion of (*a*) or (*e*) after the anomeric prefix. Ordinarily, this is not necessary.

Pyranoid rings having *two* exoplanar atoms may be subdivided according as the relationship of these two atoms is *cis* or *trans*, and *ortho*, *meta*, or *para*. The *cis*- and *trans-para* forms (boats and chairs) have already been discussed. The *trans-ortho* forms (for example, XI) are the so-called *half-chair* forms [7]; the name was originally [40] applied to cyclohexene derivatives [7], but was extended [41] to pyranoid compounds. In these forms, four adjacent ring-atoms are coplanar. In the *trans-meta* ("stretched" [42] or "skewed" [34, 43]) forms, one ring-atom (of four coplanar ring-atoms) separates two ring-atoms that lie, respectively, above and below the plane, as in XII. In all the examples depicted in figure 3, some projecting bonds are quasi.

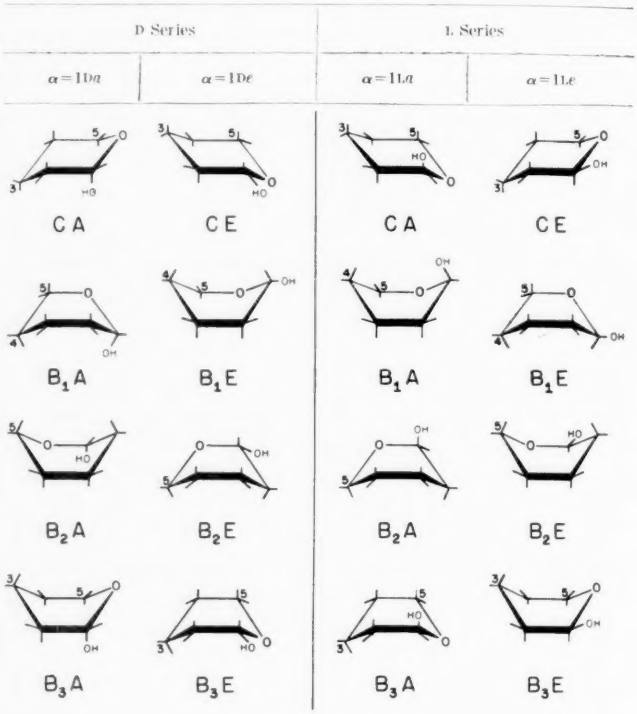

FIGURE 2. *The chair and boat conformations of pyranoid sugars of the* D *and* L *series.*

IX X XI XII

FIGURE 3. *Examples of other possible pyranoid rings.*

IX, Planar; X, sofa; XI, half-chair (*trans-ortho*); XII, skewed (*trans-meta*); dotted lines indicate coplanar atoms.

According to Reeves [34, 43], the boat forms of the pyranoid ring, like the boat forms of cyclohexane discussed by Hazebroek and Oosterhoff [42], are less rigid than the chair forms. They are flexible and can be interconverted, without angular strain, through an infinite number of intermediate shapes.

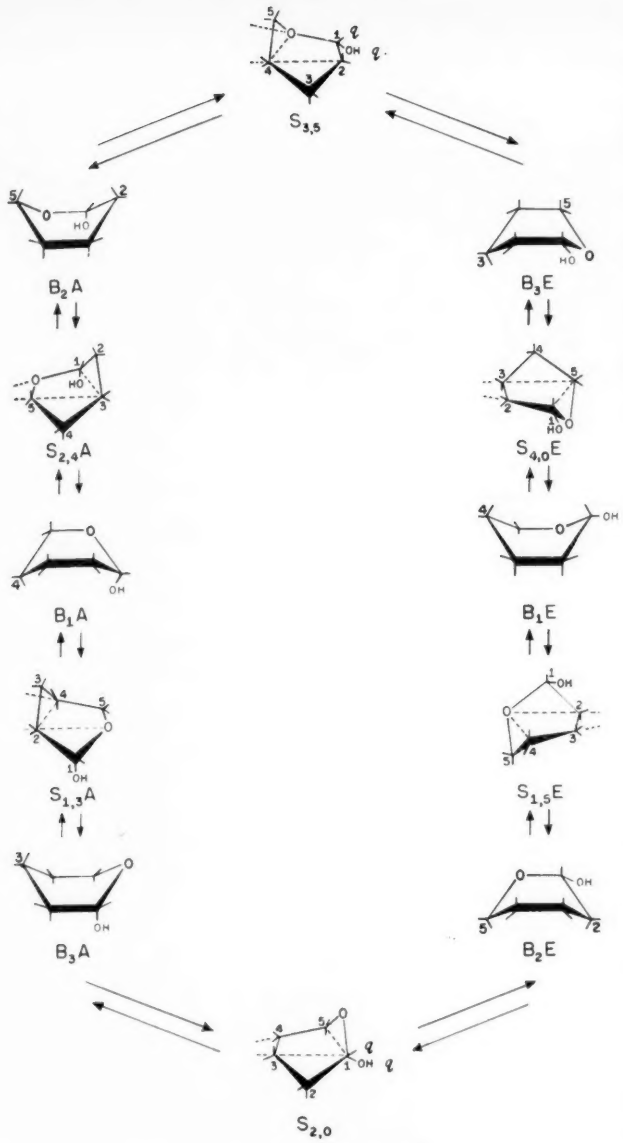

FIGURE 4. *Pathways for the interconversion of flexible forms of α-D sugars (in the boat-and-skew cycle proposed by Reeves [34]).*

B, Boat; q, quasi; S, skew; A, axial α anomeric group; E, equatorial α anomeric group.

A skew form is midway between two boat forms.[4] Figure 4 shows (with our formulas and symbols) the pathways proposed by Reeves for the interconversion of pyranoid boat- and skew-forms in a cycle. Each of the 12 forms shown has an enantiomorph (not depicted). It will be noted that the two skew forms having quasi bonds at carbon atom 1 ($S_{2,0}$ and $S_{3,5}$) are the turning points between the A and E conformations in the cycle. Although interconversion of the forms could take place without angular strain, other factors make the existence of a complete cycle improbable for many sugars and derivatives. Thus, energy barriers (arising from non-bonded interactions, hydrogen bonding, resonance effects, or solvation) would tend to restrict the molecule to a definite form.

For conformations in which the projecting bonds at the anomeric carbon atom are quasi, assignment to an A or E series may be made on the basis of the reference group at the lowest numbered asymmetric carbon atom having axial and equatorial attachments. For example, α-D-idopyranose having the $S_{2,0}$ conformation (XIII) would be called α-D-idopyranose-$S_{2,0}E_2$, where E_2 refers to the equatorial (hydroxyl) reference group at carbon atom 2.

The conformations of the 1,5-anhydroalditols, 1,5-lactones, and all other pyranoid compounds lacking an anomeric carbon atom may similarly be classified. For example,

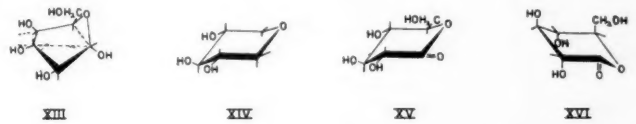

XIII XIV XV XVI

XIV is 1,5-anhydro-xylitol-CE_2; and XV and XVI are D-glucono-1,5-lactone-CE_2 and D-glucono-1,5-lactone-CA_2.

In this discussion, little attention has been devoted to conformations of specific compounds. The conformation assumed by a compound under a given set of conditions is its adopted ("preferred" or "favored") conformation. This subject will be considered in another article.

5. References

[1] W. N. Haworth, The constitution of sugars, p. 90 (Edward Arnold & Co., London, England, 1929).
[2] W. Klyne, Progr. in Stereochem. **1,** 36 (1954).
[3] O. L. Sponsler and W. H. Dore, Colloid Symposium Monograph **4,** 174 (1926).
[4] O. Hassel, Tidsskr. Kjemi Bergvesen Met. **3,** 32 (1943).
[5] C. W. Beckett, K. S. Pitzer, and R. Spitzer, J. Am. Chem. Soc. **69,** 2488 (1947).
[6] D. H. R. Barton, O. Hassel, K. S. Pitzer, and V. Prelog, Nature **172,** 1096 (1953); Science **119,** 49 (1954).
[7] D. H. R. Barton, R. C. Cookson, W. Klyne, and C. W. Shoppee, Chem. and Ind. (London) **1954,** 21.
[8] S. J. Angyal and J. A. Mills, Revs. Pure and Appl. Chem. (Australia) **2,** 185 (1952).
[9] H. D. K. Drew and W. N. Haworth, J. Chem. Soc. **1926,** 2303.
[10] E. L. Hirst and C. B. Purves, J. Chem. Soc. **123,** 1352 (1923); J. Pryde, J. Chem. Soc. **123,** 1808 (1923); W. N. Haworth, D. A. Ruell, and G. C. Westgarth, J. Chem. Soc. **125,** 2468 (1924); E. L. Hirst and G. J. Robertson, J. Chem. Soc. **127,** 358 (1925); S. Baker and W. N. Haworth, J. Chem. Soc. **127,** 365 (1925).
[11] W. Charlton, W. N. Haworth, and S. Peat, J. Chem. Soc. **1926,** 89; E. L. Hirst, J. Chem. Soc. **1926,** 350.
[12] H. Sachse, Ber. **23,** 1363 (1890); Z. physik. Chem. (Leipzig) **10,** 203 (1892).
[13] E. Mohr, J. prakt. Chem. [2] **98,** 315 (1918); **103,** 316 (1922).
[14] C. S. Hudson, J. Am. Chem. Soc. **48,** 1434 (1926); **52,** 1680 (1930).
[15] H. S. Isbell, BS J. Research **3,** 1041 (1929) RP128; **5,** 1179 (1930) RP253.
[16] H. S. Isbell and C. S. Hudson, BS J. Research **8,** 327 (1932) RP418.

[4] R. D. Guthrie (private communication) points out that there are actually two skew forms between any two boat forms. We have depicted six of the twelve skew forms.

[17] H. S. Isbell, BS J. Research **8,** 615 (1932) RP441.
[18] H. S. Isbell and W. W. Pigman, BS J. Research **10,** 337 (1933) RP534.
[19] H. S. Isbell, J. Am. Chem. Soc. **54,** 1692 (1932); J. Chem. Educ. **12,** 96 (1935).
[20] H. S. Isbell and W. W. Pigman, J. Org. Chem. **1,** 505 (1937); J. Research NBS **18,** 141 (1937) RP969.
[21] H. S. Isbell, J. Research NBS **18,** 505 (1937) RP990.
[22] H. S. Isbell, J. Research NBS **19,** 639 (1937) RP1052; **20,** 97 (1938) RP1069.
[23] H. S. Isbell and H. L. Frush, J. Research NBS **24,** 125 (1940) RP1274.
[24] O. Hassel, Quart. Revs. (London) **7,** 221 (1953).
[25] H. D. Orloff, Chem. Revs. **54,** 347 (1954).
[26] J. A. Mills, Advances in Carbohydrate Chem. **10,** 1 (1955).
[27] O. Hassel and B. Ottar, Acta. Chem. Scand. **1,** 929 (1947).
[28] R. E. Reeves, J. Am. Chem. Soc. **71,** 215 (1949).
[29] R. E. Reeves, J. Am. Chem. Soc. **71,** 1737 (1949).
[30] R. E. Reeves, J. Am. Chem. Soc. **71,** 2116 (1949).
[31] R. E. Reeves, J. Am. Chem. Soc. **72,** 1499 (1950).
[32] R. E. Reeves and F. A. Blouin, J. Am. Chem. Soc. **79,** 2261 (1957).
[33] R. E. Reeves, Advances in Carbohydrate Chem. **6,** 107 (1951).
[34] R. E. Reeves, Ann. Rev. Biochem. **27,** 15 (1958).
[35] H. S. Isbell, J. Research NBS **57,** 171 (1956) RP2707.
[36] H. S. Isbell, F. A. Smith, E. C. Creitz, H. L. Frush, J. D. Moyer, and J. E. Stewart, J. Research NBS **59,** 41 (1957) RP2772.
[37] R. D. Guthrie, Chem. and Ind. (London) **1958,** 1593.
[38] H. S. Isbell and R. S. Tipson, Science **130,** 793 (1959).
[39] E. M. Philbin and T. S. Wheeler, Proc. Chem. Soc. **1958,** 167.
[40] M. W. Lister, J. Am. Chem. Soc. **63,** 143 (1941).
[41] W. B. Whalley, J. Soc. Leather Trades' Chemists **40,** 120 (1956).
[42] P. Hazebroek and L. J. Oosterhoff, Discussions Faraday Soc. **10,** 87 (1951).
[43] R. E. Reeves, Abstracts Papers Am. Chem. Soc. **132,** 1D (1957); Chem. Eng. News **35** No. 38, 72 (1957).

WASHINGTON, D.C. (Paper 64A2–40)

JOURNAL OF RESEARCH of the National Bureau of Standards—A. Physics and Chemistry
Vol. 64A, No. 2, March–April 1960

Tritium-Labeled Compounds III. Aldoses-*1-t*[1,2]

H. S. Isbell, H. L. Frush, N. B. Holt, and J. D. Moyer

(December 16, 1959)

In a new method for preparing aldoses labeled with tritium at carbon 1, the aldonic lactone is reduced with lithium borohydride-*t* in pyridine solution. The method is suitable for preparing aldoses-*1-t* having high specific activities. The crude product contains a substantial proportion of the corresponding alditol-*1-t*, but the pure aldose-*1-t* is readily separated by fractional recrystallization or paper chromotography. By means of an isotope-dilution technique, yields were determined for the following aldoses-*1-t* and the corresponding alditols-*1-t*: D-arabinose-*1-t*, D-xylose-*1-t*, D-ribose-*1-t*, D-glucose-*1-t*, D-galactose-*1-t*, D-mannose-*1-t*, L-rhamnose-*1-t*, maltose-*1-t*, and lactose-*1-t*.

These labeled materials were also prepared by reducing the corresponding lactones with sodium amalgam in tritiated water. Although this latter method is not suitable for preparing labeled aldoses of high specific activity, the products are more readily purified than those obtained by reducing the lactones with lithium borohydride-*t*.

D-Glucose-*1-t*, obtained by each of these reduction methods, was oxidized with bromine, and the resulting D-gluconic acid was found to be nonradioactive. Hence, in the samples oxidized, tritium was present only at C1.

An apparatus used for reclaiming tritiated water by freeze-drying is depicted; it incorporates an efficient device for trapping entrained solids or liquids.

1. Introduction and Discussion

Tritium-labeled organic compounds offer vast opportunity for research in chemistry, biology, and medicine; they can be used not only to follow the course of a chemical or biological process, but also to study the behavior of hydrogen in the process. Extremely important differences in the rates of reaction for tritium and hydrogen provide a means for studying the mechanisms of chemical reactions. Because of the potential usefulness of carbohydrates position-labeled with tritium, the Organic Chemistry Section of the National Bureau of Standards has undertaken a broad program on the development of methods for their preparation and use [1, 2].[3] Previous publications have reported a simple procedure for the analysis of nonvolatile, water-soluble tritium compounds in a gas-flow, windowless, proportional counter [3], and a general-purpose manifold for conducting reactions in a closed system; in addition, detailed directions have been given for preparing lithium borohydride-*t* [4]. The present report describes methods for preparing aldoses labeled with tritium at C1.

In order to prepare aldoses-*1-t* of high activity, a process was developed in which the aldonic lactone is reduced with lithium borohydride-*t*. Previously, Wolfrom, and coworkers [5, 6] had prepared nonradioactive aldoses by reducing aldonic lactones with nonradioactive sodium borohydride. In a (presumably) similar process, Friedberg and Kaplan [7] had obtained D-glucose-*1-t* by reducing D-glucono-δ-lactone with sodium borohydride-*t*. Apparently, *lithium* borohydride had not been employed for reducing aldonic lactones to aldoses. The ease of preparation of tritiated lithium borohydride made its use for this purpose attractive. A study of the reduction of D-glucono-δ-lactone with lithium borohydride, in various solvents, showed that a fair yield of the aldose could be obtained by the dropwise addition of a pyridine solution of lithium borohydride to the lactone freshly dissolved in ice water. Pyridine appears to alter the reducing properties of the borohydride so as to decrease the tendency of the reagent to reduce the aldose to the alditol. Nevertheless, the crude product contains more or less of the alditol, depending upon the particular lactone reduced and the proportion of borohydride used. Pyridine solutions of lithium borohydride have the additional advantage of being reasonably stable and easy to handle.

Aldoses-*1-t* of low activity were prepared by reducing aldonic lactones with sodium amalgam,[4] essentially by the method developed in this laboratory for preparing C^{14}-labeled aldoses [10, 11, 12]; water-*t* was the solvent, and the reaction mixture included an acid buffer (sodium binoxalate). After the reduction step, the reaction mixture was freeze-dried, and the water-*t* recovered from one preparation was used in the next. Slight dilution of the tritium arose from hydrogen-tritium exchange between the water-*t* and the materials dissolved in it. The tritium-labeled aldoses, after removal of labile tritium by the freeze-

[1] Part of a project on the development of methods for the synthesis of radioactive carbohydrates, sponsored by the Division of Research of the Atomic Energy Commission. The tritium-labeled products described may be purchased from the National Bureau of Standards, at a price of $10 per 100 microcuries.

[2] Presented before the Division of Carbohydrate Chemistry of the American Chemical Socity at Atlantic City, N.J., on September 17, 1959.

[3] Figures in brackets indicate the literature references at the end of this paper.

[4] Topper and Stetten [8] had previously prepared D-glucose-*1-d* by reducing D-glucono-δ-lactone with sodium amalgam in deuterated water. They used Fischer's method of reduction [9], in which the acidity is maintained by the dropwise addition of mineral acid.

drying technique, were separated and purified by the procedures used in preparing the corresponding C^{14}-labeled aldoses.

The reduction of aldonic lactones with sodium amalgam does not require elaborate equipment, and is highly satisfactory for obtaining low-activity, tritium-labeled sugars (except tetroses); it is unsatisfactory for preparing materials of high activity.

When samples of D-glucose-*1-t*, prepared by each method of reduction, were oxidized with bromine [13], the resulting barium D-gluconate was found to be nonradioactive. Hence, the D-glucose had been labeled exclusively at C1. Presumably, other sugars prepared by the same reduction methods are also labeled with tritium at C1 only.

2. Experimental Procedures

2.1. Reduction of Aldonic Lactones With Lithium Borohydride-*t* in Pyridine; Determination of the Yields of Aldoses-*1-t* and of Alditols-*1-t* by the Isotope-Dilution Technique

Under an efficient hood, the reductions were conducted in a 50-ml, round-bottomed flask equipped with a magnetic stirrer and cooled in an ice bath. One millimole of lactone was efficiently stirred in the flask with 1 ml of ice water; immediately thereafter, 1 ml of a dry pyridine solution containing 0.25 millimole of lithium borohydride-*t* (having 160 μc of radioactivity) was added by drops. The mixture was kept in an ice bath for 2 hr and was then allowed to warm to room temperature. The water and pyridine were evaporated in a stream of air, and labile tritium was removed from the residue by dissolving it in 5 ml of methanol and evaporating the solvent; the latter process was repeated four times. Finally, the residue was dissolved in sufficient water to yield a total volume of 10 ml.

A 0.01-ml sample was used for studying the products by paper chromatography; the remainder, divided into two equal portions, was used for determining aldose-*1-t* and alditol-*1-t* by isotope dilution. To one portion was added 200 mg of the nonradioactive aldose, and to the other, 200 mg of the nonradioactive alditol. Each solution was deionized by passing it through a column containing 5 ml of mixed anion- and cation-exchange resins, and the effluent was concentrated substantially to dryness in a rotary still. After three successive recrystallizations of the residue from methanol by the addition of 2-propanol, the diluted aldose or alditol was assayed for radioactivity in a carboxymethylcellulose film [3]. The amount of the radioactive constituent in the diluted product was calculated from the relationship:

$$Ax = B(x+200)$$

where x is the weight of the radioactive constituent in the aliquot of the original reduction product, A is the specific activity of this constituent, and B is the specific activity of the diluted constituent. Quantity A is calculated on the assumptions (a) that the hydrogen-*t* of the reduction product has the same activity as the hydrogen-*t* of the lithium borohydride-*t* (i.e., that there is no isotope effect in the reduction) and (b) that the aldose contains one atom of hydrogen-*t* and the alditol, two atoms. The yields of aldoses-*1-t* and alditols-*1-t* formed by the reduction of a series of aldonic lactones with lithium borohydride-*t* in pyridine are given in table 1.

TABLE 1. *Yields of aldoses-1-t and alditols-1-t obtained by reducing aldonic lactones with lithium borohydride-t* [a]

Lactone	Aldose-*1-t*						Alditol-*1-t*, original product	
		Diluted product			Original			
		Sample counted (m')	cps [b]	Weight film (m)	μc/mg [c] of sample	Yield from 0.5 m. mole lactone [d]	Yield		Yield [e]
		mg		mg		mg	%		%
D-Arabono-γ-	β-D-Arabinose	0.922	61.7	20.6	0.0613	13.0	17.3	D-Arabitol	8.3
D-Xylono-γ-	α-D-Xylose	1.146	145.5	20.8	.1180	26.8	35.7	D-Xylitol [f]	4.2
D-Ribono-γ-	D-Ribose	0.794	28.7	19.6	.0315	6.5	8.7	D-Ribitol [f]	3.7
D-Glucono-δ-	α-D-Glucose	1.312	224.5	21.0	.160	47.5	52.8	D-Glucitol	0.6
D-Galactono-γ-	α-D-Galactose	0.958	92.3	19.8	.0849	22.7	25.2	D-Galactitol [f]	7.6
D-Mannono-γ-	α-D-Mannose	.838	63.2	20.5	.0688	17.7	19.7	D-Mannitol	1.6
L-Rhamnono-γ-	α-L-Rhamnose (hydrate)	1.058	87.4	19.9	.0732	19.5	21.4	L-Rhamnitol	1.3
Maltobiono-δ-	β-Maltose (hydrate)	1.012	136.9	19.8	.119	79.9	44.4	Maltitol	
Lactobiono-δ-	α-Lactose (hydrate)	1.236	174.3	20.9	.131	91.7	50.9	Lactitol (hydrate)	0.2

[a] One millimole of aldonic lactone was reduced with 0.25 millimole of lithium borohydride-*t* having an activity of 150 μc per milliatom of hydrogen-*t*. The product was divided into two equal portions; 200 mg of carrier aldose was added to one portion, and 200 mg of carrier alditol to the other.

[b] The sample, in a film of sodium *O*-(carboxymethyl)cellulose on a planchet, was counted in a windowless, gas-flow, proportional counter.

[c] Calculated from the equation $\mu c/mg = \frac{cps \times m \times k}{m'}$, where cps is the observed counts per second, and k is an empirically determined constant, in this case, 4.45×10^{-5}.

[d] Calculated from the equation above. Quantity A, in μc/mg, is based on the activity of the lithium borohydride-*t*. (See footnote a). Quantity B, in μc/mg, is the activity of the diluted product. (See previous column.)

[e] Yield of alditol-1-*t* was determined by the method shown in detail for the aldose-1-*t*, but with allowance for the fact that *two* atoms of hydrogen-*t* were introduced into the molecule of the alditol.

[f] Because of the tritium label at C1, the compound is not *meso*.

2.2 Large-Scale Preparation of Aldoses-*1-t* by Reduction of Aldonic Lactones With Lithium Borohydride-*t*

By essentially the same procedure as that described in section 2.1, but by use of a more highly radioactive lithium borohydride-*t* in a closed system [4], 0.5-g quantities of the tritium-labeled aldoses listed in table 1 were prepared; the specific activities were approximately 20 μc/mg.

Four millimoles of the aldonic lactone and a small stirring magnet were placed in a 100-ml, standard-taper flask having a side arm for the introduction of reagents through a rubber diaphragm (fig. 4 of ref. 4). The flask was attached to the general-purpose manifold of the apparatus of figure 1, reference 4, and evacuated. The connection to the manifold was closed, the flask was immersed in an ice bath set on a magnetic stirrer, and 2 ml of ice water was injected into the side-arm through the rubber diaphragm. While the lactone solution was efficiently stirred, 2 ml of a pyridine solution containing 1 millimole of lithium borohydride-*t* was injected into the system from a microburet. The mixture was kept at 0° C for 1 hr and at room temperature for 5 hr; it was then treated with approximately 1 ml of 10-percent aqueous acetic acid. The flask was immersed in liquid nitrogen, and the hydrogen-*t* generated in the reaction was transferred by means of the Toepler pump to a flask attached to the manifold; finally, the reaction flask was removed from the manifold. The solution was passed through 10 ml of cation-exchange resin, and then both labile tritium and boric acid were removed by several successive evaporations of methanol solutions to near-dryness. The residue, together with 500 mg of the nonradioactive aldose, was dissolved in water, and the solution was de-ionized with 10 ml of mixed anion- and cation-exchange resins. The salt-free solution,[5] on concentration and addition of such solvents as methanol, ethanol, or 2-propanol, gave the crystalline aldose-*1-t*, in some cases contaminated with the corresponding alditol-*1-t*. Each product was recrystallized three times from methanol, usually with the addition of 2-propanol.

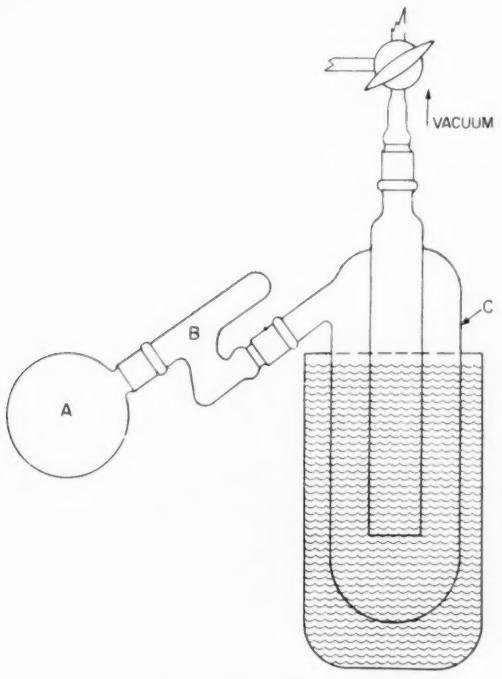

FIGURE 1. *Freeze-drying apparatus with trap for reducing mechanical losses.*

In a few preparations, difficulty was encountered in separating the aldose from the alditol. The amount of alditol-*1-t* remaining in the aldose-*1-t* after three recrystallizations was determined by the isotope-dilution technique. In each case, 2 mg of the aldose-*1-t* was mixed with 100 mg of the corresponding, nonradioactive alditol. Radioassay of the carrier alditol [3] after three recrystallizations showed that the following aldoses were pure: L-arabinose-*1-t*, D-xylose-*1-t*, D-glucose-*1-t*, L-rhamnose-*1-t*, maltose-*1-t*, and lactose-*1-t*. However, the alditol carriers derived from D-ribose-*1-t*, D-galactose-*1-t*, and D-mannose-*1-t* showed a radioactivity indicating the presence of substantial quantities of the corresponding alditol-*1-t*. These sugars were then purified by large-scale paper chromatography. The separations will be described in a later publication.

2.3. Preparation of Aldoses-*1-t* by Reduction of Aldonic Lactones With Sodium Amalgam in Tritiated Water

The reductions were first performed in a tube of the type developed for use in the synthesis of C^{14}-labeled sugars [11, 12].[6] To the tube, cooled in an ice bath, were added 4 millimoles (712 mg) of D-glucono-δ-lactone and 4 g of sodium binoxalate. Twenty milliliters of water-*t* (having 2.2 mc of radioactivity per ml) was added through the side-arm, and then while the mixture was vigorously stirred, 9.2 g of 5-percent sodium amalgam in the form of pellets [14]. After all of the amalgam had reacted (about 1 hr), the reaction mixture was transferred to a 250-ml, round-bottomed flask (flask A of fig. 1)[7] and freeze-dried. The water-*t* that collected in trap C of figure 1 was used for a subsequent preparation. The freeze-dried products from 10 successive, similar reductions were combined and neutralized with aqueous sodium hydroxide. By repeated concentration of the solution, and addition of methanol, three crops of salts (sodium oxalate and sodium gluconate) were precipitated. Finally, the mother liquor was de-ionized by means of a column of mixed ion-exchange resins. The solution, when free from ionic impurities, was con-

[5] Before concentration, solutions were tested for ionic impurities with a conductivity meter.

[6] The tube, which was 20 cm long and 2.5 cm wide, had an oblique side-arm near the top for the addition of amalgam; the tube was equipped with a stainless-steel stopper, through which a stainless-steel stirrer extended to the bottom.

[7] The freeze-drying apparatus of figure 1 depicts a highly efficient trap B, in which entrained material is caught in the side-arm. It may then be recovered by dissolving it in a solvent, and removing it with a capillary pipet.

centrated to a sirup, from which α-D-glucose-*1-t* was crystallized by the addition of methanol, and then of 2-propanol. The recrystallized aldose-*1-t* from the combined reduction products weighed 4.99 g (corresponding to a 68.5-percent yield) and had an activity of 0.08 μc/mg [3]. By use of nonradioactive D-glucose as carrier, additional α-D-glucose-*1-t*, equivalent in activity to 0.75 g of the first crop, was obtained. Thus, the yield of α-D-glucose-*1-t* was 80 percent of the lactone used.

All of the lactones [5] listed in table 1 were reduced with sodium amalgam by a procedure similar to that described above, but on a larger scale. The preparations were conducted in a 500-ml, two-necked, round-bottomed, stainless-steel flask, equipped with an efficient mechanical stirrer and cooled in an ice bath. One hundred milliliters of water-*t* and 25 to 50 millimoles of lactone were used in each reduction. For all of the aldoses except D-ribose, yields of 50 to 75 percent were obtained, without carrier. The yield of D-ribose was about 35 percent.

2.4. Proof of the Position of Label in D-Glucose-*t*; Oxidation With Bromine

A mixture of 45 mg of D-glucose-*t*, 150 mg of barium benzoate, and 3 ml of water saturated with bromine was sealed in a glass tube and kept in the dark, at room temperature, for 18 hr. The contents of the tube were mixed with about 100 mg of a decolorizing carbon and then with a solution containing 100 mg of silver sulfate in 10 ml of hot water. The mixture was filtered, and the filtrate was passed through 3 ml of cation-exchange resin. The resulting solution was then extracted with chloroform (to remove benzoic acid), neutralized with barium hydroxide, filtered, and concentrated. The barium D-gluconate was crystallized and recrystallized from water by the addition of methanol. The product showed no radioactivity when assayed in a film of sodium *O*-(carboxymethyl)cellulose.

[5] L-Arabono-γ-lactone was reduced, instead of the D form listed in the table.

The authors gratefully acknowledge the assistance of Robert E. Bailey in some of the experimental work.

3. References

[1] NBS Tech. News Bul. **43,** 121 (1959).
[2] Chem. and Eng. News **37,** No. 39, 101 (1959).
[3] H. S. Isbell, H. L. Frush, and R. A. Peterson, J. Research NBS **63A,** 171 (1959).
[4] H. S. Isbell and J. D. Moyer, J. Research NBS **63A,** 177 (1959).
[5] M. L. Wolfrom and H. B. Wood, J. Am. Chem. Soc. **73,** 2933 (1951).
[6] M. L. Wolfrom and K. Anno, J. Am. Chem. Soc. **74,** 5583 (1952).
[7] F. Friedberg and L. Kaplan, J. Am. Chem. Soc. **79,** 2600 (1957).
[8] Y. J. Topper and D. Stetten, Jr., J. Biol. Chem. **189,** 191 (1951).
[9] E. Fischer, Ber. deut. chem. Ges. **22,** 2204 (1889).
[10] H. S. Isbell, U.S. Patent No. 2,632,005, Mar. 17, 1953.
[11] H. S. Isbell, J. V. Karabinos, H. L. Frush, N. B. Holt, A. Schwebel, and T. T. Galkowski, J. Research NBS **48,** 163 (1952) RP2301.
[12] H. L. Frush and H. S. Isbell, J. Research NBS **50,** 133 (1953) RP2400.
[13] C. S. Hudson and H. S. Isbell, J. Am. Chem. Soc. **51,** 2225 (1929).
[14] H. S. Isbell, H. L. Frush, and N. B. Holt, J. Research NBS **63A,** 135 (1959).

WASHINGTON, D.C. (Paper 64A2–41)

JOURNAL OF RESEARCH of the National Bureau of Standards—A. Physics and Chemistry
Vol. 64A, No. 2, March–April 1960

Determination of Aluminum in Precipitation Hardening Stainless Steel and High Temperature Alloys

Lawrence A. Machlan, John L. Hague, and Edward J. Meros

(December 17, 1959)

A procedure is described for the determination of aluminum in high temperature alloys. Aluminum is selectively precipitated with 8-hydroxyquinoline from an ammoniacal solution of the alloy containing citrate and cyanide as complexing agents. The precipitate is ignited under oxalic acid, the oxides fused, and dissolved in acid. A caustic precipitation is made, an aliquot of the filtrate treated with hydrogen peroxide, and the aluminum precipitated with 8-hydroxyquinoline. The aluminum hydroxyquinolate is filtered on a fritted-glass crucible, dried, and weighed.

1. Introduction

One of the interesting developments in metallurgy during the last few years has been the emergence of high temperature alloys and precipitation hardening stainless steels as an important group of alloys. Many, if not most, contain aluminum as an alloying addition. All contain chromium, and varying amounts of iron, cobalt, and nickel as major constituents. Titanium, zirconium, and molybdenum are frequently present as alloying additions; less frequently, niobium and tungsten may also be used.

This combination of elements makes the determination of aluminum by chemical methods a vexing one. An embarrassingly large number of choices is available when it comes to choosing separative and determinative steps for an analysis, and most can be made to work under proper conditions; in fact, it has been said with some justification that there are almost as many methods for determining aluminum as there are analysts willing to write them. It is beyond the scope of this paper to present a comprehensive survey. The method which follows is a useful combination of steps that has been used over a period of years in the Bureau and found to have better than average reliability.

The sample, usually 2 g, is dissolved in a nitric-hydrochloric acid mixture. Citric acid is added as a complexing agent, and the solution made ammoniacal. Sodium cyanide is added to form complexes with nickel, iron, copper, and cobalt, and the aluminum precipitated by the addition of 8-hydroxyquinoline. The precipitate is filtered, ignited after the addition of oxalic acid, and the ignited residue treated with sulfuric and hydrofluoric acids to eliminate silica. The residue is fused in bisulfate, leached in hydrochloric acid, the solution partially neutralized, and a sodium hydroxide precipitation made. An aliquot of the filtrate (usually representing 1 g of sample) is treated with hydrogen peroxide and sodium cyanide, and the aluminum again precipitated with 8-hydroxyquinoline, filtered, dried, and weighed.

The separation of aluminum with 8-hydroxyquinoline in the presence of cyanide was originally described by Heczko [3] [1] in 1934. In conjunction with a sulfide separation to remove manganese, it has been used for some years as a simple routine procedure for the determination of aluminum in nitriding steels. Unfortunately the method lacks specificity, as zirconium and titanium, to name two elements, are serious interferences. Tartaric acid is usually used [6, 7] to minimize the co-precipitation of chromium, but in our experience citric acid is somewhat better in this respect. From experiments covering a range of concentrations, the amounts of citric acid and sodium cyanide were chosen as about the minimum quantities required to consistently give a reasonably clean separation of aluminum from chromium, nickel, cobalt, and iron.

A discussion of the sodium hydroxide separation is almost redundant. Much pertinent information will be found in an article by Bright and Fowler [1]. The separation serves to remove manganese, titanium, zirconium, and magnesium among others [4], as well as the remainder of the major elements. Since the latter are largely eliminated in the previous step, the precipitation is run under controlled conditions in the presence of a small addition of iron. Stainless steel beakers and polyethylene beakers and funnels can be used, and obviate the use of expensive platinum, or the use of glassware in contact with strongly alkaline solutions.

Hydrogen peroxide is added to the acidified aliquot to complex any residual titanium, niobium, vanadium, molybdenum, etc. The aluminum is precipi-

[1] Figures in brackets indicate the literature references at the end of this paper.

tated with 8-hydroxyquinoline, filtered on a glass frit, dried, and weighed. This separation was described by Lundell and Knowles [5] in 1929, and is a convenient method for removing those elements which form peroxide complexes.

The method has proved useful in the determination of aluminum in the 0.5 to 3.0 percent range in a variety of alloys. Experiments on synthetic mixtures indicate the accuracy to be of the order of one percent or better of the amount of aluminum present. The tendency of the final precipitate of the aluminum quinolate to run slightly (about 1%) high almost exactly compensates the small absorption and solubility losses. The method requires more elapsed time than some possible alternatives, due primarily to the steps involving ignition and treatment with sulfuric and hydrofluoric acids. Since these steps do not require much attention, the "working time" is usually about a day for a set of six determinations.

2. Reagents

Citric acid solution (500g/liter). Dissolve 500 g of citric acid monohydrate in 500 ml of diluted sulfuric acid (1+49)[2], dilute to 1 liter with water, and filter to remove insoluble material.

8-Hydroxyquinoline solution (75 g/liter of ethanol). Dissolve 75 g of 8-hydroxyquinoline in 900 ml of ethyl alcohol, dilute to 1 liter with ethyl alcohol, and filter.

Cyanide wash-solution. Dissolve 20 g of ammonium chloride, 20 g of ammonium citrate, and 20 g of sodium cyanide in 900 ml of water containing 25 ml of ammonium hydroxide, and dilute to 1 liter with water.

Iron solution (20 mg/ml). Dissolve 10 g of iron containing a negligible quantity of aluminum in 200 ml of diluted hydrochloric acid (1+3), cautiously oxidize with 8 to 10 ml of nitric acid, cool, and dilute to 500 ml with water.

Sodium hydroxide solution (300 g/liter). Transfer 700 ml of water and 300 g of sodium hydroxide to a polyethylene bottle, dilute to 1 liter with water, and mix well.

3. Procedure

Transfer 2 g of the sample to a 600-ml beaker, cover, and add 40 ml of diluted aqua regia (1+1) (3 parts of hydrochloric acid and 1 part of nitric acid diluted with an equal volume of water). Warm the solution on a steam bath until the sample dissolves. Add 40 ml of citric acid solution and adjust the volume of the solution with water to 250 ml. Add ammonium hydroxide until the solution is but slightly acid, add 1 g of hydroxylamine hydrochloride, neutralize to litmus paper with ammonium hydroxide, and add 10 ml in excess. Add 15 g of sodium cyanide,[3] heat to boiling, and boil 1 to 2 min. Add 25 ml or a sufficient [4] amount of 8-hydroxyquinoline solution slowly while stirring the solution vigorously. Stir the solution vigorously (best done with a mechanical stirrer) for 15 min and allow the solution to stand 15 min on the edge of the steam bath. Add paper pulp, stir the solution well to distribute the pulp, and cool to room temperature.

TABLE 1. *Results of determinations of aluminum by the recommended procedure in various synthetic mixtures*

NBS Standard Sample 169, Ni 77, Cr 20, Al 0.095

Weight of sample	Other element added	Aluminum			
		Added	Present	Found	Difference
g	*mg*	*mg*	*mg*	*mg*	*mg*
2	40 Ti		1.9	1.4	−0.5
2	40 Ti	5.0	6.9	6.5	−.4
2	40 Ti	5.0	6.9	6.7	−.2
2	40 Ti	10.0	11.9	11.7	−.2
2	40 Ti	10.0	11.9	11.8	−.1
2	40 Ti	20.0	21.9	22.2	+.3
2	40 Ti	20.0	21.9	21.7	−.2
2	40 Ti	20.0	21.9	21.9	.0
2		20.0	21.9	21.7	−.2
2	40 Ti	40.0	41.9	42.4	+.5
2	40 Ti	40.0	41.9	42.1	+.2
2	40 Ti	60.0	61.9	62.4	+.5
2	40 Ti	100.0	101.9	101.1	−.8

Filter the solution through a double thickness of close-texture filter paper fitted to a 7-cm Büchner funnel and precoated with a little filter pulp. Transfer the precipitate to the funnel, and wash 5 to 6 times with the cyanide wash solution,[5] and 2 to 3 times with water. Transfer the paper and precipitate to a platinum crucible, cover the precipitate with 5 g of oxalic acid, place the crucible in a cold muffle, and slowly ignite to 600 to 700° C. Add 1 to 2 ml of diluted sulfuric acid (1+3) and 10 to 15 ml of hydrofluoric acid to the crucible, and remove the hydrofluoric and sulfuric acids by heating on an air or sand bath. Add 1 to 2 g of potassium pyrosulfate to the crucible and fuse the salt to dissolve the oxides. Transfer the crucible and fusion to a 400-ml beaker and dissolve the fusion in 100 ml of warm diluted hydrochloric acid (1+5). Remove and wash the crucible with diluted hydrochloric acid (1+5). Add 5 ml of iron solution, nearly neutralize (as indicated by the slow redissolving of the iron precipitate) with sodium hydroxide solution (300 g/liter). Transfer 140 ml of water and 70 ml of sodium hydroxide solution to a weighed [6] 1-liter

[2] Diluted sulfuric acid (1+49) denotes 1 volume of concentrated sulfuric acid, sp gr 1.84, diluted with 49 volumes of water. If no dilution is specified, the concentrated analytical reagent is meant.

[3] With cyanide present, all operations should be conducted in a hood.

[4] A minimum addition of 25 ml of 8-hydroxyquinoline solution is recommended. In the presence of larger than usual amounts of aluminum or titanium, additional reagent may be required. For example, 40 ml of 8-hydroxyquinoline solution was used in the last experiment given in table 1.

[5] The cyanide wash solution should be handled by air or bulb.

[6] The use of "weight aliquoting" avoids the necessity of washing the precipitate and handling strongly alkaline solutions in contact with glassware. Weighing on a trip balance to the nearest half-gram or so provides adequate accuracy for the present application.

stainless steel beaker. Heat the sodium hydroxide solution to boiling, add the sample solution slowly with good stirring, and boil for 1 to 2 min. Cool the solution to room temperature, dilute with water to 500 g, stir thoroughly, and allow the precipitate to settle for a few minutes. Filter through a close-texture paper fitted to a polyethylene funnel. Discard the first 20 to 30 ml and collect approximately half of the solution in a weighed 600-ml polyethylene beaker. Reweigh the beaker to obtain the weight of the aliquot.

Transfer the filtered solution to a 600-ml glass beaker containing 25 ml of hydrochloric acid and 2 ml of citric acid solution. Neutralize the solution with ammonium hydroxide and add 10 ml in excess. Add 1 g of sodium cyanide and heat the solution to 55° to 60° C. Add 1 ml of hydrogen peroxide (30%) to the warm solution, and slowly add sufficient [7] 8-hydroxyquinoline solution while stirring the solution vigorously. Stir the solution vigorously for 15 min and allow the solution to stand 15 min on the edge of the steam bath. Cool the solution to room temperature, filter through a weighed close-fritted glass crucible, and wash the precipitate 10 to 12 times with water. Dry the crucible and precipitate for 1½ hr at 115° C, cool, and weigh.

4. Discussion and Results

The precipitation of aluminum with 8-hydroxyquinoline is restricted to a somewhat narrower *p*H range in the presence of citric acid than is the usual case using tartaric or acetic acid. A *p*H-precipitation curve for aluminum hydroxyquinolate in the presence of citric acid is given in figure 1. The recoveries involve approximately 10 mg of aluminum in a volume of 150 ml, in the presence of 1 g of citric acid. Adjustment of the *p*H was made with ammonium hydroxide and acetic acid as indicated, and the *p*H was determined on a portion of the filtrate at room temperature. The first filtrate for samples run according to the recommended procedure was usually in the *p*H range of 9.2 to 9.4, which is a satisfactory point for complete precipitation of aluminum and nearly complete solution of molybdenum and tungsten [2]. Nickel, cobalt, iron, and chromium, the major elements, are also largely eliminated in the first precipitation.

The values obtained in table 1 show that aluminum in amounts from 10 to 100 mg (corresponding to 0.5 to 5% on the aliquot used) can be determined by the recommended procedure with an error of the order of 1 percent of the amount present. The values obtained for aluminum in amounts below 10 mg (5 mg or less in the final aliquot) almost always indicated a negative bias, and the method as written is not satisfactory for alloys containing less than 0.5 percent aluminum. These data also show that titanium at the 2-percent level is not an interfering constituent.

The data in table 2 demonstrate that niobium, tantalum, molybdenum, tungsten, vanadium, phos-

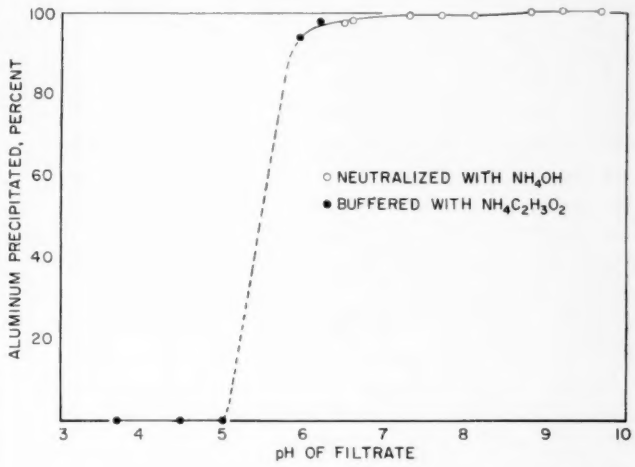

FIGURE 1. *Effect of pH on the precipitation of aluminum with 8-hydroxyquinoline in the presence of citric acid.*

TABLE 2. *Results of determinations of aluminum by the recommended procedure in the presence of possible interfering elements*

Sample number [a]	Weight of sample	Other element added [b]	Aluminum			
			Added	Present	Found	Difference
	g	*mg*	*mg*	*mg*	*mg*	*mg*
169	2	35 Nb	20.0	21.9	22.1	+0.2
169	2	35 Nb	20.0	21.9	21.8	−.1
169	2	84 Nb	20.0	21.9	22.0	+.1
169	2	82 Mo	20.0	21.9	21.9	.0
169	2	1 P	20.0	21.9	21.9	.0
169	2	10 Sn [c]	20.0	21.9	22.1	+.2
169	2	10 Sn [d]	20.0	21.9	22.1	+.2
169	2	10 Sn [e]	20.0	21.9	21.8	−.1
169	2	10 V	20.0	21.9	22.0	+.1
169	2	119 W	20.0	21.9	21.9	.0
169	2	5 Zr	20.0	21.9	21.9	.0
168	2	----------	20.0	20.4	20.3	−.1
168	2	----------	20.0	20.4	20.7	+.3

[a] NBS Standard Sample. Standard Sample 168, Cr 20, Co 41, Ni 20, Mo 4, W 4, Nb 3, Ta 1.
[b] All samples contain an addition of 40 mg of Ti.
[c] Tin added as metal at start.
[d] Tin added to solution of ignited oxides.
[e] Tin added as solution to caustic filtrate.

[7] Each mg of aluminum in the aliquot requires approximately 0.22 ml of 8-hydroxyquinoline solution. A small excess, 2 ml, is added to minimize absorption of excess reagent by the precipitate.

TABLE 3. *Results of determination of aluminum by the recommended procedure in high temperature alloys*

NBS standard sample	Aluminum				No. of determinations	Wt of sample	Type of alloy
	Certificate value	Found	Difference	Range			
	%	%	%	%		g	
349	1.23 [a]	1.23	0.0	1.22 to 1.23	6	2	Ni 57, Cr 20, Co 14, Mo 4, Ti 3, Al 1.
1188	0.77 [a]	0.76	−.01	0.76 to 0.77	3	2	Ni 73, Cr 15, Ti 2, Nb 1.
1189	1.20 [a]	1.17	−.03	1.17	3	2	Ni 73, Cr 20, Ti 2.5.
1191	1.55 [a]	1.54	−.01	1.51 to 1.55	8	2	Ni 55, Cr 19, Co 14, Mo 5, Ti 3.
1192	1.06 [a]	1.06	.0	1.06 to 1.07	5	2	Ni 57, Cr 18, Co 11, Mo 7, Ti 3.
106A	1.08	1.10	+.02	1.08	1	2	Nitriding steel.

[a] Provisional certificate values.

phorus, tin, and zirconium in amounts apt to be encountered in these alloys do not interfere. The use of NBS Standard Samples 168 and 169 as base material for the preparation of synthetic mixtures show that major amounts of nickel, cobalt and chromium do not interfere. A few values obtained on several high temperature alloys are tabulated in table 3, to show the agreement which can be expected on replicate determinations. The single run on the steel standard 106a is given to show that major amounts of iron do not interfere, but is not otherwise pertinent because simpler methods are available for this type of alloy.

5. References

[1] H. A. Bright and R. M. Fowler, BS J. Research **10,** 330 (1933).
[2] H. R. Fleck and A. M. Ward, Analyst **58,** 388 (1933); **62,** 378 (1937).
[3] T. Heczko, Chem. Ztg., **58,** 1032 (1934).
[4] G. E. F. Lundell and J. I. Hoffman, Outlines of methods of chemical analysis, p. 82. (J. Wiley and Sons, Inc., New York, N.Y., 1938).
[5] G. E. F. Lundell and H. B. Knowles, BS J. Research **3,** 93 (1929).
[6] E. C. Pigott, Iron and Steel **16,** 325 (1943).
[7] S. D. Steele and L. Russell, Iron and Steel **16,** 182 (1943).

WASHINGTON, D.C.

(Paper 64A2–42)

Selected Abstracts

Theory of diffraction in microwave interferometry, D. M. Kerns and E. S. Dayhoff, *J. Research NBS* **64B,** *No. 1, 1 (1960).*

Microwave Michelson and Fabry-Perot interferometers are respectively considered asinstances of (1) a "reflection system," consisting of a radiating-receiving system and a reflecting object (e.g., a finite mirror) and (2) a "transmission system," consisting of a radiating system and a receiving system with an object (e.g., a Fabry-Perot etalon) interposed. The basic theoretical objective is the calculation of the amplitude and phase of the (time-harmonic) received signal in the systems considered. The electromagnetic field in space transmission paths is represented in terms of continuous angular spectra of vectorial plane waves, and the elements of the systems are described by means of suitable tensor scattering matrices (having both discrete and continuous indices). Needed scattering matrices are considered known; relationships to experimentally determinable data are outlined. The general case of either the reflection or transmission system is soluble formally in terms of a series of integrals stemming from the Liouville-Neumann series solution of certain integral equations. Formulas are obtained for models of the Michelson and Fabry-Perot instruments with arbitrary radiating and receiving characteristics. The theory and various features of the instruments considered, including Fresnel-region (or quasi-optical) behavior, are illustrated by means of examples obtained by choosing relatively simple and rather hypothetical analytical expressions for the radiating and receiving characteristics.

Some solutions for electromagnetic problems involving spheroidal, spherical, and cylindrical bodies, J. R. Wait, *J. Research NBS* **64B,** *No. 1, 15 (1960).*

Solutions are presented for the low-frequency electromagnetic response of an oscillating magnetic dipole by conducting bodies of simple shape. The quasi-stationary approximation is employed throughout which is valid when the relevant dimensions of the problem are all small compared to the free-space wavelength. This amounts to matching solutions of the wave equation within the bodies to solutions of Laplace's equation outside.

Standard free-air chamber for the measurement of low energy X-rays (20 to 100 kilovolts-constant potential), V. H. Ritz, *J. Research NBS* **64C,** *No. 1, 49 (1960).*

A description of the new National Bureau of Standards "low" energy free air chamber is given. The standard chamber is designed to measure the exposure dose in roentgens for X-ray beams generated at potentials from 20 to 100 kvcp with filtrations ranging from 2 mm of beryllium to 2 mm of beryllium plus 4 mm of aluminum. The chamber has been compared with the National Bureau of Standards medium energy standard at 60, 75, and 100 kvcp with filtrations of 3, 3, and 4 mm of aluminum, respectively. The two standard chambers agreed to within 0.3 percent.

Transmittance of materials in the far infrared, E. K. Plyler and L. R. Blaine, *J. Research NBS* **64C,** *No. 1, 55 (1960).*

The transmittance of several crystal materials with thicknesses of about 5 mm has been measured from 17 to 55 μ. The crystals are sodium chloride, potassium chloride, potassium bromide, thallium bromide-iodide, cesium bromide, and cesium iodide. Also the transmittance of polyethylene containing carbon black has been measured to 100 μ and an example of its use as a filter for far infrared is given.

X-ray attenuation coefficients from 10 kev to 100 Mev, R. T. McGinnies, *NBS Circ. 583 Suppl. (1959) 15 cents.*

A revision is given of the X-ray attenuation coefficients presented in National Bureau of Standards Circular 583. Table 4 of that publication is eliminated, and a new table is given for each material for photon energies less than 100 kev. The uncertainties in the estimates of attenuation coefficients at low energies are from 3 to 5 percent, which is the same as was previously given at higher energies. The cross sections for scattering are unchanged. Two values are listed for the photoelectric cross section, one calculated from the Sauter-Stobbe formulas and the other derived from new experimental evidence. The procedures for smoothing experimental data are described and are generally the same as were used in Circular 583. In addition to the systematic coverage of the region from 10 kev to 100 Mev, some data are included for a number of elements based on experimental measurements below 10 kev and above 100 Mev. A comparison is made between calculated and experimental total attenuation coefficients at energies above 10 Mev.

Photographic dosimetry at total exposure levels below 20 mr, M. Ehrlich and W. L. McLaughlin, *NBS Tech. Note 29 (PB151388) (1959) 50 cents.*

Assemblies of commercial photographic material sandwiched between two plastic scintillators can be used to measure high-energy X- or gamma-ray exposures down to 1 mr and less. The energy dependence of the assemblies' response is much less than that of a conventional photographic dosimeter, in some instances allowing an exposure interpretation with an accuracy of ± 25 percent over the energy range from about 0.1 to 1.25 Mev. However, low-intensity reciprocity failure limits the range of applicability of the system.
Conventional photographic dosimeters, not incorporating scintillators, are usually preferable for routine personnel dosimetry. By extending the monitoring period, it may be possible to avoid personnel dosimetry below 20 mr entirely. However, by doing this, one introduces additional difficulties because of instabilities in the photographic image. In some instances, an increase in effective emulsion thickness, achieved by using stacks of identical films, may lead to an increase in emulsion sensitivity sufficient to extend the useful range of a film badge well below 20 mr, without the use of a scintillator.

Variation of the thermodynamic ideal temperature in the polystyrene-cyclohexane system, D. McIntyre, J. H. O'Mara, and B. C. Konouck, *J. Am. Chem. Soc.* **81,** *3498 (1959).*

The second virial coefficients of cyclohexane solutions of several fractions of polystyrene prepared in slightly different ways have been determined by light scattering and osmometry near the theta, or ideal, temperature. The results indicate that the ideal temperature is increased as the molecular weight is decreased. The larger increase is due to small but increasingly effective chemical interactions when an *n*-butyl mercaptan group is incorporated in the chain. A much smaller effect appears to exist even when the chain is apparently uniform.

Energy dissipation in standing waves in rectangular basins, G. H. Keulegan, *J. Fluid Mech.* **6,** *Pt. 1, 35 (1959).*

The modulus of decay of standing waves of finite height is derived by assuming that the attenuation of the waves is due to viscous losses in boundary layers close to the solid walls. Dampings are observed in six basins of varying sizes. The basins are duplicated using glass and lucite for the wall materials. With liquids wetting the walls, the losses due to viscosity are slightly increased from causes presumably related to surface tension. With a liquid not wetting the walls (distilled water and lucite), losses from surface activity, of some obscure origin, outweigh many times the losses due to viscosity in the basins of smaller sizes. For moderately large basins, for which surface activity may be neglected, the agreement between the observed and computed rates of decay is found to be satisfactory.

Total photoelectric cross sections of copper, molybdenum, silver, tantalum, and gold at 662 kev, W. F. Titus, *Phys. Rev.* **115,** *No. 2, 351 (1959).*

The photoelectric cross sections have been measured for the elements Cu, Mo, Ag, Ta, and Au using the 662 kev gamma rays from Cs^{137}. The method involved the detection of the photoelectrons in a 4π geometry. The results obtained for the cross sections have an accuracy of about 2½% and are in agreement with the values obtained from Grodstein.

Strength of synthetic single crystal sapphire and ruby as a function of temperature and orientation, J. B. Wachtman and L. H. Maxwell, *J. Am. Ceram. Soc.* **42,** *No. 9, 432 (1959).*

The modulus of rupture of sapphire single crystals was determined as a function of temperature for specimens with orientations favoring plastic deformation and for specimens with unfavorable orientations. From 600° C to 1000° C, the strength of both types increased with increasing temperature, but the increase was more pronounced for the former. Ruby specimens oriented favorably for plastic deformation also showed a large increase in strength. It is conjectured that the increase in strength results from stress relief by microscopic plastic deformation.

PILOT, the NBS multicomputer system, A. L. Leiner, W. A. Notz, J. L. Smith, and A. Weinberger, *Proc. Eastern Joint Computer Conf. (Philadelphia, Pa.), p. 164 (1958).*

At NBS a new large-scale digital system has been designed for use on a wide variety of experimental applications ranging from automatic search and interpretation of Patent Office records to real-time control of commercial aircraft traffic. Because of this wide range of intended use, the system had to combine in a single installation a variety of characteristics not ordinarily associated with one facility, namely (1) a high computation rate, (2) highly flexible control capabilities for communicating with the outside world, and (3) a wide repertoire of internal processing formats. The overall system is organized around three independently programmed computers which intercommunicate in such a way as to permit all three to work together concurrently on a common problem, each computer working on the piece of the problem for which it is individually best suited. The overall system thus provides a working model of an integrated multi-computer network.

Dimensional changes in systems of fibrous macromolecules: polyethylene, L. Mandelkern, D. E. Roberts, A. F. Diorio, and A. S. Posner, *J. Am. Chem. Soc.* **81,** *4148 (1959).*

Fibrous polyethylene of extremely high axial orientation was crosslinked by means of ionizing radiation, and the anisotropic changes in length that occur as a consequence of this process were investigated. In accord with theoretical expectations and with previous results obtained in a study of fibrous natural rubber, the length in the isotropic state subsequent to the crosslinking process increases as the crosslinking level increases. However, because of the initially higher axial orientation possessed by the polyethylene fibers much greater elongations are observed in the liquid state in this instance. As a consequence of this fact, on subsequent recrystallization a preferential axial crystalline orientation develops without the application of any external force. The melting and recrystallization of these fibers results in a reversible contractile system without the necessity of maintaining any external force. Anisotropic reversible dimensional changes of about 25% are observed, and these results are explicable on the basis of well established physical-chemical principles appropriate to macromolecular systems. These principles are then invoked to explain many of the observed anisotropic dimensional changes that occur in systems of naturally occurring fibrous proteins.

Attenuation of scattered cesium-137 gamma rays, F. S. Frantz, Jr., and H. O. Wyckoff, *Radiology* **73,** *No. 2, 263 (1959).*

Broad beam attenuation curves of the scattered radiation from teletherapy sources are necessary in designing secondary protective radiation barriers. Such attenuation curves in both Pb and concrete were obtained for a Cs^{137} source. Comparisons with the work of Dixon, et al., have also been made.

Photoproton cross sections of carbon, S. Penner and J. E. Leiss, *Phys. Rev.* **114,** *No. 4, 1101 (1959).*

The partial (γ,p) cross section of carbon in which the residual boron nucleus is left in the ground state has been measured with a thin-crystal proton spectrometer. This cross section is shown to decrease from about 10 mb at the giant resonance peak (22 Mev) to about 0.1 mb near 60-Mev photon energy. Angular distributions measured at five energies exhibit an asymmetry around 90° which increases rapidly with increasing energy. The partial cross section to the first excited state of boron is $(7\pm16)\%$ of the ground-state cross section. The partial cross section to one or more excited states of boron about 5 Mev above the ground state is comparable with the ground-state cross section above 30-Mev photon energy. In addition to the cross-section data, the measurements provide a sensitive means of calibrating the energy scales of electron accelerators at energies in the 25- to 50-Mev region.

Cryogenic engineering of hydrogen bubble chambers, B. W. Birmingham, D. B. Chelton, D. B. Mann, and H. P. Hernandez, *ASTM Bull. No. 240, 34 (TP164) 1959.*

Low-temperature material problems encountered during the development of a liquid-hydrogen bubble chamber are discussed. Properties affecting the selection of the bubble chamber material, the glass window, and the thermal radiation shield are examined. Methods of sealing the glass window to the chamber with various gaskets suitable for use at liquid hydrogen temperature (−423° F) are presented. In addition, a method of continuously maintaining the bubble chamber and contents at liquid hydrogen temperature by means of an external refrigerator is described.

Memorandum on a procedure for obtaining spectral radiant intensities of tungsten-filament lamps, 400–700 mμ, L. E. Barbrow, *J. Opt. Soc. Am. Letter to Editor* **49,** *No. 11, 1122 (1959).*

A procedure is described for computing from the candlepower and color temperature of a tungsten-filament lamp, its spectral radiant intensity in the wavelength region 400 to 700 millimicrons. A table of spectral radiant intensities per candela for seven color temperatures is included.

Paramagnetic resonance spectra of active species. Blue material from hydrazoic acid, W. B. Gager and F. O. Rice, *J. Chem. Phys.* **31,** *No. 2, 564 (1959).*

The products of hydrazoic acid that have been decomposed thermally, electrically, and photochemically have been collected and maintained at 77° K. While at this temperature, paramagnetic resonance spectra of the samples were taken, and the result in each case was a single line at $g=2.003\pm.002$. The thermally decomposed sample showed a line width of 36 gauss while the other two samples both gave a line width of 11.5 gauss. In all three cases the lines were assymetric with the low field side of the lines being broader and less intense than the high field side. The resonance spectra is compared to the optical spectra taken of similarly prepared samples. The authors believe that a mechanism similar to an *F*-center in an alkili-halide gives rise to the resonance and to the blue color.

On prediction of system behavior, J. R. Rosenblatt, *Proc. of the New York Univ.–Ind. Conf. on Reliability Theory (New York, N.Y.) p. 39 (1958).*

It is customary in theoretical discussions of prediction of system performance to assume that the relation between variables by which performance is assessed and variables describing the parts of the system can be specified by a function. The purpose of this paper is to consider some of the problems which arise in choosing the form of such a function and in specifying the relevant variables and the nature of appropriate experiments, measurements, and data.
In the context of each of a number of familiar types of mathematical model, the possible consequences of alternative choices of time units, subsystem definitions, and independence assumptions are discussed.

Argon deposition on a 4.2° K surface, S. N. Foner, F. A. Mauer, and L. H. Bolz, *J. Chem. Phys.* **31,** *No. 2, 546 (1959).*

An uncollimated beam of argon atoms was directed onto a liquid-helium-cooled surface in such a way that the incident flux could be calculated from the gas input and the geometry. The mass per unit area of the argon film was determined by measuring the attenuation of an X-ray beam diffracted by the gold substrate.
The probability of a molecule sticking on impact was calculated from the ratio of the measured mass per unit area to the integrated mass flux on the target. The value obtained for argon deposited on argon at 4.2° K was 0.60 ± 0.06.

Kinetic equation for a plasma with unsteady correlations, C. M. Tchen, *Phys. Rev.* **114,** *394 (1959).*

As a generalization of the Boltzmann equation, the kinetic equation for a plasma is derived in the form of a generalized Fokker-Planck equation, by considering unsteady correlations, including non-Markovian and nonlinear behavior. Both the binary and ternary correlations are used for many kinds of particles with different temperatures. The coefficients of the kinetic equation depend on the law of interaction for a pair of particles and are influenced by relaxation. The effective potential of friction consists of two parts: the static part corresponds to the Debye potential and is isotropic, the dynamical part is axially symmetrical about the direction of motion and causes a dynamical friction. The results show that the friction is proportional to velocity for slow particles, and inversely proportional to the square of velocity for fast particles. This tendency of the fast particles to overcome repulsion is a property connected with the "run-away" of electrons. A criterion for maximum friction is derived. The triplet interaction, which mainly affects the shielding phenomena, assures the convergence of the coefficients in case of distant interaction. Since the length scales of interaction are well determined in this way, the kinetic equation can be expected to be valid over a longer range than does the Boltzmann equation. The large scale agrees with the Debye radius, when the shielding term is linearized, as should be expected. When time relaxation is left aside and linearization is made, the kinetic equation degenerates to the classical Fokker-Planck equation with convergent coefficients.

Spectral study of a visible, short-duration afterglow in nitrogen, B. E. Beale, Jr., and H. P. Broida, *J. Chem. Phys.* **31,** *No. 4, 1030 (1959).*

In the discharge products of rapidly flowing, pure nitrogen at pressures between 4 and 15 mm Hg, an afterglow differing from the usual Lewis-Rayleigh afterglow has been found to occur approximately 5 milliseconds after the discharge. This pink-colored afterglow persists for about 2 milliseconds and is both preceded and followed by the usual yellow glow of active nitrogen. In the visible and near ultraviolet, this short-duration glow is characterized by strong emission of N_2+ and N_2 1st positive bands and weak emission of N_2 2nd positive bands. The vibrational intensity distributions of the bands are similar to that of the discharge, including strong emission from vibrational levels above the predissociation limit of the $B\,^3\Pi_g$ state. The existence of this afterglow shows the presence of highly energetic species other than nitrogen atoms after the discharge.

Cavity resonators for dielectric spectroscopy of compressed gases, H. E. Bussey and G. Birnbaum, *Rev. Sci. Instr.* **30,** *800 (1959).*

Convenient tunable sealed-off cavity resonators are described at frequencies of 1, 2, 9, and 24 kMc, for use with internal pressures up to 1000 psi. The modes of oscillation employed were TE_{01n}, TE_{11n}, and TM_{01}-hybrid, all in a circular cylinder. A convenient method for sealing an iris, applicable over a wide frequency range, was to insert a tapered Teflon plug. A Kovar-glass seal for coaxial lines is described that provides a good impedance match in a 50-ohm line. A brief summary of the measuring procedure is given, including a method of calibrating the cavity which increases considerably the accuracy of the loss measurements.

Dynamic stability of frozen radicals. II. The formal theory of model, J. L. Jackson, *J. Chem. Phys.* **31,** *No. 3, 722 (1959).*

In Part I, a model for frozen radical chain reactions of nitrogen atoms in a nitrogen molecule lattice was described. Here, a formal mathematical theory of these reactions is developed and applied. The results of the model are used to discuss the stability of frozen radical mixtures as a function of size. The theory also is used to obtain curves of free radical concentrations as a function of time when radicals are produced by irradiation of the solid at low temperatures. The formulas obtained are compared with most recent experimental results.

Method of cooling head-on photomultipliers, G. C. Harman, *Rev. Sci. Instr.* **30,** *No. 8, 742 (1959).*

A simple method of cooling the photoemissive surface of head-on photomultipliers is described. It consists of a small, specially constructed dewar with a window in its top. The dewar is charged with dry ice powder and slipped over the head of the multiplier so that it cools only the sensitive surface. The rest of the tube remains at room temperature. The dark current is reduced by a factor of at least 500.

Nonresonant microwave absorption and electric dipole moment of NO in the gaseous state, A. A. Maryott and S. J. Kryder, *J. Chem. Phys.* **31,** *No. 3, 617 (1959).*

The microwave absorption in NO has been measured by a resonant cavity method at frequencies near 9 and 23 kMc/sec and at pressures in the range 3 to 27 atmos. The major part of the absorption is due to direct Λ-type doublet transitions, although at the higher pressures, a significant contribution also comes from the low frequency wings of the pure rotational spectrum. Since the Λ-doublet separation is much smaller than the applied frequency for all significant transitions, the resulting spectrum has the nonresonant or Debye shape. From the intensity of this spectrum, the electric dipole moment was found to be 0.148 ± 0.002 debye. The effective collision cross section for random spacial reorientation of the molecules is approximately twice the kinetic collision cross section.

Bremmstrahlung cross-section formulas and related data, H. W. Koch and J. W. Motz, *Rev. Modern Phys.* **31,** *No. 4, 920 (1959).*

The present report is intended to provide a coherent summary of the bremsstrahlung cross section formulas and related data. The theoretical formulas and their specific limitations are presented in a form that is most convenient for practical calculations. In addition, estimates are given for the accuracy of these formulas for cases where comparisons can be made with experimental results. Correction factors that are available are indicated in either numerical or analytical form. A brief summary of other data pertaining to electron-electron and to thick target bremsstrahlung is also included.

The nova outburst. III. The ionization of hydrogen gas by an exciting star, J. Jefferies and S. Pottasch, *Ann. Astrophys. J.* **22,** *318 (1959).*

All quantitative nova observations for the six best observed novae are brought together and an attempt is made to explain the varied observations on the basis of a consistent model. It is shown that an ejected shell may explain both the quantitative radiative emission in the lines and the initial cooling observed in both the lines and in the continuum. For the six novae considered, the density of the shell and electron temperature in the shell are found as a function of time. The temperature and radius of the central star are also found as a function of time, and the composition of the shell is also determined.

Exploratory study, by low temperature X-ray diffraction techniques, of diborane and the products of a microwave discharge in diborane, L. H. Bolz, F. A. Mauer, and H. S. Peiser, *J. Chem. Phys.* **31,** *No. 4, 1005 (1959).*

To test the hypothesis that free radicals may be stabilized by the formation of loose, one-electron bonds with electron deficient molecules, diborane and the products of a microwave discharge in diborane have been studied by low temperature X-ray diffraction. Two crystalline phases were distinguished in ordinary diborane. An additional phase, which may be BH_3, was found in microwave-discharged diborane. Because rapid warm-up occurred spontaneously, starting at a temperature near 4.2° K, it cannot be concluded that diborane helped appreciably to stabilize the atomic hydrogen present in the microwave-discharge products.

The double bond isomerization of olefins by hydrogen atoms at −195°, M. D. Scheer and R. Klein, *J. Phys. Chem.* **63,** *1517 (1959).*

The focus of interest in low temperature chemistry coupled with the rather unusual nature of this low temperature reaction dictates the prompt disclosure of this information in the form of a note.

Other NBS Publications

Journal of Research, Section 64D, No. 2, March–April 1960, 70 cents.

Optimum frequencies for outer space communication. George W. Haydon.
The joint use of the ordinary and extraordinary virtual height curves in determining ionospheric layer profiles. L. R. O. Storey.
Measured statistical characteristics and narrow band teletype message errors on a single sideband 600 mile long ultrahigh frequency tropospheric radio link. E. F. Florman and R. W. Plush.
Impedance of a corner-reflector antenna as a function of the diameter and length of the driven element. A. C. Wilson.
The electric field at the ground plane near a top-loaded monopole antenna with special regard to electrically small L- and T-antennas. H. Lottrup Knudsen and T. Larsen.
Terrestrial propagation of very-low-frequency radio waves, a theoretical investigation. James R. Wait.
Aurora of October 22/23, 1958, at Rapid City, South Dakota. F. E. Roach and E. Marovich.

Journal of Research, Section 64B, No. 1, January–March 1960, 75 cents.

Theory of diffraction in microwave interferometry. D. M. Kerns and E. S. Dayhoff. (See above abstract.)
Some solutions for electromagnetic problems involving spheriodal, spherical, and cylindrical bodies. James R. Wait. (See above abstract.)
Kantorovich's inequality. Morris Newman.
A symmetric continuous poker model. A. J. Goldman and J. J. Stone.
Moebius function on the lattice of dense subgraphs. R. E. Nettleton and M. S. Green.
The minimum of a certain linear form. Karl Goldberg.
Space of k-commutative matrices. Marvin Marcus and N. A. Khan.
Selected bibliography of statistical literature, 1930 to 1957: I. Correlation and regression theory. Lola S. Deming.
Selected bibliography of statistical literature, 1930 to 1957: II. Time series. Lola S. Deming.

Journal of Research, Section 64C, No. 1, January–March 1960, 75 cents.

Power loss and operating temperature of tires, R. D. Stiehler, M. N. Steel, G. G. Richey, J. Mandel, and R. H. Hobbs.
Effects of antioxidants on asphalt durability, B. D. Beitchman.
Temperature stratification in a nonventing liquid helium Dewar, L. E. Scott, R. F. Robbins, D. B. Mann, and B. W. Birmingham.
Expansion engines for hydrogen liquefiers, E. H. Brown.
A statistical chain-ratio method for estimating relative volumes of mail to given destinations. N. C. Severo and A. E. Newman.

Standard free-air chamber for the measurement of low energy X-rays (20 to 100 kilovolts-constant potential), V. H. Ritz. (See above abstract.)

Transmittance of materials in the far infrared, E. K. Plyler and L. R. Blaine. (See above abstract.)

Equipment and method for photoelectric determination of image contrast suitable for using square wave targets, F. W. Rosberry.

Formation of silver sulfide in the photographic image during fixation, C. I. Pope.

Capacitor calibration by step-up methods, T. L. Zapf.

CRPL exponential reference atmosphere, B. R. Bean and G. D. Thayer, NBS Monograph 4 (1959) 45 cents.

Preservation of documents by lamination, W. K. Wilson and B. W. Forshee, NBS Monograph 5 (1959) 20 cents.

Screw-thread standards for federal services 1957. Amends in part H28 (1944) (and in part its 1950 Supplement), NBS Handb. H28 (1957)—Part II (1959) 75 cents.

Hydraulic research in the United States—1959, H. K. Middleton, NBS Misc. Pub. 227 (1959) $1.25.

Frequency dependence of VHF ionospheric scattering, J. C. Blair, NBS Tech. Note 9 (PB151368) (1959) 75 cents.

Some applications of statistical sampling methods to outgoing letter mail characteristics, N. C. Severo, A. E. Newman, S. M. Young, and M. Zelen, NBS Tech. Note 16 (PB151375) (1959) $2.75.

Radio noise data for the International Geophysical Year July 1, 1957–December 31, 1958, W. Q. Crichlow, C. A. Samson, R. T. Disney, and M. A. Jenkins, NBS Tech. Note 18 (PB151377) (1959) $2.50.

Variations of gamma cassiopeiae, S. R. Pottasch, NBS Tech. Note 21 (PB151380) (1959) 75 cents.

Communication theory aspects of television bandwidth conservation, W. C. Coombs, NBS Tech. Note 25 (PB151384) (1959) 50 cents.

Distribution of mail by destination at the San Francisco, Los Angeles, and Baltimore Post Offices, N. C. Severo and A. E. Newman, NBS Tech. Note 27 (PB151386) (1959) $1.50.

A history of vertical-incidence ionosphere sounding at the National Bureau of Standards, S. C. Gladden, NBS Tech. Note 28 (PB151387) (1959) $2.00.

Aerodynamic phenomena in stellar atmospheres—A bibliography, NBS Tech. Note 30 (PB151389) (1959) $1.25.

Resistance diode bridge circuit for temperature control, L. H. Bennett and V. M. Johnson, NBS Tech. Note 34 (PB151393) (1959) 50 cents.

Atomic weights, E. Wichers, ch. 6, Treatise on analytical chemistry, pt. 1. Theory and practice, vol. 1, sec. B. Application of chemical principles, p. 161 (The Interscience Encyclopedia, Inc., New York, N.Y., 1959).

Concept and determination of *p*H, R. G. Bates, ch. 10. Treatise on analytical chemistry, pt. 1. Theory and practice, vol. 1, sec. B. Application of chemical principles, p. 361 (The Interscience Encyclopedia, Inc., New York, N.Y., 1959).

Electrode potentials, R. G. Bates, ch. 9. Treatise on analytical chemistry, pt. 1. Theory and practice, vol. 1, sec. B. Application of chemical principles, p. 319 (The Interscience Encyclopedia, Inc., New York, N.Y., 1959).

Principles and methods of sampling, W. W. Walton and J. I. Hoffman, ch. 4. Treatise on analytical chemistry, pt. 1. Theory and practice, vol. 1, sec. A. Analytical chemistry: Its objectives, functions, and limitations, p. 67 (The Interscience Encyclopedia, Inc., New York, N.Y., 1959).

System loss in radio-wave propagation, K. A. Norton, Letter to Editor, Proc. IRE **47** No. 9, 1661 (1959).

The oxide films formed on copper single crystal surfaces in pure water. 1. Nature of the films formed at room temperature, J. Kruger, J. Electrochem. Soc. **106** No. 10, 847 (1959).

Strain gauge calibration device for extreme temperatures, R. M. McClintock, Rev. Sci. Instr. **30,** No. 8, 715 (1959).

Rapid insertion device for coaxial attenuators, A. Y. Rumfelt and R. J. Como, Rev. Sci. Instr. **30,** No. 8, 687 (1959).

Trapped energetic radicals, J. L. Franklin and H. P. Broida, Ann. Rev. Phys. Chem **10,** 145 (1959).

Electrode potentials, p. 319, and Concept and determination of *p*H, p. 361, R. G. Bates, pt. 1, vol. 1, Treatise on analytical chemistry, Edited by I. M. Kolthoff and P. J. Elving (Interscience Pub. Co., New York, N.Y., 1959).

Diode in feedback loop makes stable transistor bias circuit, G. F. Montgomery, Electronic Design **7,** 54 (1959).

Investigation of creep behavior of structural joints under cyclic loads and temperatures, L. Mordfin, N. Halsey, and G. E. Greene, NASA Tech. Note D–181, p. 37 (1959).

Dimensional stability of impregnated sole leather, B. H. Fouquet, J. Am. Leather Chemists' Assoc. **LIV,** No. 10, 544 (1959).

Theoretical problems of reliability measurement and prediction, J. R. Rosenblatt, Proc. of the Third Exploratory Conf. on Missile Model Design for Reliability Prediction at White Sands Missile Range (New Mexico) p. 29 (1959).

Accuracy and precision: Evaluation and interpretation of analytical data, W. J. Youden, ch. 3. Treatise on analytical chemistry, pt. I. Theory and practice, vol. 1, sec. A. Analytical chemistry: Its objectives, functions and limitations, p. 47 (The Interscience Encyclopedia, Inc., New York, N.Y., 1959).

Microwave reflectometer techniques, G. F. Engen and R. W. Beatty, IRE Trans. on Microw. Theory and Tech. **MTT-7,** No. 3, 346 (1959).

Dependence of mechanical strength of brittle polycrystalline specimens on porosity and grain size, F. P. Knudsen, J. Am. Ceram. Soc. **42,** No. 8, 376 (1959).

Theory of dielectric relaxation in molecular crystals, J. D. Hoffman, Archives des Sciences, Soc. Phys. et Hist. Nat. de Geneve **12,** 36 (1959).

Denture reliners—direct, hard, self-curing resin, G. M. Brauer, E. E. White, Jr., C. L. Burns, and J. B. Woelfel, J. Am. Dental Assoc. **59,** 270 (1959).

A porcelain reference electrode conductive to sodium ions for use in molten salt systems, R. J. Labrie and V. A. Lamb, J. Electrochem. Soc. **106,** No. 10, 895 (1959).

Ceramic wafer tubes for modular units, C. P. Marsden, sec. on Components and Materials, Electronics **32,** No. 39, 94 (1959).

Magnified and squared VSWR responses for microwave reflection coefficient measurements, R. W. Beatty, IRE Trans. on Microw. Theory and Tech. **MTT-7,** No. 3, 346 (1959).

Low-temperature tensile properties of copper and four bronzes, R. M. McClintock, D. A. Van Gundy, and R. H. Kropschot, ASTM Bull. No. 240, 34 (TP177) (1959).

A nomenclature for conformations of pyranoid sugars and derivatives, H. S. Isbell and R. S. Tipson, Science **130,** No. 3378, 793 (1959).

On the convergence of the Rayleigh quotient iteration for the computation of the characteristic roots and vectors. III (General Rayleigh quotient and characteristic roots with linear elementary divisors) A. M. Ostrowski, Arch. Rat. Mech. Anal. **3,** 325 (1959).

On the convergence of the Rayleigh quotient iteration for the computation of the characteristic roots and vectors. IV (Generalized Rayleigh quotient for nonlinear elementary divisors) A. M. Ostrowski, IV Arch. Rat. Mech. Anal. **3,** 341 (1959).

Observations of the ionosphere over the south geographic pole, R. W. Knecht, J. Geophys. Research **64,** No. 9, 1243 (1959).

Atomic electron affinities, F. Rohrlich, Nature **183,** 244 (1959). A discussion of federal specifications GS–X–620 and L–F–310 for dental X-ray apparatus and dental X-ray film, G. C. Paffenbarger, A. F. Forziati, and M. P. Kumpula, J. Am. Dental Assoc. **59,** 472 (1959).

An additional lunar influence on equatorial E_s at Huancayo, R. W. Knecht, Research Note J. Atmospheric and Terrest. Phys. **14,** 348 (1959).

On artificial geomagnetic and ionospheric storms associated with high-altitude explosions, S. Matsushita, J. Geophys. Research **6,** 1149 (1959).

An intermittent-action camera with absolute time calibration, R. G. Hefley, R. H. Doherty, and E. L. Berger, IRE Wescon Conv. Record **3,** pt. 6, 129 (1959).

The earth and its environment, S. Chapman, Proc. IRE **47,** No. 2, 137 (1959).

Note on quiet-day vertical cross sections of the ionosphere along 75° W geographic meridian, J. W. Wright, Letter J. Geophys. Research **64,** 1631 (1959).

Effect of atomic tests on radio noise, C. A. Samson, Letter Nature **184,** 538 (1959).

Short-time stability of a quartz-crystal oscillator as measured with an ammonia maser, A. H. Morgan and J. A. Barnes, Letter Proc. IRE **47,** 1782 (1959).

Electromagnetic radiation from cylindrical structures, J. R. Wait (Pergamon Press, New York, N.Y., 1959).

Interplanetary gas. I: Hydrogen radiation in the night sky, J. C. Brandt and J. W. Chamberlain, Astrophys. J. **130,** 670 (1959).

Some clinical applications of research findings in dental materials, G. C. Paffenbarger, Ohio Dental J. **33,** No. 3, 218 (1959).

Liquid helium cryostat with an integral superconducting resonator, E. Maxwell and F. A. Schmidt, Suppl. Bull. Inst. Intern. Froid, Commission 1, Delft, Holland, Annexe 1958–1, p. 95 1958).

Sporadic *E* observed on VHF oblique incidence circuits, E. K. Smith, in North Atlantic Treaty Organization. Sporadic *E* ionization; Ionospheric Research Meeting, AGARD Avionics Panel, Cambridge, England, Sept. 1958 (AGARDograph 34) p. 129 (1958).

Low-temperature transport properties of copper and its dilute alloys: Pure copper, annealed and cold-drawn, R. L. Powell, H. M. Roder, and W. J. Hall, Phys. Rev. **115,** 314 (1959).

**Publications for which a price is indicated (except for Technical Notes) are available only from the Superintendent of Documents, U.S. Government Printing Office, Washington 25, D.C. (foreign postage, one-fourth additional). Technical Notes are available only from the Office of Technical Services, U.S. Department of Commerce, Washington 25, D.C. (order by PB number.) Reprints from outside journals and the NBS Journal of Research may often be obtained directly from the author.*

UNITED STATES
GOVERNMENT PRINTING OFFICE
DIVISION OF PUBLIC DOCUMENTS
WASHINGTON 25, D.C.

OFFICIAL BUSINESS

PENALTY FOR PRIVATE USE TO AVOID
PAYMENT OF POSTAGE, $300
(GPO)

JOURNAL OF RESEARCH of the National Bureau of Standards
A. Physics and Chemistry

Vol. 64A, No. 2

March–April 1960

Contents

Page

A carbon-14 beta-ray standard, benzoic acid-7-C^{14} in toluene, for liquid scintillation counters. W. F. Marlow and R. W. Medlock. 143

A comparison of experimental and theoretical relations between Young's modulus and the flexural and longitudinal resonance frequencies of uniform bars. S. Spinner, T. W. Reichard, and W. E. Tefft. 147

Determination of copolymer composition by combustion analysis for carbon and hydrogen. Lawrence A. Wood, Irving Madorsky, and Rolf A. Paulson. 157

Some effects of aging on the surface area of portland cement paste. C. M. Hunt, L. A. Tomes, and R. L. Blaine. 163

Conformations of the pyranoid sugars. I. Classification of conformers. H. S. Isbell and R. S. Tipson. 171

Tritium-labeled compounds III. Aldoses-*1-t*. H. S. Isbell, H. L. Frush, N. B. Holt, and J. D. Moyer. 177

Determination of aluminum in precipitation hardening stainless steel and high temperature alloys. Lawrence A. Nachlan, John L. Hague, and Edward J. Meros. 181

Publications of the National Bureau of Standards. 185

For sale by the Superintendent of Documents, U.S. Government Printing Office, Washington 25, D.C. Price 70 cents (single copy)
Subscription price: $4.00 a year; $0.75 additional for foreign mailing.

UNITED STATES GOVERNMENT PRINTING OFFICE, WASHINGTON : 1960